Titre: Title:	Etalonnage géométrique des machines-outils par barre à billes en vue de prédire leur performance
Auteur: Author:	Yousefali Abbaszadeh-Mir
Date:	2001
Type:	Mémoire ou thèse / Dissertation or Thesis
Référence: Citation:	Abbaszadeh-Mir, Y. (2001). Etalonnage géométrique des machines-outils par barre à billes en vue de prédire leur performance [Ph.D. thesis, École Polytechnique de Montréal]. PolyPublie. https://publications.polymtl.ca/7064/

URL de PolyPublie: PolyPublie URL:	https://publications.polymtl.ca/7064/
Directeurs de recherche: Advisors:	
Programme: Program:	Unspecified

INFORMATION TO USERS

This manuscript has been reproduced from the microfilm master. UMI films the text directly from the original or copy submitted. Thus, some thesis and dissertation copies are in typewriter face, while others may be from any type of computer printer.

The quality of this reproduction is dependent upon the quality of the copy submitted. Broken or indistinct print, colored or poor quality illustrations and photographs, print bleedthrough, substandard margins, and improper alignment can adversely affect reproduction.

In the unlikely event that the author did not send UMI a complete manuscript and there are missing pages, these will be noted. Also, if unauthorized copyright material had to be removed, a note will indicate the deletion.

Oversize materials (e.g., maps, drawings, charts) are reproduced by sectioning the original, beginning at the upper left-hand corner and continuing from left to right in equal sections with small overlaps.

ProQuest Information and Learning
300 North Zeeb Road, Ann Arbor, MI 48106-1346 USA
800-521-0600

UNIVERSITÉ DE MONTRÉAL

ÉTALONNAGE GÉOMÉTRIQUE DES MACHINES-OUTILS PAR BARRE À BILLES EN VUE DE PRÉDIRE LEUR PERFORMANCE

YOUSEFALI ABBASZADEH-MIR
DÉPARTEMENT DE GÉNIE MÉCANIQUE
ÉCOLE POLYTECHNIQUE DE MONTRÉAL

THÈSE PRÉSENTÉE EN VUE DE L'OBTENTION
DU DIPLÔME DE PHILOSOPHIAE DOCTOR
(GÉNIE MÉCANIQUE)
SEPTEMBRE 2001

UNIVERSITÉ DE MONTRÉAL

ÉCOLE POLYTECHNIQUE DE MONTRÉAL

Cette thèse intitulée:

ÉTALONNAGE GÉOMÉTRIQUE DES MACHINES-OUTILS PAR BARRE À BILLES EN VUE DE PRÉDIRE LEUR PERFORMANCE

présentée par: ABBAZADEH-MIR Yousefali

en vue de l'obtention du diplôme de: Philosophiae Doctor

a été dûment acceptée par le jury d'examen constitué de:

M. BALAZINSKI Marek, Ph.D., président

M. FORTIN Clément, Ph.D., membre et directeur de recherche

M. MAYER René, Ph.D., membre et codirecteur de recherche

M. BARON Luc, Ph.D., membre

M. RIVEST Louis, Ph.D., membre

DÉDICACE

À mon épouse Fatemeh,

à ma mère,

et à la mémoire de mon père.

REMERCIEMENTS

L'auteur tient à remercier toutes les personnes qui ont collaboré de près ou de loin à la réalisation de cette thèse.

Plus particulièrement, ces remerciements s'adressent à Messieurs Clément Fortin et René Mayer mes directeurs de recherche, pour m'avoir dirigé et soutenu tout au long de ce travail, pour leurs conseils judicieux ainsi que pour la disponibilité dont ils ont fait preuve.

Je tiens à remercier Messieurs Marek Balazinski et Luc Baron, professeurs à l'École Polytechnique de Montréal et Monsieur Louis Rivest, professeur à l'École de Technologie Supérieure de Montréal, d'avoir accepté de participer au jury d'examen de cette thèse. Je remercie également Monsieur Richard Hurteau, professeur à l'École Polytechnique de Montréal, d'avoir accepté d'être représentant du doyen.

Mes remerciements vont également au Ministre de la science et de la technologie d'Iran pour son aide financière partielle.

J'aimerais tout spécialement remercier ma famille pour leurs constants encouragements et leur appui tout au long de mes études. J'adresse également mes remerciements les plus sincères à mon épouse Fatemeh.

RÉSUMÉ

La caractérisation et la modélisation de la performance des machines-outils et des autres équipements de soutien sont essentielles pour obtenir des piéces usinées de grande précision.

Cette problématique s'applique à bon nombre d'industries manufacturières, dans les domaines de l'aérospatiale, de l'automobile, de la machine-outil, des fabricants d'équipements lourds, ainsi qu'aux petites et moyennes entreprises sous-traitantes en usinage pour les grands donneurs d'ordre.

Le comportement d'une machine-outil et son habileté à suivre les trajectoires programmées doivent être définis. Leur influence sur la génération de pièces ou de surfaces doit être connue. Un parcours d'outil réel est estimé en analysant les erreurs générées par la machine.

La présente thèse vise l'atteinte de deux objectifs. Le premier est le développement d'une procédure pour identifier les erreurs géométriques sur une machine-outil multi-axes. Le second objectif vise, une fois les erreurs de la machine-outil identifiées, à évaluer sa capacité à positionner l'outil aux coordonnées spécifiées.

Les inexactitudes géométriques d'une machine-outil influencent fortement la qualité des pièces usinées. Dans un premier temps, une approche systématique est développée pour l'étalonnage des paramètres d'écarts géométriques indépendants de la position (PEGIPs). Ces écarts incluent les mauvais alignements articulaires ainsi que les entre-axes et les écarts de zéro dans le cas d'articulations rotoïdes d'une machine-outil à cinq axes. Un modèle cinématique de machine-outil à cinq axes est développé en employant les matrices de transformation homogène et en y incorporant les écarts géométriques. Nous avons utilisé ce modèle pour produire des mesures virtuelles, une matrice d'observation ainsi qu'une procédure de prédiction d'erreurs. La matrice d'observation a été développée sur la base d'un modèle nominal de machine-outil, des configurations de la machine-

outil et de sa topologie. Cette matrice a été utilisée pour calculer la sensibilité de l'erreur en bout d'outil par rapport à la pièce versus les sources d'erreurs géométriques. La barre à billes magnétique et télescopique (BBMT) a été utilisée pour acquérir des lectures de longueur pour un certain nombre de configurations de la machine. Une stratégie de choix est proposée afin de représenter un groupe complet et minimal de paramètres d'écarts pour la machine-outil. Ce modèle est par la suite étalonné à l'aide de mesures de la variation de la longueur de la barre à bille pour des configurations machines qui nominalement devraient résulter en des variations nulles de cette longueur. Une série de critères est adoptée pour valider les paramètres identifiés. Finalement plusieurs essais ont été faits pour montrer que la méthode utilisée est valide. Les essais montrent des résultats excellents pour les valeurs des paramètres identifiés ainsi que pour la prédiction des erreurs de localisation de l'outil par rapport à la pièce.

Dans un deuxième temps, un modèle est développé afin d'étalonner une machine-outil à cinq axes pour les paramètres d'erreurs géométriques dépendants de la position (PEGDPs) en utilisant la barre à billes télescopique. Les différentes positions décrivent le mouvement non-idéal d'un joint. Le modèle est basé sur l'identification des PEGIPs et il utilise une fonction polynomiale pour l'identification des PEGDPs. Les sources d'erreurs de la machine-outil ont été individuellement modélisées par les polynômes de Chebychev et intégrées dans la matrice d'observation. Le polynôme de Chebychev a été utilisé pour ses avantages sur la procédure de calcul. Les coefficients des polynômes sont calculés suite à la résolution d'un système d'équations linéaires constitué de la matrice d'observation augmentée et des lectures de la barre à billes. Puis, les polynômes sont utilisés pour prédire l'erreur de bout d'outil pour des coordonnées articulaires données. Étant donné la redondance entre les paramètres d'erreur, une stratégie a été développée pour choisir un nombre minimal mais complet de coefficients. Ensuite, une méthode de barre à billes à trois ancrages successifs et sollicitant différents aspects de la cinématique est employée pour identifier les coefficients. Finalement, des critères sont utilisés pour évaluer si les paramètres identifiés peuvent atteindre nos objectifs.

La prévision de la capacité de la machine-outil à produire une pièce dans les tolérances est évaluée en considérant les coefficients des polynômes des paramètres identifiés au cours du déplacement de l'outil. Dans les systèmes de CAO/FAO actuels, la trajectoire de l'outil (ou des données CL (« cutter location ») définissant la position de l'outil par rapport à la pièce) est directement obtenue à partir de la courbe ou de la surface à usiner. Les coordonnées articulaires qui sont utilisées pour commander la machine-outil sont calculées à partir de ces donnés CL et d'un modèle cinématique inverse. Un modèle cinématique direct enrichi des PEGDPs permet de générer la trajectoire prédite de l'outil. Une comparaison est faite entre les deux trajectoires et une évaluation est effectuée pour vérifier si la machine-outil actuelle est capable de produire la pièce avec les tolérances désirées. Une méthodologie est aussi présentée pour intégrer cet outil dans un système de CAO/FAO et GAO (gamme assistée par ordinateur).

ABSTRACT

The modelling, characterization, and performance assessment of machine tools and other supporting equipment are essential to obtain highly accurate machined parts.

The behaviour of a machine tool including sources of errors must be defined and their influence on the generation of the part faces or surfaces quantified. A predicted machined surface is then generated which considers the existing errors on the machine tool.

The development of a procedure to identify the geometric errors on a multi-axis machine tool is the main objective pursued in this research. Once the errors are identified, predicting the performance of the machine tool for a machining operation on a surface is the second objective of this work.

This concept would benefit to a broad spectrum of manufacturing industries, including aerospace, automotive, machine tool, and heavy equipment manufacturers, as well as small manufacturing enterprises that provide machining services to these large industrial groups.

The geometric inaccuracies of a machine tool strongly influence the quality of machined parts. A systematic approach is developed for the calibration of the position independent geometric error parameters (PIGEPs) such as the joint misalignments of a five-axis machine tool. A kinematics model of such a machine tool is developed using the homogenous transformation matrix and incorporates geometric errors. This machine tool model was used to generate the virtual measurements, observation matrix and error prediction procedure. An observation matrix is developed based on the machine tool nominal model, configurations and topology. This matrix is used to calculate the sensitivity of the tool-location error to the geometric error sources. Then a telescoping magnetic ball bar (TMBB) is used to gather length readings for a number of machine configurations. From an error identification procedure and through a strategy of

selection of error parameters, a set of error parameters are selected which represent a complete and minimal set of error parameters for a five axis machine tool. A series of criteria is presented for the acceptance of the identified parameters. Finally several tests are presented to validate the method through simulation. These show excellent results both for the parameter values and for the tool versus workpiece error prediction.

As a further step, a procedure is developed to calibrate a five-axis machine tool for position dependent geometric errors parameters (PDGEPs) again using the telescoping ball-bar. These PDGEP describe the non-ideal motion of joints. The model is based on the development of the PIGEP identification and uses polynomial functions for modelling the PDGEP error model. The machine tool error sources are individually modelled by Chebychev polynomials and integrated in the observation matrix. The Chebychev polynomials are used because of their advantages for computing purposes. The coefficients of these polynomials are calculated through a set of linear equations made of the observation matrix and ball-bar readings. Then, the identified polynomials are used to predict the tool-tip error for a given joint coordinate values. Details of the observation matrix generation are presented and a complete identification procedure has been developed to identify the parameters. Because of redundancies amongst error parameters, a strategy was developed to select parameters from each group of redundant parameters. For the complete identification procedure, firstly, a minimal but complete number of coefficients are selected. Then, a three-socket ball-bar strategy is used to identify these parameters. Finally, some criteria are used to evaluate whether the identified parameters are valid. The Simulation of the entire calibration procedure are developed based on Matlab™.

Predicting the performance of a machine tool before machining a part is an important task in order to improve the dimensional accuracy of parts. The prediction of performance of machine tool to perform a task is estimated by considering the identified machine tool error parameters in the tool path generation. In current CAD/CAM systems, the tool path (or CL data) is directly generated from the curves or surfaces to be

machined. The joint coordinate values corresponding to the CL data are then calculated through an inverse kinematics model. A second CL data file is generated on the basis of the nominal joint coordinate and of the geometric error sources of the machine tool. A comparison is made between these two data set and then an assessment is made to verify whether or not the actual machine tool is capable of producing parts within desired tolerances. A methodology is also presented to integrate this tool within a CAD/CAM and computer-aided process planning (CAPP) environment.

TABLE DES MATIÈRES

LISTE DES TABLEAUX

LISTE DES FIGURES

INTRODUCTION

Pour être concurrentiel sur les marchés globaux, il faut fabriquer des produits de haute qualité à des prix compétitifs. Cela exige un haut degré de contrôle sur les processus et les ressources de fabrication.

L'avenir de la fabrication réside dans l'utilisation de machines-outils flexibles. Dans un tel environnement, la caractérisation et la modélisation de la performance des machines-outils et d'autres équipements de soutien sont essentiels.

Les machines-outils sont des éléments critiques dans la fabrication de pièces discrètes, qui représentent un bon pourcentage des opérations de fabrication en Amérique du Nord [NIST, 2000]. Les utilisateurs principaux de machines-outils sont des ateliers d'usinage sous-traitant, l'aérospatiale, la défense, les industries de l'automobile, l'agriculture, la machinerie électrique et l'industrie des appareils domestiques.

La gamme de fabrication consiste à formuler des processus de fabrication et à identifier les ressources qui doivent être employées pour convertir un matériau brut de sa forme initiale à une forme finale déterminée par le bureau d'étude. Les logiciels de génération de gammes assistée par ordinateur doivent offrir un soutien au gammiste en lui donnant un accès direct à la définition du produit, aux ressources de fabrication, aux méthodes de fabrication et en lui fournissant des outils d'analyse.

La caractérisation d'une machine-outil est difficile à réaliser étant donné le grand nombre de sources d'erreurs géométriques, thermiques et dynamiques dont les effets sur la précision des pièces sont complexes. Les méthodes actuelles d'essais sont complexes, nécessitent beaucoup de temps et exigent un haut degré d'expertise en métrologie. De plus, l'effet des paramètres de performance est difficile à mettre en évidence dans les dispersions de pièces obtenues dans des conditions de coupe réelles.

L'augmentation de la performance des machines-outils est critique pour l'amélioration de la précision générale (qualité). De plus, l'augmentation de la performance générale de

fabrication est critique quant à elle pour rencontrer les demandes du marché (coûts, temps). Des tolérances plus serrées sont exigées pour l'interchangeabilité, l'assemblage automatique, la miniaturisation, l'intégration, la performance et la fiabilité. La précision des machines-outils doit être augmentée pour atteindre ces exigences. L'évaluation et l'augmentation de la performance des machines-outils jouent un rôle critique dans l'amélioration de cette précision. L'identification des erreurs de la machine-outil et les modèles de prédiction de la performance sont des tâches cruciales pour l'amélioration de la performance des machines-outils.

Les erreurs quasi-statiques des machines-outils sont définies comme étant les erreurs de positions relatives entre l'outil et la pièce qui varient lentement en fonction du temps et rapidement après une collision du système. Ces erreurs sont reliées à la structure de la machine-outil. Il a été avancé que les erreurs quasi-statiques représentent environ 70% de toutes les erreurs attribuables à une machine-outil [Ragunath 1985]. La capacité d'identifier de telles erreurs pourrait donc faire diminuer de façon significative le nombre de pièces rebutées et augmenter la précision de la machine.

L'identification des paramètres d'erreur de la machine-outil est un pas important pour améliorer la précision dimensionnelle de pièces puisque ces informations peuvent être employees pour la compensation d'erreurs. Ces informations sont aussi utilisées pour prévoir la performance de la machine et générer des gammes réalisables. Une fois les erreurs identifiées pour une machine-outil, la prédiction de la performance de cette machine peut être évaluée. Cela peut être fait en prédisant le résultat de l'usinage suite à une opération suggérée par la gamme.

Une gamme est valide quand elle peut produire une pièce dans un intervalle de tolérance désiré. La production d'une pièce précise est fortement dépendante de la précision de la machine-outil. Donc, l'identification des erreurs de la machine et la prédiction de sa performance peut aider le gammiste à choisir une machine-outil appropriée afin d'exécuter un processus avec la précision désirée.

Ce travail contribue à développer les outils qui peuvent aider le gammiste à produire une gamme valide. Ces outils sont l'identification des erreurs géométriques de la machine-outil et la prédiction de performance de ces machines pour exécuter une trajectoire avec la tolérance requise. Ils peuvent servir à un grand nombre d'industries manufacturières, y compris l'aérospatiale, l'automobile, le domaine de la machine-outil et les fabricants d'équipements lourds, tant pour les petites entreprises industrielles qui fournissent l'usinage aux grands groupes industriels que pour ces derniers.

Identification des erreurs géométriques de la machine-outil

La connaissance de l'état de la machine-outil peut aider les gammistes à choisir une ressource appropriée pour des opérations sur une pièce pendant le développement de la gamme. Les recherches sur les machines-outils à commande numérique (MOCN) montrent que de telles machines peuvent se détériorer considérablement même dans un environnement idéal [Shin et al 1991]. Afin d'usiner des pièces de grande précision il est donc nécessaire de caractériser la machine sur une base régulière. L'intérêt pour accroître la précision de la machine-outil est bien reconnu en raison des demandes de tolérances de plus en plus serrées sur les pièces à usiner.

Parmi les sources d'erreurs de la machine on distingue les erreurs géométriques des composants de machine et des structures, les erreurs provoquées par les distorsions thermiques, les erreurs de déflexions causées par les forces de coupe, les erreurs d'asservissement et enfin les erreurs algorithmiques de contrôle et de commande. Cependant les erreurs géométriques et thermiques sont parmi les plus importantes [Donmez et al. 1987, Hocken 1980, Ragunath 1985].

Les erreurs géométriques des machines-outils proviennent des imperfections de fabrication, des mauvais alignements et de la déformation statique de composants de la machine ou de l'usure de cette dernière. Celles-ci incluent des paramètres d'erreurs géométriques indépendants de la position (PEGIPs) qui décrivent la localisation relative

des joints rotoïdes et prismatiques successifs de la machine ainsi que les paramètres d'erreurs géométriques dépendants de la position (PEGDPs) décrivant le mouvement non-idéal d'un joint. Ces erreurs pourraient être réduites par l'amélioration structurelle de la machine-outil, c'est à dire par l'amélioration de sa conception et de la qualité de ses composants. Cependant, il y a dans de nombreux cas, des limitations physiques à la précision qui ne peuvent pas être surmontées par des techniques de conception et de production des machines-outils. L'identification de ces sources d'erreur a reçu beaucoup d'attention ces dernières années, en vue de compenser leurs effets par des corrections soit au niveau des programmes CN, soit en modifiant les signaux provenant des encodeurs.

Prédiction de performance de la machine-outil

La précision dimensionnelle et géométrique des pièces produites sur une machine-outil dépend de la précision de la machine et du processus d'usinage. Avec une machine-outil à CN, le but primordial est d'automatiser les processus d'usinage. La prédiction de la performance des machines-outils peut faire diminuer énormément le nombre de pièces rebutées et contribuer à la validation des gammes d'usinage avant leur exécution dans l'atelier. La connaissance de l'état de la machine-outil sélectionnée et du processus d'usinage sont les clefs pour prévoir les défauts sur la pièce usinée.

"La précision d'une pièce est définie comme étant le degré de conformité de la pièce finie aux spécifications dimensionnelles et géométriques" [Hocken 1980]. La prédiction de la performance de la machine-outil consiste à déterminer si la machine dans son état actuel est capable d'accomplir une opération avec une tolérance spécifiée. Pour cela nous devons connaître l'état de la machine-outil choisie, le type de processus choisi et les limites de spécification que les concepteurs imposent à une pièce donnée.

Il est clair que l'analyse de la gamme de fabrication qui prévoit l'état de précision des pièces à usiner est nécessaire parce qu'elle aide à faire un changement plus tôt dans le cycle de développement.

La connaissance de la précision des machines-outils et de ses effets sur la pièce produite donne un avantage pour intégrer le système de génération de gamme assistée par ordinateur "Computer Aided Process Planning (CAPP)" dans un système de CAO/FAO. Elle permet aux ingénieurs de fabrication de prévoir la forme de la pièce avant d'engager les moyens réels de production. Cet outil donne l'information pour réduire le temps de production et augmenter la qualité des pièces.

Le développement d'une procédure d'identification permettant de trouver les erreurs géométriques sur une machine-outil multi-axes est le premier objectif de cette recherche. La procédure utilise la barre à billes télescopique comme appareil de mesures industrielles pour acquérir l'information à partir de la machine-outil et utilise aussi des fonctions polynomiales pour représenter les erreurs de mouvement des machines d'une façon paramétrique. L'usinage exact sera réalisé en considérant les erreurs existantes sur la machine-outil qui apparaissent lors du déplacement de l'outil. La pièce doit être analysée afin de s'assurer qu'elle peut rencontrer la tolérance désirée. La prédiction de la performance de la machine-outil avant d'exécuter une opération d'usinage est l'autre objectif de ce travail.

Organisation de la thèse

La thèse a été rédigée sur la base d'articles qui en forment le corps. Le présent chapitre donne une vue générale de la problématique et du besoin d'avoir des machines précises pour produire des pièces de grande qualité. Les chapitres 1 et 2 présentent respectivement la revue de littérature et la synthèse du sujet de la thèse.

Le chapitre 3 présente la méthodologie d'identification des PEGIP sur une machine-outil à cinq axes. Le travail qui constitue ce chapitre est présenté dans l'article intitulé

"Theory and simulation for the identification of the link geometric errors for a five axis machine tool using a telescoping magnetic ball-bar". Cet article a été soumis à la revue "International Journal of Production Research".

Le Chapitre 4 présente une méthodologie d'identification et une procédure de simulation pour identifier les erreurs dues aux inexactitudes géométriques de composants de machine-outil pendant leur mouvement, soit les PEGDP. Ce travail est présenté dans un article intitulé "Calibration of a Five-Axis Machine Tool Link and Motion Errors Using a Telescoping Magnetic Ball-Bar". L'article a été soumis à la revue "International Journal of Machine Tools and Manufacture".

Le chapitre 5 présente un concept pour prévoir les erreurs de l'outil versus la position de la pièce résultant des sources d'erreurs géométriques PEGIP PEGDP pour une tâche d'usinage donnée. Le contenu de ce travail est présenté dans l'article intitulé "Tool path error prediction of a five-axis machine tool with geometric errors". Cet article a été soumis à la revue "Journal of Engineering Manufacture".

Enfin une conclusion générale et des recommandations sont présentées.

CHAPITRE 1: REVUE BIBLIOGRAPHIE

1.1 La gamme assistée par ordinateur «GAO»

La gamme décrit en détail les méthodes pour qu'une pièce puisse être fabriquée à partir de la matière première jusqu'au produit fini. Au cours de ces dernières années, les systèmes de GAO ont été reconnus comme un élément clé dans les systèmes de fabrication intégrés par ordinateur. Malgré les efforts énormes réalisés dans le développement de système de GAO, les avantages de GAO dans la vie réelle des environnements industriels doivent encore être établis [Elmaraghy et al 1993]. Durant les trois dernières décennies, plus de 300 articles ont été publiés dans ce domaine. Beaucoup d'articles clé ont été consacrés au développement de GAO [Leung 1996]. Weill et al [Weill et al 1982] ont examiné des systèmes de GAO et ont étudié des problèmes techniques dans le développement de GAO, du choix de processus à la rédaction de feuilles de processus. Trois ans plus tard, Eversheim et Schulz [Eversheim et Schulz 1985] ont passé en revue plus de 50 systèmes de GAOs. Un an plus tard, une autre étude extensive a été effectuée par Wysk et al [Wysk et al 1986] dans laquelle plus de 25 systèmes ont été examinés. D'autres travaux ont été faits par Alting et Zhang [Alting et Zhang 1989] et Elmaraghy et al [Elmaraghy et al 1993].

Pendant les 30 dernières années plusieurs systèmes de GAO développés ont été basés sur l'approche par variantes, tandis qu'actuellement les approches génératives et semi-génératives sont largement adoptées. Dans l'approche par variantes, les pièces sont groupées dans des familles de pièces où un code unique est produit pour chaque famille et une gamme standard développée à l'avance. La planification d'une nouvelle pièce est exécutée en identifiant et récupérant des gammes existantes pour des pièces semblables et en faisant des modifications nécessaires pour convenir à la nouvelle pièce [Chang et Wysk 1985; Tempelhof 1980]. Les systèmes GAO semi-génératifs et génératifs constituent la génération suivante où le concept de "la gamme standard" a été remplacé par un système informatique capable de prendre des décisions spécifiques sur l'opération

à exécuter pour produire une pièce. Dans ce type de système de GAO, les tableaux de décision ou les arbres de décision sont décrits par le codage de la technologie de groupe (TG) et des arrangements de classification ou des langages de description de pièces spéciales [Ham et Lu 1989; Eversheim et Cobanoglu 1989]. Au début des années 1980, les techniques d'intelligence artificielle (IA) ont été introduites en GAO. Beaucoup de systèmes GAO ont été mis en œuvre par des techniques IA soit par les systèmes de "bases de connaissance" ou des systèmes "experts" [Chang et Wysk 1985]. Chacun d'entre eux a des avantages et des inconvénients. De nombreuses sociétés industrielles ont acquis des systèmes GAO pour l'intégration de la conception et de la production afin de compenser le manque de gammistes experts. Malgré la prévision optimiste des chercheurs sur le progrès de systèmes GAO et leur implantation dans l'industrie dans le proche avenir, cette prévision est toujours incertaine. Beaucoup de grandes entreprises ont dû établir leurs propres groupes de recherche pour développer leurs propres systèmes de GAO. Des petites et moyennes entreprises peuvent se permettre seulement le système GAO existant qui a été développé par des organisations de recherche ou des universités.

On peut aussi voir que la gamme de fabrication s'applique à une grande variété de processus de fabrication incluant l'enlèvement de métal, l'addition de métal (le moulage, l'injection, le prototypage rapide), le soudage, le traitement de surface, l'inspection et l'assemblage, etc. À cet égard un système de gamme assisté par ordinateur multidisciplinaire développé par Fortin et al [Fortin et al 1997] est un bon exemple.

1.2 Les erreurs de machine-outil

Une machine-outil à cinq-axes a la capacité de positionner et d'orienter simultanément l'outil coupant dans son espace de travail. C'est ce qui fait qu'une telle machine-outil est si versatile. Dû au besoin accru de composants usinés de haute complexité géométrique et de grande précision, les demandes sur les MOCN à cinq-axes ont fortement augmenté. Ces machines ont aussi d'autres avantages tels [Trankle 1980]: (a) une bonne adaptation

géométrique de l'outil de coupe à la surface de la pièce; (b) une correction technique de l'alignement de l'outil de coupe le long de sa trajectoire de fraisage et (c) la réduction du nombre de gabarits et de montages. D'autres part, la précision de ces machines sophistiquées est limitée par de nombreuses erreurs qui proviennent de plusieurs sources aussi bien cinématiques, thermiques que dynamiques.

L'amélioration de la performance des machines-outil est critique pour l'amélioration de la précision générale et de la performance de fabrication pour rencontrer les demandes du marché. De plus des tolérances plus serrées sont exigées pour l'interchangeabilité, l'assemblage automatique, la miniaturisation, l'intégration, la performance et la fiabilité. La précision des machines-outils doit être augmentée pour atteindre ces exigences. L'évaluation et l'augmentation de la performance des machines-outils jouent un rôle critique dans l'amélioration de cette précision. L'identification des erreurs des machines-outil et les modèles de prédiction de la performance sont des tâches cruciales pour l'amélioration de la précision de ces dernières.

Plusieurs chercheurs ont concentré leurs efforts sur les erreurs associées aux machines-outils. La cinématique des corps rigides est une des techniques de modélisation les plus couramment utilisées pour la caractérisation d'erreurs de machine-outil [Donmez et al 1986, Donmez et al 1987, Duffie et Malmberg 1987, Hocken et al 1977].

En contrepartie, Kiridena et Ferreira [Kiridena et Ferreira 1993] ont utilisé la méthode de modélisation de Danevit-Hartenberg (D-H) et ont développé un modèle qui a montré les effets des erreurs de positionnement des axes de la machine sur l'exactitude de pose (position et orientation) de l'outil de coupe dans sa zone de travail.

Sur la base d'un modèle à corps rigide, Zhang et al. [Zhang et al 1985] ont calculé les erreurs géométriques d'une machine à mesurer tridimensionnelle, et ont successivement appliqué la compensation d'erreurs par logiciel aux machines, obtenant ainsi une amélioration d'un facteur de 10 de l'exactitude de la machine.

Elshennawy et Ham [Elshennawy et Ham 1990] ont aussi utilisé la cinématique de corps rigide pour développer un modèle pour des machines et ont appliqué une technique de compensation d'erreurs pour améliorer la performance de ces machines par un facteur moyen de quatre.

En supposant des caractéristiques d'erreurs élémentaires linéaires, Ferreira et Liu [Ferreira et Liu 1993] ont combiné différentes sources d'erreurs pour former un modèle complet d'erreurs volumétriques de la machine en utilisant la cinématique des corps rigides. Les paramètres du modèle ont été exprimés comme les fonctions de 15 mesures d'erreurs faites à neuf points sur les bords d'une zone de travail cubique.

Sur la base des concepts développés par Ferreira et Liu [Ferreira et Liu 1993], Kiridena et Ferreira [Kiridena et Ferreira 1994a, 1994b, 1994c] ont présenté une approche pour le développement d'un modèle d'erreur quasi-statique du $n^{ième}$ ordre pour les MOCNs.

Zhang, Ouyang et Lu [Zhang et al 1988] ont proposé une methode de déplacement pour l'étalonnage de la géométrie de la machine. En mesurant l'erreur de déplacement le long de 22 lignes dans la zone de travail, les erreurs volumétriques d'une machine-outil à trois axes ont été déterminées.

Kreng, Liu et Chu [Kreng et al 1994] ont développé un modèle pour exprimer l'erreur observée dans une zone de travail d'un centre d'usinage à trois axes comme une fonction de ses erreurs élémentaires. En utilisant une palette de montage personnalisée pour évaluer les erreurs, les paramètres du modèle d'erreur ont pu être mis à jour périodiquement. Les résultats expérimentaux ont indiqué que l'erreur peut être prévue dans un intervalle de $25\mu m$ lorsque cette méthode est appliquée.

Shin, Chin et Brink [Shin et al 1991] ont établi une procédure de caractérisation complète pour les centres usinages de MOCN et ont démontré que les caractéristiques statiques et dynamiques peuvent être extraites de sept essais de caractérisation complémentaires.

Mou et Liu [Mou et Liu 1992, 1994] ont développé une méthode de correction d'erreurs qui utilise des pièces de référence comme des échantillons «artefacts» de métrologie . Ils ont proposé une méthodologie adaptative en adoptant des conditions de machine-outil actuelles obtenues à partir de divers détecteurs et en modifiant ensuite les coefficients de modèle d'erreurs pour l'évaluation et la compensation plus précise d'erreurs [Mou et Liu 1995, Mou et al 1995a, Mou et al 1995b].

Beaucoup d'attention a été portée ces deux dernières décennies à l'utilisation d'instruments beaucoup plus simples pour acquérir les données représentatives de l'état géométrique de la machine. Un des instruments les plus populaires est la barre à billes magnétique télescopique (BBMT) [Bryan 1982a, Bryan 1982b] destinée à remplacer les étalons circulaires pour les essais de circularité sur des machines-outils. Kunmann et Waldele [Kunmann et Waldele 1983] ont utilisé le test de la barre à billes fixe pour évaluer les erreurs de déplacement et les erreurs de perpendicularité d'une machine à mesurer tridimensionnelle (MMT). L'effet de ces erreurs sur les erreurs de position de la MMT a été formulé et ces dernières peuvent donc être évaluées. La barre à billes a été largement utilisée pour les machines outils à trois axes prismatiques [Kakino et al 1993] et elle permet aussi la mesure de nombreux paramètres quasi-statiques et dynamiques via l'essai des trajectoires circulaires. Driels [Driels 1993] a utilisé une barre à billes de longueur fixe pour étalonner les paramètres d'erreurs géométriques indépendants de la position d'un robot industriel avec une chaîne cinématique simple composée de six joints rotoïdes. La formulation D-H modifiée est utilisée pour éviter le problème de la modélisation D-H en présence d'axes rotoïdes nominalement parallèles. En 1997, Pahk [Pahk 1997] a employé la barre à billes télescopique et a développé un concept de polynômes pour identifier des erreurs de machine-outil à trois axes.

Depuis cet article publié en 1997, nous n'avons pas trouver d'autres articles reliés de près à ce domaine.

1.3 La prédiction de performance d'une machine-outil

Une caractéristique géométrique, telle une surface complexe usinée par fraisage peut présenter des défauts géométriques en raison de divers facteurs, y compris des erreurs géométriques de la machine-outil, des variations de température, des erreurs de contrôle de mouvement, des vibrations, des erreurs de géométrie de l'outil de coupe, et de déflexion et des erreurs de calcul de génération de sa trajectoire. Beaucoup de travail a été fait pour identifier les erreurs géométriques et thermiques sur les machines-outils tel que discuté précédemment.

Pour la planification de l'usinage d'une surface, plusieurs stratégies peuvent être utilisées pour améliorer la qualité et la productivité du processus d'usinage. Ce sont la stratégie de vitesse d'avance adaptative, la stratégie de trajectoire de l'outil et la stratégie de contrôle de surface. Pour la stratégie de vitesse d'avance adaptative, l'avance est ajustée selon une certaine contrainte de production (Wang 1988; Fussell et Srinivasan 1989; Yazar et al 1992; Fussell et al 1992). Pour la stratégie de trajectoire d'outil, les directions des trajectoires d'outils sont choisies sur la base de certains critères, par exemple, la force de coupe, etc.

La trajectoire de l'outil est générée par la cinématique inverse de données d'emplacement de l'outil de coupe «CL» ("cutter location"), où les données CL sont les positions et les orientations du bout de l'outil et qui peuvent être produites directement à partir d'un logiciel de CAO/FAO. Morishing et al [Morishing et al 1999] ont appliqué un espace de configuration 3D pour éviter la collision de l'outil en générant la trajectoire de l'outil pour une géométrie complexe. Huang [Huang et Olivier 1995] ont développé une méthodologie pour créer la trajectoire de l'outil d'une machine-outil cinq axes sur la base de la technique de division spatiale qui incorpore des calculs de proximité progressifs entre des surfaces de conception et celles usinées. Kim et Kim [Kim et Kim 1993] ont présenté un concept de trajectoire d'outil paramétrique pour produire la trajectoire précise de l'outil pour l'usinage de pièces sculptées. Leu et al. ont développé une

méthodologie pour vérifier la trajectoire de l'outil en fonction de la déflexion de l'outil [Leu et al 1997, Leu et al 1998]. Frey [Frey et al 1997] a développé un concept dans lequel un volume balayé est défini par les fonctions du mouvement et de la forme de l'outil. Le travail de Frey correspond à une catégorie d'outils dont la forme peut être produite à partir d'une surface de révolution. Cette méthode ne produit pas de volume d'usinage précis puisque le volume d'usinage est produit à partir de l'opération de balayage d'une surface de révolution menée par une courbe directrice qui ne peut pas coïncider avec la trajectoire d'outil afin de produire le même volume. Donc, en fonction du type de courbe paramétrique utilisée pour produire la courbe directrice, la précision des surfaces générées peut changer. Nous ne pouvons pas utiliser cette méthode pour une pièce complexe parce qu'il n'y a aucune base mathématique pour créer un volume exact quand les trajectoires d'outil se croisent. Ces travaux sont utiles pour l'opération de rectification puisque l'outil dans ce type d'opération est une surface de révolution.

Dans le travail présent, nous portons notre attention sur la prédiction des erreurs dimensionnelles résultantes des erreurs géométriques d'une machine-outil multi-axes pour une opération. Nous considérons l'influence de l'état géométrique des machines-outils, le processus choisi et la tolérance imposée sur la précision d'une pièce usinée.

CHAPITRE 2: SYNTHÈSE

2.1 Identification des erreurs de machine-outil

Le but est d'identifier les erreurs géométriques des membrures ainsi que les erreurs de mouvement des machines-outils à cinq-axes. Pour cela nous utilisons la cinématique de corps rigide pour générer le Jacobien d'identification qui définit l'effet des sources d'erreurs sur la pose de l'outil par rapport à la pièce. Nous obtenons l'information en utilisant une barre à billes télescopique.

2.1.1 La machine-outil et le modèle d'erreur

Dans le domaine de la machine-outil, nous pouvons définir deux familles de paramètres d'erreurs géométriques: les paramètres d'erreurs géométriques indépendants de la position (PEGIP) et les paramètres d'erreurs géométriques dépendants de la position (PEGDP). Contrairement au PEGDPs, le PEGIPs ne varie pas pendant le mouvement de la machine. Des exemples de PEGIPs sont la perpendicularité, le parallélisme, la séparation d'axes rotoïdes et les erreurs au zéro (joint offset).

En général, le modèle cinématique d'une machine-outil peut être obtenu en attachant rigidement un repère pièce "w" à la table et un repère d'outil "t" au point d'attache d'outil. Du repère de base ou fondation F, nous définissons une branche d'outil (t = tool) et une branche de pièce (w = workpiece) employant leur matrice de transformation homogène (MTH), ${}^{F}\boldsymbol{T}_{t}$ et ${}^{F}\boldsymbol{T}_{w}$ respectivement. Le ${}^{i}\boldsymbol{T}_{j}$ dénote un MTH 4 x 4 qui représente la pose (la position et l'orientation) de repère i à un repère j. Alors, la pose de t relative à w est donnée comme suit:

$$ {}^{w}T_{t} = [{}^{F}T_{w}]^{-1} \cdot {}^{F}T_{t} \qquad (1) $$

La topologie ZFYXAC de machine-outil cinq-axes Matsuura MC-760VX est illustrée à la figure 2.1.

Figure 2.1 Machine-outil Matsuura à cinq axes.

Les coordonnées articulaires de la fraiseuse Matsuura sont définies comme θ = [z y x a c]^T. À θ = [0 0 0 0 0]^T les repères de tous les joints coïncident (voir la figure 2.2). Il peut aussi être noté que l'axe x (de vecteur unitaire *i*) du repère articulaire X est nominalement aligné avec l'axe x d'un repère articulaire A, et l'axe z du repère articulaire Z est nominalement aligné avec la broche pour toutes les valeurs de θ.

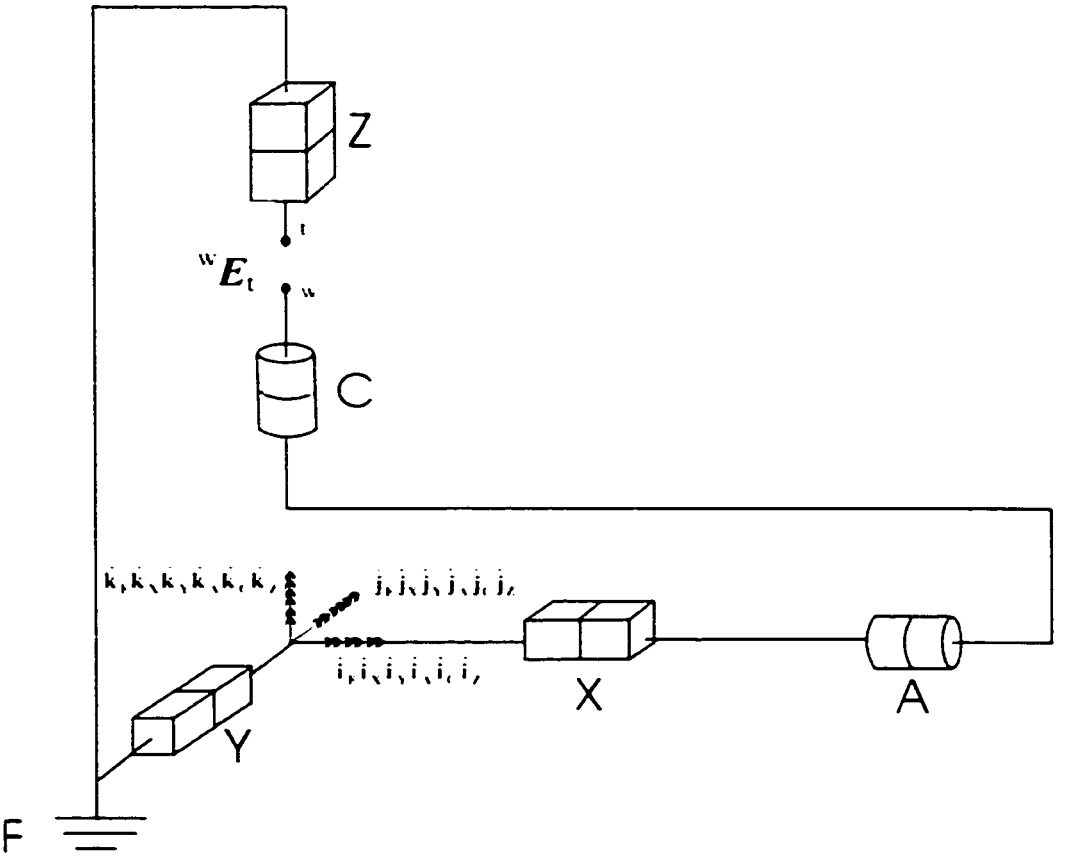

Figure 2.2 Repères articulaires pour des coordonnées articulaires nulles.

La MTH pour une membrure non-idéale incluant les valeurs nominales, les imperfections dans les membrures (PEGIPs) et les joints (PEGDPs) peut être modélisée en utilisant 3 MTHs (voir la figure 2.3).

$$\boldsymbol{D}_S = \boldsymbol{D}_{1S}\,\boldsymbol{D}_{2S}\,\boldsymbol{D}_{3S} \qquad (2)$$

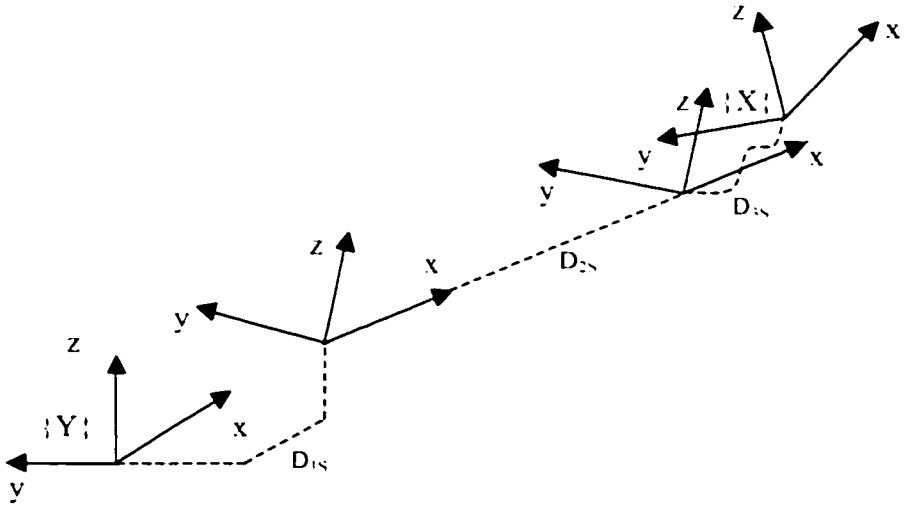

Figure 2.3 MTHs d'une combinaison membrure-joint d'axe {Y} à l'axe {X} avec erreurs.

$\boldsymbol{D}_{IS}$ est la membrure nominale MTH définie comme suit:

$$\boldsymbol{D}_{IS} = \boldsymbol{trans}(\dot{\mathbf{i}}, a_{X,S})\ \boldsymbol{trans}(\dot{\mathbf{j}}, a_{Y,S})\ \boldsymbol{trans}(\dot{\mathbf{k}}, a_{Z,S})\ \boldsymbol{rot}(\dot{\mathbf{k}}, \alpha_{Z,S})\ \boldsymbol{rot}(\dot{\mathbf{j}}, \alpha_{Y,S})\ \boldsymbol{rot}(\dot{\mathbf{i}}, \alpha_{X,S}) \qquad (3)$$

Où $\boldsymbol{trans}(\dot{\mathbf{i}}, a_{X,S})$ est une MTH pour une transformation linéaire par une valeur de $a_{X,S}$ le long de la direction $\dot{\mathbf{i}}$; $\boldsymbol{rot}(\dot{\mathbf{j}}, \alpha_{Y,S})$ est une MTH pour une rotation de $\alpha_{Y,S}$ autour de $\dot{\mathbf{j}}$; $\dot{\mathbf{i}}$, $\dot{\mathbf{j}}$ et $\dot{\mathbf{k}}$ sont des vecteurs unitaires; $a_{X,S}$, $a_{Y,S}$ *et* $a_{Z,S}$ sont les positions linéaires nominales; $\alpha_{X,S}$, $\alpha_{Y,S}$ et $\alpha_{Z,S}$ sont les positions angulaires nominales. Pour la machine-outil Matsuura, S représente Z, Y, X, A et C et tous les paramètres nominaux sont nuls. $\boldsymbol{D}_{2S}$ décrit le mouvement nominal du repère articulaire.

$\boldsymbol{D}_{2S}$ = ***trans***(**dir**.s) pour une articulaire prismatique; (4)

$\boldsymbol{D}_{2S}$ = ***rot***(**dir**.*s*) pour une articulaire rotoïde.

Pour une articulation prismatique **dir** est $\mathbf{i}$, $\mathbf{j}$ et $\mathbf{k}$ et s (la coordonnée articulaire) est x, y ou z, pour X, Y, Z respectivement. Tandis que pour un articulaire rotoïde ***dir*** est $\mathbf{i}$ pour A et $\mathbf{k}$ pour C et s est a ou c, l'angle de déplacement articulaire.

$\boldsymbol{D}_{3S}$ décrit les erreurs de forme du mouvement articulaire ou PEGDPs (voir la figure 2.4).

$$\boldsymbol{D}_{3S} = \mathbf{trans}(\mathbf{i}.e_{xS})\,\mathbf{trans}(\mathbf{j}.e_{yS})\,\mathbf{trans}(\mathbf{k}.e_{zS})\,\mathbf{rot}(\mathbf{k}.\gamma_{zS})\,\mathbf{rot}(\mathbf{j}.\gamma_{yS})\,\mathbf{rot}(\mathbf{i}.\gamma_{xS}) \qquad (5)$$

Où e_{xS}, e_{yS}, e_{zS} sont les erreurs de déplacement le long du S^{eme} joint et γ_{xS}, γ_{yS}, γ_{zS} sont les erreurs angulaires (roulis, tangage et lacet) le long du joint (voir la figure 2.3 et 2.4). Tous les termes d'erreur du mouvement articulaire sont calculés comme des fonctions de la position et seront définis par des polynômes.

$\boldsymbol{D}_S$ sera utilisé pour calculer la résultante des erreurs de positionnement pour n'importe quelle machine multi-axes avec une combinaison arbitraire d'articulations rotoïdes et prismatiques. Notez qu'un tel modèle utilise un nombre excédentaire de paramètres.

L'outil et la pièce sont modélisés via des MTHs constantes $\boldsymbol{T}_t$ et $\boldsymbol{T}_w$ respectivement. La branche pièce place le repère de la pièce tandis que la branche d'outil place le repère de bout d'outil, tous les deux dans le repère de base F. À cause des diverses erreurs décrites de la machine, le bout d'outil actuel et la pièce ne coïncident pas. Cette erreur ${}^{w}\boldsymbol{E}_t$ (voir la figure 2.2) est calculée comme suit:

la branche d'outil est donnée par,

$${}^{F}\boldsymbol{T}_t = \boldsymbol{D}_z\,\boldsymbol{T}_t \qquad (6)$$

et la branche de pièce est

$${}^{F}\boldsymbol{T}_w = \boldsymbol{D}_S\,\boldsymbol{D}_x\,\boldsymbol{D}_a\,\boldsymbol{D}_c\,\boldsymbol{T}_w. \qquad (7)$$

La chaîne cinématique complète peut être obtenue comme :

$$ {}^{F}\boldsymbol{T}_{t} = {}^{F}\boldsymbol{T}_{w} \; {}^{w}\boldsymbol{E}_{t} \tag{8} $$

et finalement :

$$ {}^{w}\boldsymbol{E}_{t} = [{}^{F}\boldsymbol{T}_{w}]^{-1} \; {}^{F}\boldsymbol{T}_{t} . \tag{9} $$

Les MTHs servent à générer la mesure virtuelle sur la machine-outil qui est utilisée pour l'étalonnage, et produire la matrice Jacobienne d'identification $\boldsymbol{J}$, qui exprime la sensibilité de ${}^{w}\boldsymbol{E}_{t}$ par rapport aux paramètres d'erreur.

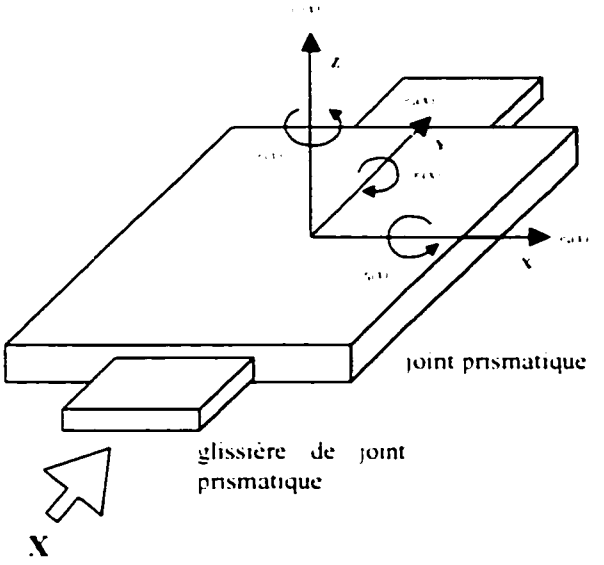

Figure 2.4 Les erreurs linéaires et angulaires le long de l'articulation X d'une machine-outil.

Ce modèle est utilisé à deux fins. La première est la prédiction d'erreurs pour une tâche d'usinage donnée. La seconde est pour la simulation de processus d'étalonnage par barre à billes. Elle permet alors la génération d'indications virtuelles pour une machine imparfaite.

2.1.2 Les fonctions polynomiales

Pour une machine-outil typique à cinq-axes (3 axes prismatiques et 2 axes rotoïdes), il y a 30 (5×6) erreurs géométriques variables mentionnées ci-dessus et 8 constantes incluant une erreur de perpendicularité entre les axes Y et X; deux erreurs d'alignement entre l'axe A et les X et Y; un biais angulaire pour l'axe A; une erreur de perpendicularité entre les axes C et A; une distance axe à axe articulaire entre A et C et finalement deux erreurs de perpendicularité pour l'axe Z [Mayer et al. 2000].

Dans ce travail, nous présentons le comportement d'erreurs de composants sur la machine-outil comme des fonctions polynomiales pendant leurs mouvements le long du guide. Cela signifie que ces erreurs, pour une position donnée, peuvent être calculées une fois que les coefficients de polynôme correspondants ont été identifiés.

Pour représenter le mouvement de composant de machine-outil, le polynôme de Chebychev [Rivlin 1974] est choisi. Ce polynôme a des caractéristiques orthogonales et peut produire un meilleur nombre de conditionnement pour le Jacobien d'identification, réduisant ainsi l'impact du bruit de mesure expérimental sur la solution. La forme générale du polynôme de Chebychev est :

$$T_n(x) = \cos n? \tag{10}$$

où n est un entier non-négatif, $x=\cos\theta$ et $0 \le ? \le p$. $T_n(x)$ est défini dans l'intervalle $-1 \le x \le 1$. Le polynôme Chebychev de 3eme degré est utilisé dans ce travail et il est défini comme suit:

$$p(x) = c_0T_0 + c_1T_1 + c_2T_2 + c_3T_3. \tag{11}$$

où

$$
\begin{aligned}
T_0(x) &= 1 \\
T_1(x) &= x \\
T_2(x) &= 2x^2 - 1 \\
T_3(x) &= 4x^3 - 3x
\end{aligned}
\qquad (12)
$$

Et c_0, c_1, c_2, c_3 sont les coefficients.

Les coefficients des polynômes pour tous les paramètres d'erreur seront calculés dans la procédure d'identification d'erreur.

2.1.3 Procédure de mesure

Un programme est développé pour simuler la mesure sur une machine-outil cinq axes en utilisant la barre à billes. La figure 2.5a montre la barre à billes télescopique à deux billes. La barre à billes sera installée sur la machine telle qu'une bille est placée sur la table et l'autre attachée à la broche (voir la figure 2.5b). En utilisant la barre à billes, les mesures sont limitées à la mesure de la distance entre les deux centres des billes. Quand une commande est donnée à la machine d'aller à une position, la barre à billes indique la distance mesurée et supposée exacte entre le repère de l'outil et la pièce. En pratique les erreurs de mesure d'une barre à billes sont très petites, étant de l'ordre de 0,5 µm. Cette erreur a été aussi considérée comme négligeable pour le présent travail. Cette information peut être calculée à partir du modèle actuel (quand les paramètres d'erreur sont présentés dans le modèle) de machine-outil. De plus, la distance nominale entre ces deux points peut aussi être calculée en utilisant le modèle nominal de la machine-outil. Ces données seront obtenues pour un nombre suffisant de configurations. Le nombre de configuration dépend du nombre de coefficients de tous les polynômes et le nombre d'erreurs de PEGIPs pour l'étalonnage.

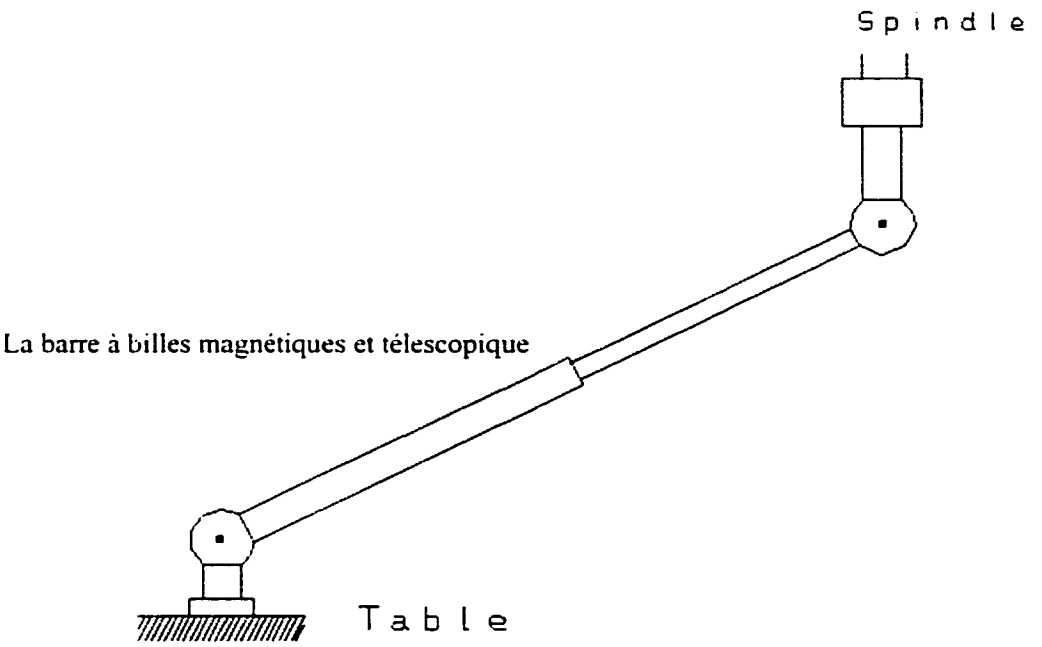

Figure 2.5a Une barre à billes télescopique employée pour l'acquisition de données.

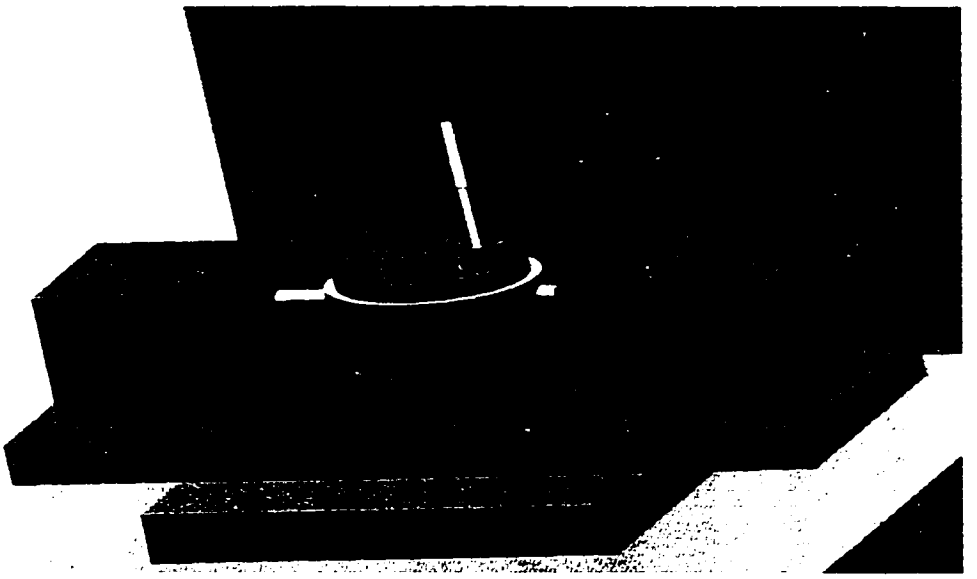

Figure 2.5b Installation de la barre à billes sur la machine-outil.

2.1.4 Génération de la matrice d'observation

Comme mentionnée plus tôt, une des applications des MTHs est de créer la matrice Jacobienne d'identification dont les éléments sont formés par les éléments de la matrice de transport qui elle-même est une fonction de la matrice de transformation homogène. Le rôle de la matrice de transport est de transformer le torseur d'erreurs $[e_x\ e_y\ e_z\ \gamma_x\ \gamma_y\ \gamma_z]^T$ de l'origine à la fin d'un composant, ou de l'origine d'un repère à l'origine d'un autre repère [Craig 1989, Cloutier et Mayer 1999, Hayati 1998] comme on peut le voir dans l'équation ci-dessous:

$$ {}^{\{B\}}\boldsymbol{dt}_B = {}^{B}_{A}\boldsymbol{C}\,{}^{\{A\}}\boldsymbol{dt}_A \tag{13} $$

$$ \text{si } {}^{A}_{B}\boldsymbol{T} = \begin{bmatrix} {}^{A}_{B}\boldsymbol{R} & {}^{\{A\}A}\boldsymbol{P}_B \\ 000 & 1 \end{bmatrix} \quad \Rightarrow \quad {}^{B}_{A}\boldsymbol{C} = \begin{bmatrix} {}^{A}_{B}\boldsymbol{R}^T & {}^{A}_{B}\boldsymbol{R}^T\left[{}^{\{A\}A}\boldsymbol{P}_B \times\right]^T \\ O & {}^{A}_{B}\boldsymbol{R}^T \end{bmatrix}. \tag{14} $$

La matrice Jacobienne lie les données obtenues par la barre à billes avec les sources d'erreurs. La signification des symboles de ces équations est présentée dans les articles qui se trouvent dans les chapitres 3 et 4. La formule correspondante est :

$$ \left[{}^{\{t\},f}\boldsymbol{t}_t\right] = \left[{}^{\{t\},f}_{t}\boldsymbol{J}\right]\cdot[\boldsymbol{dP}] \tag{15} $$

Le Jacobien représente la sensibilité des données obtenues par la barre à billes aux sources d'erreurs géométriques de la machine-outil. Il est développé sur la base de la topologie de la machine-outil, de sa géométrie, des positions articulaires et des fonctions polynomiales. L'équation (15) permet de calculer les erreurs de bout d'outil par rapport à la pièce exprimées sur le repère outil. ${}^{\{t\},f}\boldsymbol{t}_t$ est une matrice colonne (6m)-par-1. ${}^{\{t\},f}_{t}\boldsymbol{J}$ est le Jacobien avec 6m-par-n éléments et $\boldsymbol{dP}$ est le vecteur du paramètre d'erreur n-par-1. Dans cette équation, f représente le "feature" et t représente l'outil ("tool"). Le nombre de poses et de paramètres sont représentés par m et n respectivement.

Chaque colonne de cette matrice est associée à un des paramètres d'erreur de la machine-outil. Cependant, certaines colonnes n'ont pas de conséquences sur les erreurs de la

machine-outil puisqu'elles sont utilisées pour représenter des paramètres de fixation de la barre à billes. Donc, les colonnes correspondantes sont inutiles et doivent être enlevées de la matrice d'observation. Puisque chaque paramètre d'erreur de composants est présenté comme une fonction polynomiale de degré 3, chacun sera représenté par 4 coefficients. Ainsi, chacune de ces colonnes sera étendue d'une quantité correspondante au nombre de coefficients.

2.1.5 Procédure d'identification des erreurs

Puisque nous avons l'information de la machine-outil à partir des données obtenues par la barre à billes, les paramètres d'erreurs peuvent être calculés à partir de l'équation (15). Dans cette équation, $^{[1]}\boldsymbol{t}$, est le résultat de mesure de la barre à billes en une matrice colonne et $\boldsymbol{J}$ est une matrice non-carrée. Cette équation est linéaire. De plus, due à la matrice $\boldsymbol{J}$, la théorie de l'inverse généralisé [Noble et Daniel, 1977] a été appliquée pour identifier les paramètres $\boldsymbol{dP}$:

$$\boldsymbol{dP} = \boldsymbol{J}^{+} \cdot \boldsymbol{t} \tag{16}$$

où $\boldsymbol{J}^{+}$ est appelé l'inverse généralisé de Moore-Penrose de $\boldsymbol{J}$ qui peut être calculé à partir de la décomposition aux valeurs singulières (SVD pour "Singular Value Decomposition"):

$$\boldsymbol{J}^{+} = \boldsymbol{V}\boldsymbol{S}^{+}\boldsymbol{U}^{\mathrm{T}} \tag{17}$$

Pour diminuer l'influence des erreurs de mesure de $\boldsymbol{\tau}$ sur $\boldsymbol{\delta P}$ dans l'équation (16), nous devons produire une matrice $\boldsymbol{J}$ ayant un petit nombre de conditionnement c($\boldsymbol{J}$) [Noble et Daniel, 1977], où:

$$c(\boldsymbol{J}) = \|\boldsymbol{J}\| . \|\boldsymbol{J}^{-1}\| \tag{18}$$

$$\|\boldsymbol{J}\|_1 = \max_{1 \le j \le m} \sum_{i=1}^{m} |a_{ij}| . \tag{19}$$

2.2 Prédiction de la performance de machines-outils et vérification de la trajectoire d'outil.

Une évaluation de la qualité des pièces produites peut être faite par la prédiction d'erreurs et la vérification de la trajectoire d'outil et du volume qui sera enlevé sur la pièce. Pour faire cela, un fichier d'exigences de processus est produit sur la base de la gamme de fabrication. Ce fichier contient l'information détaillée sur la géométrie nominale de la pièce, le type de processus, la position, la taille et la tolérance des caractéristiques à usiner et aussi la position, la forme et la dimension de l'outil coupant. Ensuite la trajectoire nominale de l'outil peut être produite directement d'un système de CAO/FAO. Cette trajectoire est modifiée en considérant les erreurs identifiées de la machine-outil à ces positions. Le volume généré après chacune de ces trajectoires (trajectoire nominale et trajectoire réelle) mène à deux surfaces différentes nommées surface nominale et surface réelle. Les formes nominale et actuelle sont comparées et le résultat évalué selon la précision désirée de la pièce. Cette analyse aide le gammiste à choisir la machine-outil appropriée pour le processus choisi. Une procédure de compensation pourrait alors être suggérée pour améliorer la trajectoire actuelle de l'outil afin de produire le volume dans la tolérance souhaitée.

2.3 Procédure de simulation, résultats et vérification

Une BBMT (barre à billes magnétique et télescopique) d'une longueur médiane de 13 "(L=13") a été employée pour mesurer la position relative de l'outil par rapport à la pièce d'une machine-outil cinq-axes (voir la figure 2.5a et 2.5b). Une série de configurations a été utilisée dans la zone de travail de la machine-outil et la distance entre la broche et la pièce est restée aux environs de L. La trajectoire circulaire n'a pas été utilisée.

Pour chaque configuration, la position relative de l'outil par rapport à la table a été calculée pour deux cas: a) en absence d'erreurs sur les composants de la machine-outil pour calculer ${}^{w}\boldsymbol{E}_{t}^{\text{prédit}}$, b) et en présence d'erreurs sur les composants de machine-outil

pour calculer ${}^{w}\boldsymbol{E}_{t}^{reel}$ La différence entre ces deux matrices est l'erreur de pose causée par les imperfections géométriques de la MOCN.

Pour chaque pose une ligne de la matrice Jacobienne d'identification sera produite. Ensuite une matrice Jacobienne d'identification sera générée en utilisant l'analyse mathématique de la matrice.

Un ancrage simple de la barre à billes est employé pour acquérir l'information de la machine-outil pour l'identification des PEGIPs. La méthode de trois-ancrages ou trois montages séparés (figure 4.9) est utilisée pour acquérir l'information de la machine-outil pour l'identification de PEGDPs. Le nombre de configurations pour chaque cas dépend du nombre de paramètres à identifier et aussi du nombre de conditionnements de la Jacobienne.

Les données acquises par la barre à billes et la Jacobienne d'identification sont utilisées pour évaluer les paramètres d'erreur en solutionnant un système d'équations linéaires. Les termes connus dans ce système sont les différences entre les longueurs de la barre à billes prévues et mesurées et la matrice de Jacobienne. Les paramètres identifiés sont alors employés pour prédire l'erreur de position de bout d'outil versus la pièce par le modèle cinématique direct incorporant l'effet des erreurs géométriques. Cette procédure nous aidera à prédire la performance de la machine-outil. Les résultats de la simulation pour identifier les PIGEPs et PDGEPs ainsi que la procédure de vérification sont expliqués aux chapitres 3 et 4.

2.4 Organisation de la thèse

La thèse a été rédigée essentiellement sur la base d'articles scientifiques. Le chapitre 1 présente la revue de littérature. Le chapitre 2 donne une vue générale de la problématique concernant le besoin d'une gamme de fabrication valide ainsi que le besoin d'avoir des machines pour produire des pièces de précision.

Le chapitre 3 présente la méthodologie d'identification des PEGIPs sur une machine-outil à cinq axes. Ces paramètres constants sont les mauvais alignements articulaires et la séparation d'axes rotoïdes. Le concept utilise une barre à billes télescopique pour identifier les sources d'erreurs géométriques d'une machine-outil à cinq axes. On propose un certain nombre de critères pour vérifier si les paramètres identifiés prédisent bien le comportement non-idéal de la machine.

Le Chapitre 4 présente une méthodologie d'identification et une procédure de simulation pour identifier les erreurs dues aux inexactitudes géométriques des composants de la machine-outil pendant leur mouvement (soit les PEGDPs). Ces sources d'erreur sont individuellement modélisées comme des fonctions polynomiales de la coordonnée articulaire individuelle de la machine-outil. Les données essentielles ont été acquises à l'aide de la barre à billes.

Le chapitre 5 présente un concept pour prévoir les erreurs de l'outil versus la position de la pièce résultant des sources d'erreurs géométriques PEGIP/PEGDP pour une tâche d'usinage donnée. La prédiction de la performance de la machine-outil pour exécuter une tâche spécifique est évaluée par l'analyse de deux versions des positions de bout d'outil (CL = cutter location) d'une courbe ou d'une surface. La première version est le produit d'un système de CAO/FAO et la deuxième considère les erreurs de machine-outil identifiées. Une méthodologie est aussi présentée pour intégrer cet outil dans un système de GAO.

Une conclusion générale et des recommandations pour le travail futur sont présentées à la fin de la thèse.

CHAPITRE 3: THEORY AND SIMULATION FOR THE IDENTIFICATION OF THE LINK GEOMETRIC ERRORS FOR A FIVE AXIS MACHINE TOOL USING A TELESCOPING MAGNETIC BALL-BAR

Y. A. MIR, J.R.R. MAYER*, G. CLOUTIER, and C. FORTIN

Mechanical Engineering Department
Ecole Polytechnique de Montréal

Submitted in June 2001, to the International Journal of Production Research
*To whom correspondence should be addressed: rene.mayer@meca.polymtl.ca

3.1 Présentation du chapitre et liens utiles

Dans ce chapitre les paramètres d'erreurs géométriques indépendants de la position d'une machine-outil sont présentés. Une approche systématique, pour identifier certaines de ces erreurs sur une machine-outil à cinq axes a été élaborée. Une méthode basée sur l'analyse mathématique des singularités de systèmes linéaires est utilisée pour aider à choisir une série minimale mais suffisante de paramètres d'erreur pour l'étalonnage d'une machine-outil. Une série de 8 paramètres d'erreurs de machine a été choisie parmi un potentiel de 30 paramètres. On propose un certain nombre de critères pour vérifier que les paramètres identifiés prévoient exactement les erreurs de position de la machine réelle. Finalement on montre l'efficacité numérique de cette méthode par des simulations.

3.2 Abstract

The position invariant geometric inaccuracies of a machine tool are the first to influence the quality of machined parts. A systematic approach is presented to identify some of these errors on a five-axis machine tool. The methodology is applied to the link error parameters such as joint misalignments, angular offset and rotary axis separation distance. A method based on the mathematical analysis of singularities of linear systems is used to assist in selecting a minimal but sufficient set of link error parameters for the calibration of a machine tool. A number of criteria are proposed in order to verify that the identified parameters accurately predict the positioning errors of the true machine. Finally the numerical effectiveness of this method is shown through simulations.

Keywords: Five-axis machine tool, geometric errors, calibration, telescoping magnetic ball bar, link errors identification.

3.3 Introduction

A five-axis machine tool has the ability to simultaneously position and orient its cutting tool in some co-ordinate system defined in the workspace. This is what makes such a machine tool so versatile. With an increasing need for machined components with growing geometric complexity and high dimensional accuracy, the demands on five-axis CNC machine tools has been steadily increasing. Other advantages of five-axis machines include (Trankle 1980): (a) good geometric accommodation of the location of cutter relatively to the surface of the workpiece; (b) technically correct alignment of the cutter along its milling path; and (c) a small number of jigs, fixtures and especially set-ups.

The geometric deviations of a machined workpiece are due in part to errors in the machine tool structure, and also to the effects occurring during the machining process. Not only do the identification of machine tool errors and the prediction of its performance help the process planners select an appropriate machine for specific

operations during process plan development, it can also be used for error compensation. Research on CNC machines shows (Shin et al. 1991) that such complex surface may deteriorate substantially even in an ideal environment. This demonstrates the necessity for characterisation on a regular basis to ensure or assess the performance of production machines. The importance of tracking and enhancing machine tool accuracy is well recognised due to the increasingly tight tolerance demands on machined parts.

Many parameters influence the positioning accuracy of machine tools. These can be divided into two main groups. The first group includes the position independent geometric error parameters (PIGEPs), also called link error parameters, such as joint misalignments, angular offsets and rotary axes separation errors which describe the relative location of the machine's successive rotary and prismatic joints. The second group is made of the position dependent geometric error parameters (PDGEPs), also called motion errors, describing the non-ideal motion of each joint, such as the scale error, straightness errors, yaw, pitch and roll of prismatic joints and the angular error, tilts, radial and axial errors of rotary joints.

Investigators have addressed the machine tool error identification problem from different perspectives. Rigid body kinematics is one of the most common used modelling techniques for machine tool error characterisation (Hocken et al. 1977, Donmez et al. 1986, Donmez et al. 1987, Duffie and Malmberg 1987). General homogenous transformation matrices (HTMs) are generally used to build the direct kinematic model since they can easily accommodate both link and motion error modelling. In contrast Kiridena and Ferreira (Kiridena and Ferreira 1993) used the Denavit-Hartenberg (D-H) method to construct the HTMs, and developed a model that showed the effects of the link errors PIGEPs on the pose accuracy (position and orientation) of the cutting tool relatively to the workpiece. The possible extension of the D-H method to motion error has not been documented.

Designed to measure many error parameters, methods, instruments and set-ups exist and are well documented, for example in the national standards (ASME B5.54 1992). However, such procedures are relatively involved in terms of equipment and operator expertise. On the other hand, much attention has been given over the past two decades or so to the use of much simpler devices to gather data, which are representative of the machine geometric status. One of the most popular devices is the telescoping magnetic ball bar (TMBB) (Bryan 1982, part I & II), which was intended to replace the circular comparison standards of the circular test for machine tools. Kunmann and Waldele (1983) used a fixed ball bar test to estimate the linear displacement errors and squareness error of a co-ordinate measurement machine (CMM). The effect of those error sources on the position errors of the CMM was formulated and estimated. The ball bar has been extensively used for three prismatic joint machine tools (Kakino et al. 1993), and allows the measurement of numerous quasi-static and dynamic parameters including all three squarenesses via circular test paths. However, its usefulness with five-axis machine tools has not yet been investigated.

In the field of robotics, Driels (1993) used a fixed-length ball bar to calibrate the PIGEPs of an industrial robot made of a single serial kinematic chain of six rotary joints. A modified D-H formulation was used to avoid the problem occurring with D-H modelling in the presence of nominally parallel rotary joint axes. Although it is widely accepted in the modelling of industrial robots, D-H modelling is rarely used in the field of machine tools.

In this paper a method is proposed based on the use of a single, low cost and widely accepted instrument amongst machine tool users, the TMBB, to identify the PIGEPs of a five-axis machine tool. In effect the TMBB offers the potential for a quick and efficient means of machine calibration even in five-axis machines. However, since the ball bar does not measure individual error parameters, but rather provides a "snapshot" of the effects of combined errors, a complete five-axis kinematic model must be used for the data analysis. The general modelling approach allowing up to 6 parameters per joint is

used instead of the modified D-H modelling approach. It has the advantage of having its joint frames follow the convention used for machine tool. Furthermore it does not have the numerical problems associated with the original D-H modelling approach when near parallel joints are present. However, it results in extraneous and redundant parameters thus requiring a strategy to reduce the number of parameters for calibration purposes. The paper describes a strategy based on the analysis of the size, rank, condition number and singular value decomposition of the sensitivity Jacobian matrix to assist in the removal of redundant parameters. This is followed by the calibration theory and simulation procedure. The simulations are conducted using the Matlab® language for a machine tool with a ZFYXAC topology (such as a Matsuura MC-760VX five-axis CNC).

3.4 Five axis machine tool forward geometric model

The kinematic model of a machine tool allows the calculation of the location of the tool relative to the part feature as a function of joint co-ordinate. From the base or foundation frame F we define a tool branch, which locates the tool t in the base frame F, and a workpiece feature branch, which locates the workpiece feature w in the base frame F. These branches are modelled using homogenous transformation matrices (HTM) ${}^{F}\boldsymbol{T}_{t}$ and ${}^{F}\boldsymbol{T}_{w}$ respectively. ${}^{i}\boldsymbol{T}_{j}$ denotes a 4-by-4 HTM representing the pose (position and orientation) of frame i with respect to frame j. The ZFYXAC topology of the Matsuura five axis machine tool is shown in figure 3.1. The joint co-ordinates of the machine are defined as $\boldsymbol{\theta} = [z\ y\ x\ a\ c]^{T}$. At $\boldsymbol{\theta} = [0\ 0\ 0\ 0\ 0]^{T}$ we define the reference frames of all joints so they nominally coincide with the intersection of axes A and C (see figure 3.2). This differs from the definition of the origin by the controller of the machine tool but serves the current purpose better, and simple zero offsets provide consistency between the two systems. Note that the x axis of the X joint frame (unit vector $\hat{\mathbf{i}}_{X}$) is nominally aligned with the x-axis of the A joint frame (unit vector $\hat{\mathbf{i}}_{A}$), and that the z-axis of the Z joint frame (unit vector $\hat{\mathbf{k}}_{Z}$) is nominally aligned with the spindle for all values of $\boldsymbol{\theta}$.

Each non-ideal link and nominal joint combination can be modelled using 3 HTMs (see Figure 3.3).

$$\boldsymbol{D}_S = \boldsymbol{D}_{1S}\,\boldsymbol{D}_{2S}\,\boldsymbol{D}_{3S} \tag{20}$$

Two link HTMs describe the nominal location and the location error between two successive joints.

$\boldsymbol{D}_{1S}$ is the nominal link HTM from the previous joint frame to the current S joint frame.

$$\boldsymbol{D}_{1S} = \boldsymbol{trans}(\mathbf{i}, a_{x,S})\,\boldsymbol{trans}(\mathbf{j}, a_{y,S})\,\boldsymbol{trans}(\mathbf{k}, a_{z,S})\,\boldsymbol{rot}(\mathbf{k}, \alpha_{z,S})\,\boldsymbol{rot}(\mathbf{j}, \alpha_{y,S})\,\boldsymbol{rot}(\mathbf{i}, \alpha_{x,S}) \tag{21}$$

where for example $\boldsymbol{trans}(\mathbf{i}, a_{x,S})$ produces a HTM of a linear translation by a value $a_{x,S}$ along the $\mathbf{i}$ direction; $\boldsymbol{rot}(\mathbf{j}, \alpha_{y,S})$ produces a HTM for a rotation of $\alpha_{y,S}$ around $\mathbf{j}$; $\mathbf{i}$, $\mathbf{j}$, and $\mathbf{k}$ are unit vectors; $a_{x,S}$, $a_{y,S}$ and $a_{z,S}$ give the nominal joint position; $\alpha_{x,S}$, $\alpha_{y,S}$ and $\alpha_{z,S}$ give the nominal joint orientation. For the target machine tool S represents Z, Y, X, A, and C and all nominal parameters are null.

$\boldsymbol{D}_{2S}$ describes the link imperfection due to the presence of the PIGEPs.

$$\boldsymbol{D}_{2S} = \boldsymbol{trans}(\mathbf{i}, e_{x,S})\,\boldsymbol{trans}(\mathbf{j}, e_{y,S})\,\boldsymbol{trans}(\mathbf{k}, e_{z,S})\,\boldsymbol{rot}(\mathbf{k}, \gamma_{z,S})\,\boldsymbol{rot}(\mathbf{j}, \gamma_{y,S})\,\boldsymbol{rot}(\mathbf{i}, \gamma_{x,S}) \tag{22}$$

where $e_{x,S}$, $e_{y,S}$, $e_{z,S}$, $\gamma_{x,S}$, $\gamma_{y,S}$ and $\gamma_{z,S}$ are the PIGEPs of the S link.

The joint HTM $\boldsymbol{D}_{3S}$ describes the nominal motion of the joint frame.

$$\boldsymbol{D}_{3S} = \boldsymbol{trans}(\text{dir}, s) \text{ for prismatic joint; } \boldsymbol{D}_{3S} = \boldsymbol{rot}(\text{dir}, s) \text{ for a rotary joint} \tag{23}$$

where for prismatic joints **dir** is $\mathbf{i}$, $\mathbf{j}$, or $\mathbf{k}$ and s (the joint co-ordinate) is x, y or z, for joints X, Y, or Z respectively. Whereas for rotary joints ***dir*** is $\mathbf{i}$ for joint A, and $\mathbf{k}$ for joint C, and s is a or c, the displacement angle.

$\boldsymbol{D}_S$ will be used to calculate the resultant positioning errors for any multi-axis machine with an arbitrary serial combination of rotary and prismatic joint. Note however that

such a model almost certainly contains redundant parameters, i.e. more parameters then are strictly necessary to describe the non-ideal machine links geometry.

Finally the tool and workpiece features are modelled via constant HTMs $\boldsymbol{T}_t$ and $\boldsymbol{T}_w$ respectively. Thus the tool branch is modelled by

$$^{F}\boldsymbol{T}_t = \boldsymbol{D}_Z\boldsymbol{T}_t \tag{24}$$

and the workpiece feature branch is modelled as

$$^{F}\boldsymbol{T}_w = \boldsymbol{D}_Y\boldsymbol{D}_X\boldsymbol{D}_Z\boldsymbol{D}_C\boldsymbol{T}_w. \tag{25}$$

The complete kinematic chain can be closed by defining a tool versus workpiece location HTM $^{w}\boldsymbol{T}_t$ as follows.

$$^{F}\boldsymbol{T}_t = {}^{F}\boldsymbol{T}_w \; {}^{w}\boldsymbol{T}_t \tag{26}$$

and finally:

$$^{w}\boldsymbol{T}_t = [{}^{F}\boldsymbol{T}_w]^{-1} \, {}^{F}\boldsymbol{T}_t. \tag{27}$$

In general $^{w}\boldsymbol{T}_t$ is simply the tool frame location observed from, and expressed in, the workpiece feature frame. If the joint co-ordinates used in equation (27) are at their nominal values, i.e those which would position and orient the tool to its desired location given a perfect machine geometry, then $^{w}\boldsymbol{T}_t$ present the position and orientation of tool on workpiece frame, otherwise it represent also the presence of link errors. The HTMs can be used to: a) generate simulated measurement data on the machine tool for its calibration, and b) generate the sensitivity Jacobian matrix $\boldsymbol{J}$, which expresses the sensitivity of $^{w}\boldsymbol{T}_t$ to the error parameters.

3.5 Sensitivity Jacobian matrix generation

From the nominal link definitions and joint co-ordinates, the sensitivity Jacobian matrix $\boldsymbol{J}$ is obtained using the Newton-Euler equation. The sensitivity Jacobian matrix is built using transport matrices. A transport matrix is generated using a HTM, and is used to

propagate the effect of an error twist $[e_x\ e_y\ e_z\ \gamma_x\ \gamma_y\ \gamma_z]^T$ occurring at frame A onto another frame B rigidly connected to frame A as follows :

$$ {}^{\{B\}}\boldsymbol{dt}_B = {}^{B}_{A}\boldsymbol{C}\,{}^{\{A\}}\boldsymbol{dt}_A \tag{28} $$

where ${}^{\{B\}}\boldsymbol{dt}_B$ is an error twist in B, expressed in frame B, ${}^{\{A\}}\boldsymbol{dt}_A$ is an error twist in A, expressed in frame A, and ${}^{B}_{A}\boldsymbol{C}$ is a 6×6 transport matrix (Craig 1989, Cloutier and Mayer 1999). The transport matrix ${}^{B}_{A}\boldsymbol{C}$ can be formed using HTM ${}^{B}_{A}\boldsymbol{T}$ as follows:

$$ {}^{B}_{A}\boldsymbol{C} = \begin{bmatrix} {}^{A}_{B}\boldsymbol{R}^T & {}^{A}_{B}\boldsymbol{R}^T\left[{}^{\{A\}}{}^{A}\boldsymbol{P}_B \times\right]^T \\ 0_{3\times3} & {}^{A}_{B}\boldsymbol{R}^T \end{bmatrix} \tag{29} $$

where ${}^{A}_{B}\boldsymbol{R}$ and ${}^{\{A\}}{}^{A}\boldsymbol{P}_B$ can be extracted from the following

$$ {}^{A}_{B}\boldsymbol{T} = \begin{bmatrix} {}^{A}_{B}\boldsymbol{R} & {}^{\{A\}}{}^{A}\boldsymbol{P}_B \\ 000 & 1 \end{bmatrix}. \tag{30} $$

For example for a ZFYXAC machine (see figure 3.2), the sensitivity Jacobian matrix, ${}^{\{T\}}_{T}\boldsymbol{J}$ representing the sensitivity of the tool-tip versus workpiece feature location to the machine tool geometric errors parameters is expressed as:

$$ {}^{\{T\}}_{T}\boldsymbol{J} = \left[-{}^{T}_{F}\boldsymbol{C}\,{}^{F}_{T}\boldsymbol{C}^{-1}\,{}^{\{T\},F}_{T}\boldsymbol{J} \quad {}^{\{T\},F}_{T}\boldsymbol{J}\right] \tag{31} $$

where

$$ {}^{\{T\},F}_{T}\boldsymbol{J} = \left[{}^{T}_{F}\boldsymbol{C} \quad {}^{T}_{Y}\boldsymbol{C} \quad {}^{T}_{X}\boldsymbol{C} \quad {}^{T}_{A}\boldsymbol{C} \quad {}^{T}_{C}\boldsymbol{C} \quad {}^{T}_{A}\boldsymbol{C} \quad {}^{T}_{T}\boldsymbol{C}\right|_{6\times(1+6)} \tag{32} $$

$$ {}^{\{T\},F}_{T}\boldsymbol{J} = \left[{}^{T}_{F}\boldsymbol{C} \quad {}^{T}_{Z}\boldsymbol{C} \quad {}^{T}_{A}\boldsymbol{C} \quad {}^{T}_{T}\boldsymbol{C}\right|_{6\times(1+6)} \tag{33} $$

and

$$ {}^{F}_{T}\boldsymbol{C}^{-1} = {}^{F}_{T}\boldsymbol{C} \tag{34} $$

In equation (32), ${}^{\{T\},F}_{T}\boldsymbol{J}$ propagates the effects of all error twists occurring in the feature branch , ${}^{T}_{T}\boldsymbol{C}$ is $I_{6\times6}$, and other elements of this equation are calculated as follows:

$$
\begin{aligned}
{}^{W}_{I}\boldsymbol{C} &= {}^{F}_{I}\boldsymbol{C}\cdot{}^{W}_{F}\boldsymbol{C}\\
{}^{C}_{W}\boldsymbol{C} &= {}^{W}_{I}\boldsymbol{C}\cdot{}^{C}_{W}\boldsymbol{C}\\
{}^{A}_{C}\boldsymbol{C} &= {}^{C}_{I}\boldsymbol{C}\cdot{}^{A}_{C}\boldsymbol{C}\\
{}^{B}_{A}\boldsymbol{C} &= {}^{A}_{I}\boldsymbol{C}\cdot{}^{B}_{A}\boldsymbol{C}\\
{}^{Y}_{B}\boldsymbol{C} &= {}^{B}_{I}\boldsymbol{C}\cdot{}^{Y}_{B}\boldsymbol{C}\\
{}^{T}_{F}\boldsymbol{C} &= {}^{Y}_{I}\boldsymbol{C}\cdot{}^{T}_{F}\boldsymbol{C}
\end{aligned}
\qquad (35)
$$

The $\boldsymbol{C}$ matrices in equation (31) are used for combining the tool and feature branches. In equation (33), ${}^{[t],F}_{t}\boldsymbol{J}$ propagates the effects of all error twists in the tool branch, ${}^{T}_{t}\boldsymbol{C}$ is $I_{6\times6}$ (a 6×6 identity matrix), and other elements of this equation are calculated as follows:

$$
\begin{aligned}
{}^{S}_{T}\boldsymbol{C} &= {}^{T}_{t}\boldsymbol{C}\cdot{}^{S}_{T}\boldsymbol{C}\\
{}^{Z}_{S}\boldsymbol{C} &= {}^{S}_{T}\boldsymbol{C}\cdot{}^{Z}_{S}\boldsymbol{C}\\
{}^{F}_{Z}\boldsymbol{C} &= {}^{Z}_{S}\boldsymbol{C}\cdot{}^{F}_{Z}\boldsymbol{C}
\end{aligned}
\qquad (36)
$$

Finally the tool error twist relative to the feature frame and expressed in the tool frame caused by small values of all potential position independent geometric error parameters can be approximated by a linear system as follows:

$$
{}^{[t],F}\boldsymbol{dt}_{t} = {}^{[t],F}\boldsymbol{J}_{t}\cdot\boldsymbol{dP} \qquad (37)
$$

3.6 Complete and Minimal Set of PIGEPs

There are potentially 42 PIGEPs for modelling a five-axis machine tool in order to predict the pose error of the tool with respect to the workpiece feature. There are 6 PIGEPs per axis, 6 error parameters for positioning and orienting a part on the table, and finally 6 error parameters for positioning and orienting the tool in the spindle. These error parameters are listed in table 3.1.

Although complete in the sense that it can represent any real geometric condition of a machine, this set of parameters is not minimal in the sense that it does not use the minimum number of error parameters necessary and sufficient. Its use would lead to a numerically ill-conditioned system (and thus unidentifiable). This is supported by the

widely accepted equation for serial chains (Everett and Hsu 1988, Everett and Suryohadiprojo 1988)

$$n = 4r + 2p + 6 \tag{38}$$

where n is the number of independent model parameters, and r and p are the number of rotary and prismatic joints respectively. In the present context n becomes the minimum number of PIGEPs required to fully describe the tool versus workpiece pose error. For most 5-axis machine tools, $p = 3$ and $r = 2$ yielding $n = 20$. This total can be confirmed by direct construction of the machine model. Let start building the machine with the Y-joint. It requires no parameter as it is the only joint so far. Then let's add the X-joint which moves along $\hat{\mathbf{i}}_Y$ which is nominally perpendicular to the Y-joint or $\hat{\mathbf{j}}_Y$ and so requires a single perpendicularity error parameters, $\gamma_{Z,X}$, with respect to z axis of the Y-joint, $\hat{\mathbf{k}}_Y$ (itself imposed perpendicular to the Y-axis and X-axis). Then let's add the A-joint which is nominally perpendicular to $\hat{\mathbf{j}}_X$ and $\hat{\mathbf{k}}_X$ (or nominally parallel to $\hat{\mathbf{i}}_Y$) and so requires $\gamma_{Y,A}$ and $\gamma_{Z,A}$. The A-joint also requires an angular offset which is the non-alignment of $\hat{\mathbf{k}}_Y$ and $\hat{\mathbf{k}}_X$ and the associated parameter $\gamma_{X,A}$. The C-joint axis of rotation is nominally perpendicular to $\hat{\mathbf{i}}_A$ and so requires $\gamma_{Y,C}$. Also, the C-joint axis nominally intersect the A-joint axis and so requires $e_{Y,C}$. Finally, the Z-axis is nominally perpendicular to $\hat{\mathbf{j}}_Y$ and $\hat{\mathbf{i}}_X$ and requires $\gamma_{X,Z}$ and $\gamma_{Y,Z}$. In summary, the 8 link error parameters are (in the case of the ZFYXAC machine topology) 1 squareness error between the X and Y axes; 2 alignment errors between the A and X axes; 1 angular offset for the A axis; 1 squareness error between the C and A axes; 1 axis to axis distance between joints A and C and finally 2 squareness errors between the Z and the Y axes respectively. Finally there are 6 additional error parameters required to define the workpiece feature frame and another 6 for the tool frame (for a rotating tool, 5 parameters would suffice).

3.6.1 Strategy to select a complete and minimal set of parameters

A mathematical analysis of the $\boldsymbol{J}$ matrix, using its rank, condition number, and singular value decomposition guides the process of parameter selection in order to define a complete and minimal set.

The presence of redundant parameters leads to a singular $\boldsymbol{J}$ matrix that has columns which are linear combination of others. A singular value decomposition (SVD) based method is proposed to locate the mutually dependent columns (Noble, 1977) and select redundant parameters for their removal. A singular value decomposition of an m×n real matrix $\boldsymbol{J}$ is any factorisation of the form

$$\boldsymbol{J} = \boldsymbol{U}\boldsymbol{S}\mathrm{V}^{\mathrm{T}} \tag{39}$$

where $\boldsymbol{U}$ is an m×m orthogonal matrix, $\boldsymbol{V}$ is an n×n orthogonal matrix, and $\boldsymbol{\Sigma}$ is an m×n diagonal matrix, $\sigma_{ij} = 0$ if $i \neq j$ and $\sigma_{ij} = \sigma_i \geq 0$. The quantities σ_i are called the singular values of $\boldsymbol{J}$, and the columns of $\boldsymbol{U}$ and $\boldsymbol{V}$ are called the left and right singular vectors. Here m is the total number of poses multiplies by 6 and n is the total number of parameters and is also the initial number of singular values.

Another useful property is the rank of $\boldsymbol{J}$, *rank*($\boldsymbol{J}$), which represents the maximum number of independent columns or the maximum number of independent parameters. It corresponds to the number of non-zero singular values. An m×n matrix with $m \geq n$ is said to be of full rank if *rank*($\boldsymbol{J}$) = n or rank deficient if *rank*($\boldsymbol{J}$) < n.

A redundant parameter can manifest itself in a number of ways in the $\boldsymbol{J}$ matrix:

1) Its associated column may be null showing no effect on the tool versus workpiece feature error.

2) Its associated column may be identical to one or more others.

3) Its associated column may be a linear combination of others, which means that the effect of a parameter can be exactly reproduced by a linear combination of these. These parameters then constitute a group of confounded parameters. Note that 1) and 2) are special cases of 3.

Finally the condition number of matrix $\boldsymbol{J}$ is:

$$\mathrm{Cond}(\boldsymbol{J}) = \frac{\sigma_{max}}{\sigma_{min}} \tag{40}$$

where σ_{max} and σ_{min} are the largest and smallest singular values of $\boldsymbol{J}$ respectively. If $\boldsymbol{J}$ is rank deficient, then $\sigma_{min} = 0$ and $Cond(\boldsymbol{J})$ is said to be infinite.

Using the notions of rank, condition number, size, and the SVD, we can analyse whether or not the matrix is singular, how many independent columns exist, what columns are dependent and to what degree.

3.6.2 Parameters selection procedure

In order to select the parameters of the complete and minimal model the authors analyse the position and orientation sensitivity to all machine parameters at 30 machine configurations. A configuration is specified by a set of joint co-ordinate values. The size of the sensitivity Jacobian matrix is 6m×42 (with in this case m = 30), its condition number is 1.91E+17 and its rank is 20, indicating that 22 error parameters are redundant. It was easily noted that many columns of matrix $\boldsymbol{J}$ were identical. Thus the parameters associated with these columns have identical effects on machine positioning errors, and therefore are perfectly confounded. The groups of confounded parameters are shown in table 3.3. In such cases, keeping one parameter of each group is sufficient. The last line of table 3.2 shows the parameters that are kept from each group. A total of 21 parameters were removed. The reduced $\boldsymbol{J}$ matrix has a condition number of 2.9E+16, a rank of 20, and a size of 180×21. As can be seen in table 3.2, from the group of

confounded parameters we retained those parameters associated with the workpiece and tool, since the observed effect can be completely related to these parameters and not to machine imperfection. These selected parameters are $e_{x,t}$, $e_{y,t}$, $e_{z,t}$, $e_{z,w}$, and $\gamma_{z,t}$. Regarding the around-x group, from the group made of $\gamma_{x,z}$ and $\gamma_{x,y}$, $\gamma_{x,y}$ was eliminated since the y joint is the first joint of the workpiece branch and its direction defines the machine foundation y-axis. Thus we retained $\gamma_{x,z}$ which is one of the perpendicularity error of joint Z. For the other around-x group, $\gamma_{x,A}$ is the joint angle offset of the A rotary joint, and was selected because of it is a variable that is defined and adjustable in many machine controllers. For the around-y group, $\gamma_{y,z}$ is the other perpendicularity error of joint Z.

The remaining 21 error parameters are listed in table 3.3. The reduced $\boldsymbol{J}$ matrix has a condition number of 2.9E+16, and a rank of 20, so one error parameter is still redundant. A group of confounded parameters is found through a detail analysis of the last column of V (equation 39), that corresponding to the null singular value of the $\boldsymbol{J}$ matrix. This group of confounded parameters includes $\gamma_{z,C}$, $e_{x,w}$, $e_{y,w}$ and $\gamma_{z,w}$. Removing one of those confounded parameters eliminates the redundancy, and leads to a complete and minimal parameter set. The angular offset of the C-axis $\gamma_{z,C}$ is removed, since it is confounded with the workpiece location error parameters and so is defined during a set-up procedure prior to machining. Once this parameter is removed the size and rank of the sensitivity Jacobian matrix becomes 20, and the condition number dropped to 87. The reduced $\boldsymbol{J}$ matrix is now well conditioned since there is no redundant parameter and named reduced sensitivity Jacobian matrix $\boldsymbol{J}_r$. Amongst the remaining 20 parameters are the tool and part parameters, w and t, each requiring 6 error parameters. These are application dependent, and do not define machine PIGEPs. As a result, we now have 8 machine tool parameters, as listed in table 2.4, which – if known – completely determine the relative pose error of the tool with respect to the workpiece, that can result from any link geometric imperfections of the machine.

3.7 Calibration Procedure

3.7.1 Ball bar single setup method

The use of a commercial telescoping magnetic ball bar (TMBB) is planned to measure the distance between a point rigidly attached to the spindle and another rigidly attached to the workpiece table. Ball bar measurements are limited to the ball to ball length variation from a reference length. Therefore, the tool to workpiece position, obtained from equation (27), must be oriented along the ball bar axis. Effectively a feature ball frame is defined with its z-axis aligned with the ball bar measuring direction and the tool to workpiece positions are oriented into this frame using oriented matrix $\boldsymbol{R}$. The oriented matrix $\boldsymbol{R}$ is calculated as (see figure 3.4):

$$\begin{aligned} &\boldsymbol{R}=\boldsymbol{R}_1*\boldsymbol{R}_2 \\ &\boldsymbol{R}_1=\boldsymbol{rot}(\hat{\mathbf{k}}, \beta-90) \qquad \text{where } \beta=\text{atan2}(d_y, d_x) \text{ and} \\ &\boldsymbol{R}_2=\boldsymbol{rot}(\hat{\mathbf{i}}_1, -\gamma) \qquad \text{where } \gamma=\text{atan2}(d_{xy}, d_z). \end{aligned} \tag{41}$$

where d (in figure 3.4) is the distance between frames w and t, d_x, d_y, d_z are the Cartesian co-ordinates of frame t in frame w and d_{xy} is the oriented of d on the xy plan. $\boldsymbol{R}$ is used at the end of each branch to orient the feature and tool frame along the ball-bar axis. For example, the feature branch equation (25) changes to:

$${}^{F}\boldsymbol{T}_w = \boldsymbol{D}_Y\boldsymbol{D}_X\boldsymbol{D}_A\boldsymbol{D}_C\boldsymbol{T}_w\boldsymbol{R} \tag{42}$$

This effectively aligns one of the axes of the reference frame of expression of the translation components of the error twist with the ball bar axis. As a result, the new component corresponding to the aligned axis directly provides the virtual distance measurement of the TMBB. This will allow the generation of an identification Jacobian matrix where each line represents the effect of the machine parameters onto the ball to ball distance thus maintaining the availability of a linear system of equations. Having instead calculated the distance from the initial unaligned components (with the squares and square root operations thus required) would have not permitted the development of a

linear system. As will be shown later, the availability of a linear system greatly simplifies solving for the unknowns parameters.

For generating the ball bar measurement at each configuration, the position of the tool branch ball relative to the workpiece branch ball is calculated for two cases: a) with the machine tool parameters at their estimated values from which ${}^{w}\boldsymbol{T}_{t}^{predicted}$ is calculated, and b) for a true machine tool from which ${}^{w}\boldsymbol{T}_{t}^{true}$ is calculated. The difference between the ball to ball distances obtained from ${}^{w}\boldsymbol{T}_{t}^{true}$ and ${}^{w}\boldsymbol{T}_{t}^{predicted}$ respectively, represents the virtual measurement value for one configuration. These differences for all test configurations are concatenated vertically to form the measured data column matrix $\Delta \boldsymbol{b}$. The ball to ball distance is calculated directly from the norm of the translation vector contained within the HTMs ${}^{w}\boldsymbol{T}_{t}^{true}$ and ${}^{w}\boldsymbol{T}_{t}^{predicted}$.

A TMBB with a length of L = 13 is simulated (see figure 3.5a and 3.5b). A series of arbitrary configurations are selected in the workspace of the machine tool, which nominally maintain the ball bar length of L.

3.7.2 Identification Jacobian matrix

Because the TMBB does not detect the individual pose coordinates, it is essential to verify that all 8 machine PIGEPs as well as the six additional parameters that define the positions of the ball bar ends can be observed by the test procedure. The identification Jacobian matrix $\boldsymbol{J}_{I}$ propagates the effects of the PIGEPs onto the ball bar readings. The orientation in the direction of the ball-bar produces one line of the identification Jacobian matrix from six lines of the reduced sensitivity Jacobian matrix, $\boldsymbol{J}_{r}$, for each configuration.

3.7.3 Procedure simulation

The data acquired by the ball bar procedure and the identification Jacobian matrix is used to estimate the unknown error parameters by solving the following system of linear equations.

$$?\boldsymbol{b} = \boldsymbol{J}_{\mathrm{I}} \cdot \boldsymbol{dP}. \tag{43}$$

where $\Delta\boldsymbol{b}$ has m×1 elements, $\boldsymbol{J}_{\mathrm{I}}$ is the identification Jacobian matrix with m×n elements, and $\boldsymbol{dP}$ is the error parameter column matrix with n×1 elements. There are n = 14 unknown parameters (with 8 PIGEPs and 3 positioning errors for each ball position).

In order to reduce the effect of measurement noise, more configurations than are strictly necessary will be used resulting in an over-determined system for equation (43). The resulting $\boldsymbol{J}_{\mathrm{I}}$ matrix is rectangular, and a solution for $\boldsymbol{\delta P}$ can be obtained as follows:

$$\boldsymbol{dt} = \boldsymbol{J}_{\mathrm{I}}^{+} ?\boldsymbol{b} \tag{44}$$

where $\boldsymbol{J}_{\mathrm{I}}^{+}$ is the pseudo-inverse of $\boldsymbol{J}_{\mathrm{I}}$.

The known terms in this system are the differences between predicted and measured ball-bar lengths and the identification Jacobian matrix. Because equation (44) is a local linearisation, the Newton method (Ciarlet 1998) has been used to converge towards a solution for the unknown parameter values through an iteration procedure. The identified parameters are then used to predict the tool versus feature positioning errors using equation (27). The details of the calibration simulation procedure are illustrated in figure 3.6 and proceeds as follows:

1. Set the $\mathrm{PIGEP}_{\mathrm{ident}}$ to their nominal (null) values and all potential errors parameters PIGEPs (table 3.1) to their non null true values.
2. Calculate the difference between the true and the predicted ball bar lengths, $\Delta\boldsymbol{b}$, for all machine configuration used for the ball bar test using the true tool pose ${}^{w}\boldsymbol{T}_{t}^{\mathrm{true}}$ (calculated using PIGEPs) and the predicted one ${}^{w}\boldsymbol{T}_{t}^{\mathrm{pred}}$ (calculated using $\mathrm{PIGEP}_{\mathrm{ident}}$) in equation (27).
3. Generate the identification Jacobian matrix with $\mathrm{PIGEP}_{\mathrm{ident}}$ for all machine configuration used for the ball bar test .
4. Solve $\Delta\boldsymbol{b} = \boldsymbol{J}_{\mathrm{I}} \Delta\mathrm{PIGEP}$ and update $\mathrm{PIGEP}_{\mathrm{ident}} = \mathrm{PIGEP}_{\mathrm{ident}} + \Delta\mathrm{PIGEP}$

5. Repeat 2, 3 and 4 until ΔPIGEP is smaller than some convergence criteria compatible with the application context (e.g. simulation with or without noise on the data, virtual or real machine and data etc.)

3.7.4 Criteria of verification of the identified parameters

The following criteria are used to verify the usefulness of the solution for tool versus workpiece location error prediction:

1. If we impose non-zero values to the complete and minimal parameter set, are the identified parameters identical to the real parameters ?
2. If we impose non-zero values on all potential error parameters then is the calculated twist, representing the position and orientation of the tool relative to the workpiece identical for the true and identified parameters for configurations other than those used for the calibration procedure?

3.8 Simulation results

Thirty machine configurations (poses) were used for the identification. Another 60 configurations are used for verification group. Two simulation tests were conducted and the results are shown in table 3.5. In test A, error values are imposed to all potential machine PIGEPs. Errors are also added to the ball bar attachments. The identified PIGEPs are different from the true ones, as expected, due to redundancies amongst the parameters of the maximum and complete model. However, close inspection of the ball bar residuals and of the calculated pose, both for the calibration configurations and the verification groups, show that the identified model is functionally identical to the true one. In test B, only the complete and minimal parameter set have non-zero true errors. In this case, as anticipated, the identified error values are identical (accounting for computer resolution) to the true ones.

For both tests the generated effective identification Jacobian matrix has a rank of 14 and a conditioning number around 100, which is very satisfactory especially when noise is present on the data.

3.9 Conclusion

An approach has been proposed and simulated for the calibration of the position independent geometric error parameters (link errors) of a five-axis machine tool from data acquired using a telescoping magnetic ball bar. A five-axis machine tool kinematic model is developed using homogenous transforms, and incorporating the geometric errors. This model is used to generate the virtual measurements, sensitivity Jacobian matrix and predicted errors. The sensitivity Jacobian matrix quantifies the sensitivity of the tool-tip pose versus the workpiece to geometric error sources.

A complete and minimal set of 8 machine parameters is selected from the potential 30 parameters of the complete and maximal parameter set. This reduction process uses properties such as the size, rank and condition number of the sensitivity Jacobian matrix as well as its singular value decomposition to help pinpoint redundancies amongst parameters. Simulations conducted using specially written programs in Matlab® show that the parameters of the complete and minimal set are identified successfully thus supporting the use of a TMBB for the calibration of the link errors of a five axis machine tool.

Acknowledgements

This work was performed with the support of NSERC Grants N° 155677-98 and 36396-98, and its code used several functions from Matlab libraries built under NSERC Grants N° OGP0138478 and OGP0121639.

References

American Society of Mechanical Engineering, 1992, ASME B5.54, Methods for Performance Evaluation of Computer Numerically Controlled Machining Center.

BRYAN, J. B., 1982, A simple method for testing measuring machine and machine tools Part 1: Principles and applications. *Precision Engineering*, **4**(2).

BRYAN, J. B., 1982, A simple method for testing measuring machine and machine tools Part 2: Construction details. *Precision Engineering*, **4**(2).

CIARLET, P.G., 1998, Introduction à l'analyse numérique matricielle et à l'optimisation (Masson, ISBN 2100041673).

CLOUTIER, G., and MAYER, J. R. R., 1999, Modelisation de Machine en Fabrication Mecanique. Course offered in Mechanical Engineering Department, Ecole Polytechnique de Montreal.

CRAIG, J. J., 1989, Introduction to Robotics, Mechanics and Controls (Addison-Wesley, second Edition, ISBN 0201095289).

DONMEZ, M. A., BLOMQUIST, D. S., HOCKEN, R. J., LIU, C. R. and BARASH, M. M., 1986, A general methodology for Machine Tools Accuracy Enhancement by Error Compensation. *Precision Engineering*, Vol. **8**, No. **4**, pp. 187-196.

DONMEZ, M. A., LIU, C. R. and BARASH, M. M., 1987, A generalized Mathematical Model for Machine Tool Errors, Modeling, Sensing, and Controlling of Manufacturing Process. *ASME Winter Annual Conference*, PED-Vol. 23/DSC-Vol. 4, pp. 231-243.

DRIELS, M. R., 1993, Using Passive End-Point Motion Constraints to Calibrate Robot Manipulators. Trans. of the ASME, Vol. **115**, 560-566.

DUFFIE, N. A. and MALMBERG, S. J., 1987, Error Diagnosis and Compensation Using Kinematic Model and Position Error data. *Annals of CIRP*, Vol. 36, No. 1, pp. 355-358.

EVERETT, L. J. and HSU T.-W., 1988, The theory of kinematic parameter identification for industrial robots. *Transaction of ASME, Journal of Dynamic Systems, Measurement and Control*, **110**, pp. 96-100.

EVERETT, L. J. and SURYOHADIPROJO, A. H., 1988, A study of kinematic models for forward calibration of manipulators. *IEEE International Conference on Robotics and Automation*, pp. 798-800.

HOCKEN, R. J., SIMPSON, J. A, BORCHARDT, B., LAZAR, J., REEVE and C. STEIN, P., 1977, *Three Dimension Metrology*, *Annals of CIRP*, Vol. 26, No. 1, pp. 403–408.

KIRIDENA V. and FERREIRA P. M., 1993, Mapping the Effects of Positioning Errors on the Volumetric Accuracy of Five-axis CNC Machine Tools. *International Journal of Machine Tools & Manufacture*, V33, n3, pp. 417–437.

KUNMANN, H. and WALDELE, F., 1983, On Testing Coordinate Measuring Machines (CMM) with Kinematic Reference Standards (KRS). *Annals of CIRP*, Vol. 32(1).

KAKINO, Y., IHARA Y. and SHINOHARA, A., 1993, Accuracy Inspection of NC Machine Tools by Double Ball Bar Method (Hanser Publishers, ISBN 3446174303).

NOBLE, B. and DANIEL, J. W., 1977, Applied linear algebra (Prentice-Hall, second edition, ISBN 0130413437).

SHIN, V. C., CHIN, H. and BRINK, M. J., 1991, Characterisation of CNC machining centers. *Journal of Manufacturing System*, Vol. 10, No. 5.

TRANKLE, H., 1980, Effects of position errors in five-axis milling processes. Ph.D. Dissertation, Stuttgart University, Federal Republic of Germany.

Table 3.1 All potential PIGEPs for the Matsuura five axis machine tool.

Frame	Position error parameters			Angular error parameters		
Y	$e_{x,Y}$	$e_{y,Y}$	$e_{z,Y}$	$\gamma_{x,Y}$	$\gamma_{y,Y}$	$\gamma_{z,Y}$
X	$e_{x,X}$	$e_{y,X}$	$e_{z,X}$	$\gamma_{x,X}$	$\gamma_{y,X}$	$\gamma_{z,X}$
A	$e_{x,A}$	$e_{y,A}$	$e_{z,A}$	$\gamma_{x,A}$	$\gamma_{y,A}$	$\gamma_{z,A}$
C	$e_{x,C}$	$e_{y,C}$	$e_{z,C}$	$\gamma_{x,C}$	$\gamma_{y,C}$	$\gamma_{z,C}$
Z	$e_{x,Z}$	$e_{y,Z}$	$e_{z,Z}$	$\gamma_{x,Z}$	$\gamma_{y,Z}$	$\gamma_{z,Z}$
W	$e_{x,W}$	$e_{y,W}$	$e_{z,W}$	$\gamma_{x,W}$	$\gamma_{y,W}$	$\gamma_{z,W}$
T	$e_{x,T}$	$e_{y,T}$	$e_{z,T}$	$\gamma_{x,T}$	$\gamma_{y,T}$	$\gamma_{z,T}$

Table 3.2 Groups of perfectly confounded parameters and selected parameter for each group.

	Groups of confounded error parameters							
Frame	x direction	y direction	z direction		around x		around y	around z
Y	$e_{x,Y}$	$e_{y,Y}$	$e_{z,Y}$		$\gamma_{x,Y}$		$\gamma_{y,Y}$	$\gamma_{z,Y}$
X	$e_{x,X}$	$e_{y,X}$	$e_{z,X}$			$\gamma_{x,X}$	$\gamma_{y,X}$	
A	$e_{x,A}$	$e_{y,A}$	$e_{z,A}$			$\gamma_{x,A}$		
C	$e_{x,C}$			$e_{z,C}$		$\gamma_{x,C}$		
Z	$e_{x,Z}$	$e_{y,Z}$	$e_{z,Z}$		$\gamma_{x,Z}$		$\gamma_{y,Z}$	$\gamma_{z,Z}$
W				$e_{z,W}$				
T	$e_{x,T}$	$e_{y,T}$	$e_{z,T}$					$\gamma_{z,T}$
The selected parameter								
	$e_{x,T}$	$e_{y,T}$	$e_{z,T}$	$e_{z,W}$	$\gamma_{x,Z}$	$\gamma_{x,A}$	$\gamma_{y,Z}$	$\gamma_{z,T}$

Table 3.3 Complete and not minimal parameter set after removal of the confounded parameters.

Frame	x direction	y direction	z direction	around x	around y	around z
Y						
X						$\gamma_{z,X}$
A				$\gamma_{x,A}$	$\gamma_{y,A}$	$\gamma_{z,A}$
C		$e_{y,C}$			$\gamma_{y,C}$	$\gamma_{z,C}$
Z				$\gamma_{x,Z}$	$\gamma_{y,Z}$	
W	$e_{x,W}$	$e_{y,W}$	$e_{z,W}$	$\gamma_{x,W}$	$\gamma_{y,W}$	$\gamma_{z,W}$
T	$e_{x,T}$	$e_{y,T}$	$e_{z,T}$	$\gamma_{x,T}$	$\gamma_{y,T}$	$\gamma_{z,T}$

Table 3.4 Complete and minimal machine PIGEPs for the Matsuura five axis machine tool.

Frame	x direction	y direction	z direction	around x	around y	Around z
Y						
X						$\gamma_{Z,X}$
A				$\gamma_{Y,A}$	$\gamma_{Y,A}$	$\gamma_{Z,A}$
C		$e_{Y,C}$			$\gamma_{Y,C}$	
Z				$\gamma_{Y,Z}$	$\gamma_{Y,Z}$	

Table 3.5 Results of simulations A and B for the values of the error parameters. The linear errors (e) are in inch and the angular errors (γ) are in radian.

PIGEPs name	Simulation A		Simulation B		
	True values	Identified values	True values	Identified values	Identification errors
$e_{x,1}$	0.0040		0		
$e_{y,1}$	0.0160		0		
$e_{z,1}$	0.0010		0		
$\gamma_{x,1}$	0.0040		0		
$\gamma_{y,1}$	0.0080		0		
$\gamma_{z,1}$	0.0020		0		
$e_{x,2}$	0.0070		0		
$e_{y,2}$	0.0030		0		
$e_{z,2}$	0.0020		0		
$\gamma_{x,2}$	0.0020		0		
$\gamma_{y,2}$	-0.0080		0		
$\gamma_{z,2}$	-0.0060	-0.0060	-0.0060	-0.0060	-3.3E-16
$e_{x,3}$	0.0060		0		
$e_{y,3}$	0.0020		0		
$e_{z,3}$	0.0015		0		
$\gamma_{x,3}$	0.0030	0.0050	0.0500	0.0500	-7.8E-16
$\gamma_{y,3}$	0.0060	0.0060	0.0060	0.0060	4.0E-16
$\gamma_{z,3}$	-0.0040	-0.0040	-0.0040	-0.0040	-5.0E-16
$e_{x,4}$	0.0020		0		
$e_{y,4}$	0.0030	0.0030	0.0030	0.0030	-2.8E-15
$e_{z,4}$	0.0070		0		
$\gamma_{x,4}$	0.0000		0		
$\gamma_{y,4}$	0.0040	0.0040	0.0110	0.0110	-7.0E-17
$\gamma_{z,4}$	0.0000		0		
$e_{x,5}$	0.0020		0		
$e_{y,5}$	-0.0010		0		
$e_{z,5}$	0.0110		0		
$\gamma_{x,5}$	0.0030	-0.0010	0.0300	0.0300	-2.3E-16
$\gamma_{y,5}$	0.0030	0.0030	0.0350	0.0350	9.0E-17
$\gamma_{z,5}$	0.0035		0		
$e_{x,6}$	0.0070	0.0070	0.0070	0.0070	-1.2E-15
$e_{y,6}$	0.0060	0.0060	0.0060	0.0060	1.4E-15
$e_{z,6}$	0.0030	0.0100	0.0030	0.0030	-1.1E-15
$\gamma_{x,6}$	0.0000		0		
$\gamma_{y,6}$	0.0000		0		
$\gamma_{z,6}$	0.0000		0		
$e_{x,7}$	0.0040	-0.0131	0.0040	0.0040	2.0E-15
$e_{y,7}$	0.0070	-0.0149	0.0070	0.0070	-1.2E-15
$e_{z,7}$	0.0090	0.0156	0.0090	0.0090	-1.9E-15
$\gamma_{x,7}$	0.0000		0		
$\gamma_{y,7}$	0.0000		0		
$\gamma_{z,7}$	0.0000		0		

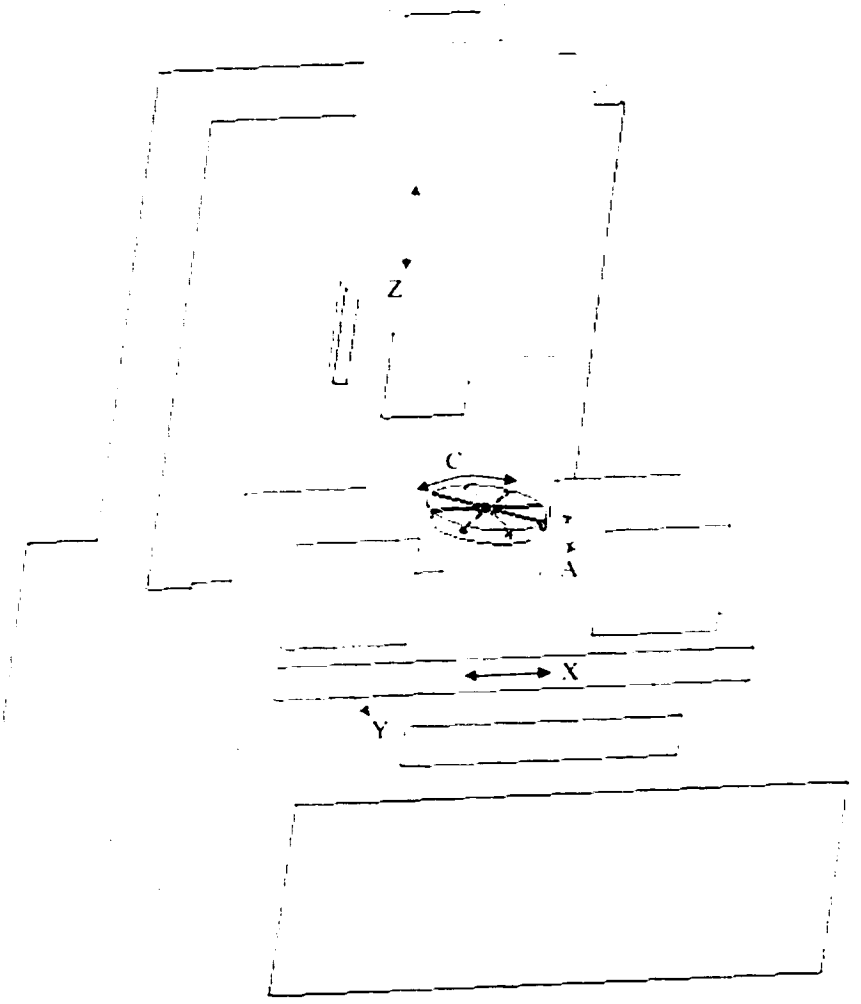

Figure 3.1 3D wire-frame representation of the Matsuura five-axis machine tool.

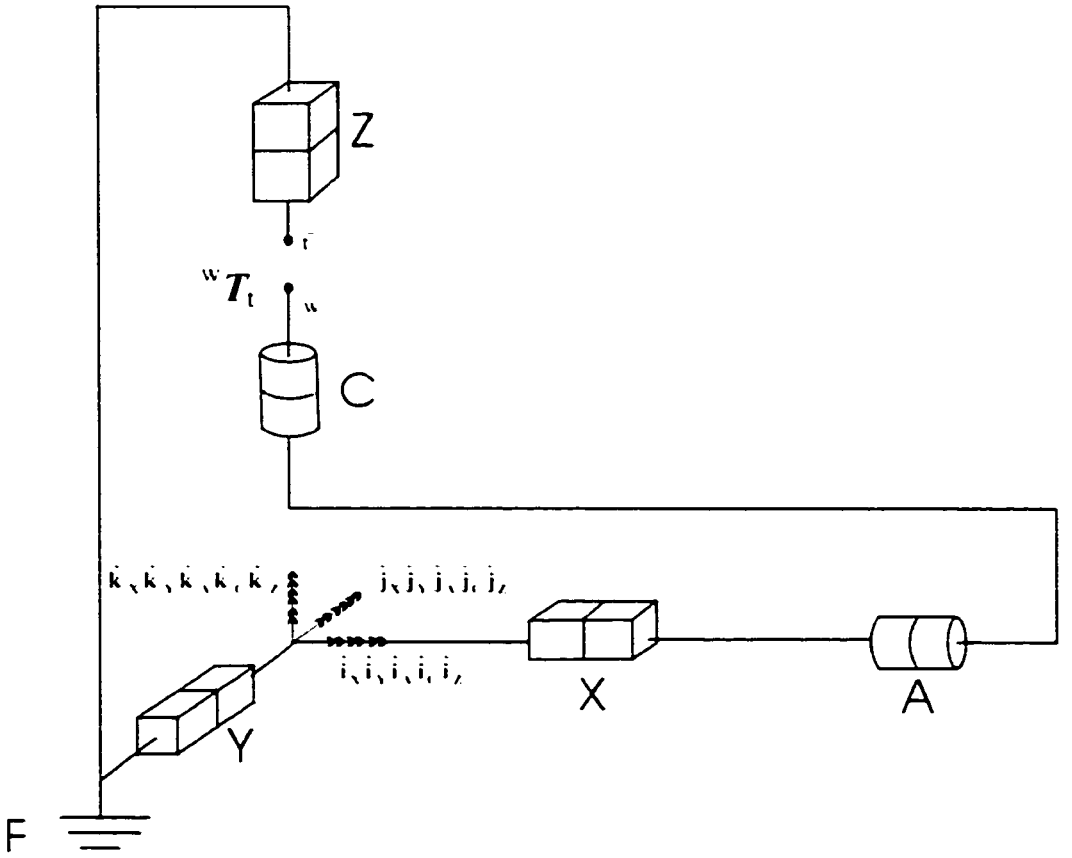

Figure 3.2 Joint frames at joint coordinates $\theta=[0\ 0\ 0\ 0\ 0]^{T}$.

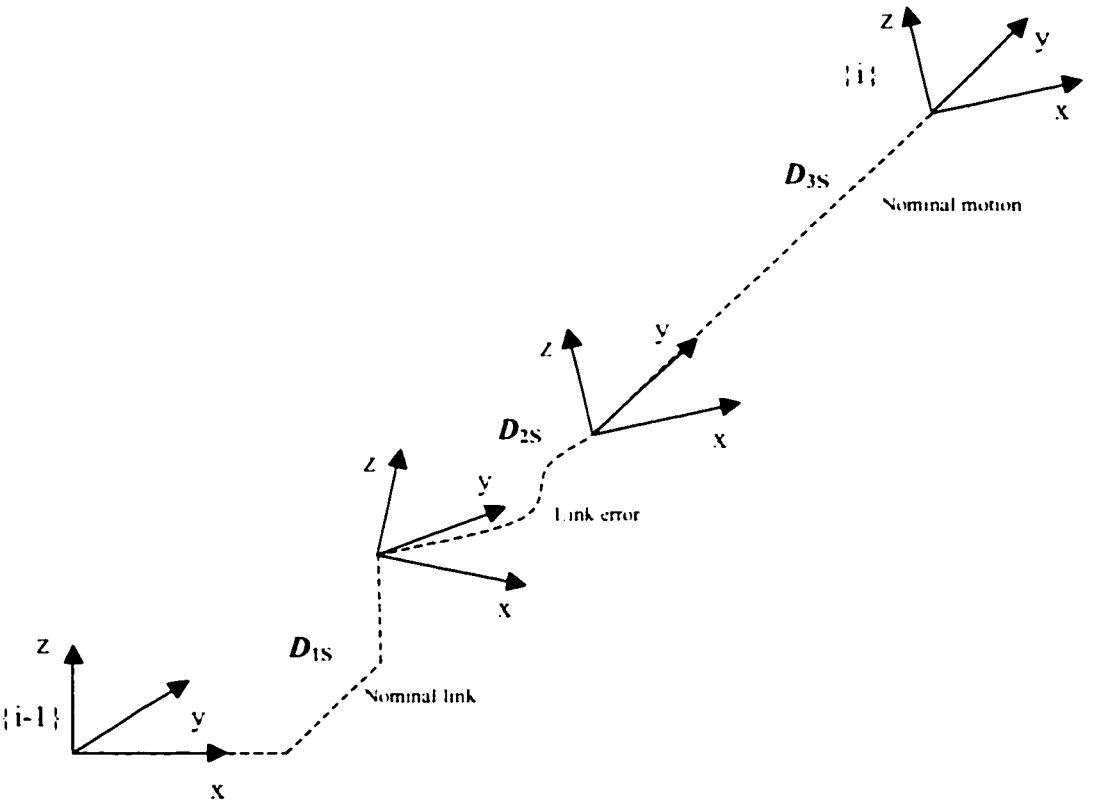

Figure 3.3 Sub-HTM of each link joint transformation

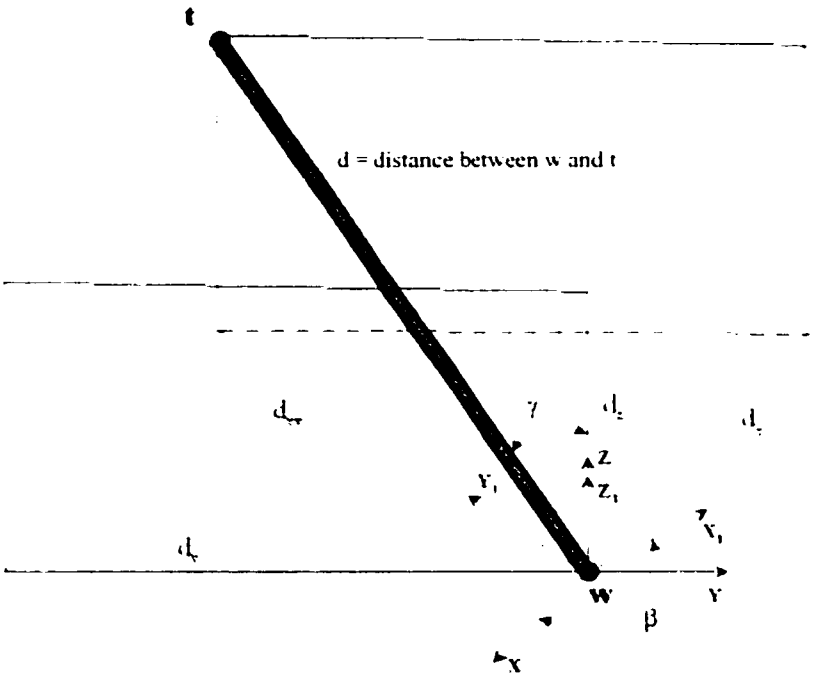

Figure 3.4 Orientation of measurement in direction of ball-bar.

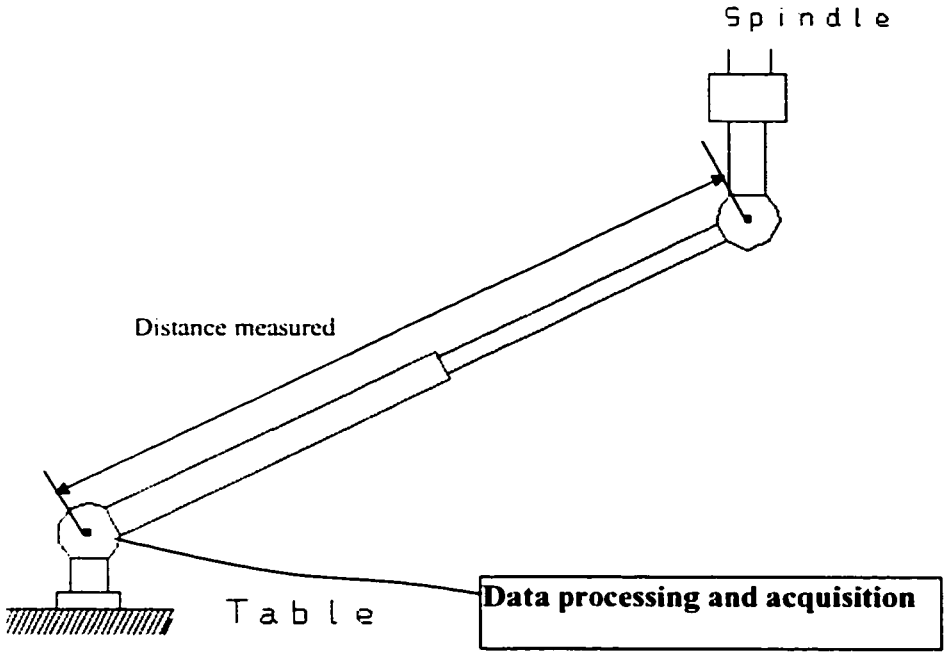

Figure 3.5a Ball-bar schema.

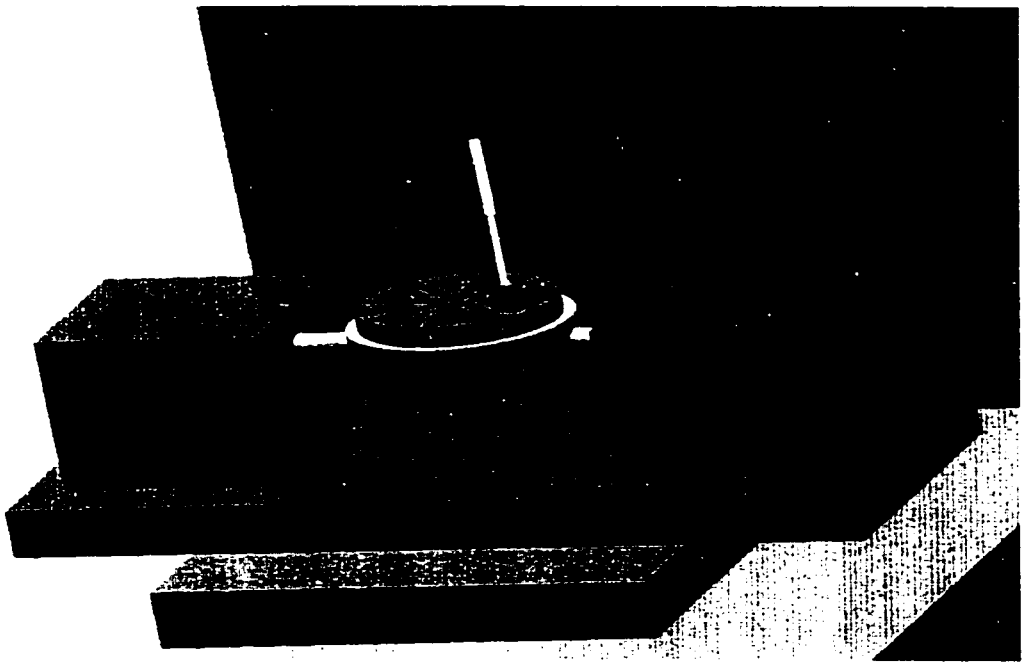

Figure 3.5b Ball-bar fixed to the part table and spindle of the machine tool.

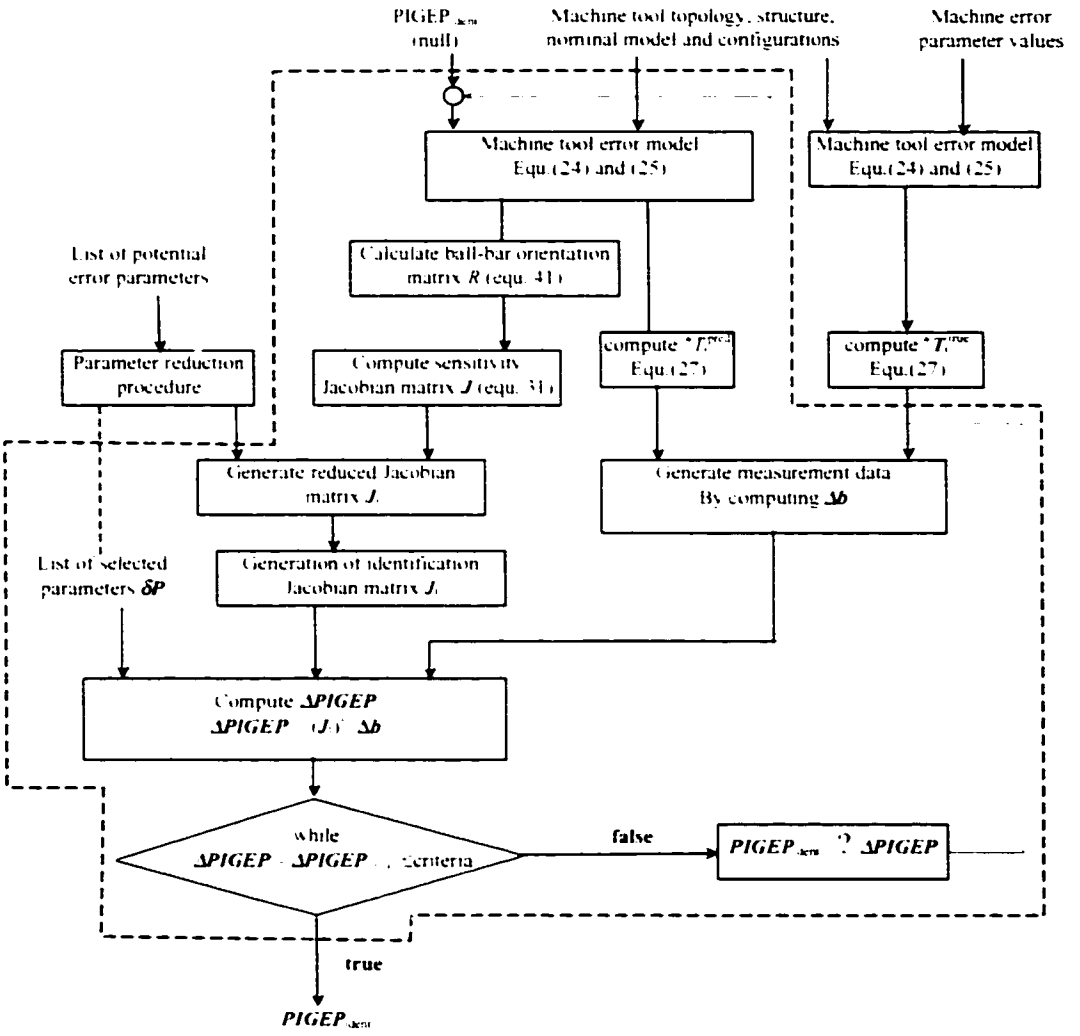

Figure 3.6 Graph presenting the simulation algorithem for PIGEPs.

CHAPITRE 4: CALIBRATION OF A FIVE-AXIS MACHINE TOOL LINK AND MOTION ERRORS USING A TELESCOPING MAGNETIC BALL-BAR

Y. A. Mir, J.R.R. Mayer*, and C. Fortin

Mechanical Engineering Department
Ecole Polytechnique de Montréal

Submitted in June 2001 to the International Journal of Machine Tools and Manufacture

*To whom correspondence should be addressed: rene.mayer@meca.polymtl.ca

4.1 Présentation du chapitre et liens utiles

Dans ce chapitre on propose une méthode qui utilise une barre à billes magnétique télescopique pour identifier la liaison et les erreurs de mouvement sur une machine - outil à cinq axes. La solution mathématique utilise une matrice de sensibilité Jacobienne qui exprime la sensibilité des déplacements du bout d'outil par rapport à la pièce tenant compte des sources d'erreurs géométriques de la machine. Les sources d'erreur de mouvement sont individuellement modélisées comme des fonctions polynomiales de chaque position articulaire de la machine-outil. Par suite de la présence initiale d'un grand nombre de coefficients de polynôme nécessaires pour le modèle, une stratégie a été développée pour réduire le nombre de ces coefficients à une série minimale-complète. On propose aussi des formules pour calculer le nombre nécessaire de paramètres pour une cinématique donnée de la machine outil. Les coefficients inconnus et les paramètres de positions de billes ont été calculés par un système d'équations linéaires faites d'une matrice Jacobienne d'identification et des lectures de barre à billes.

4.2 Abstract

Many parameters influence the quality of machined parts. Amongst them are the link errors which describe the relative location between the machine's successive rotary and prismatic joints and, the motion errors, describing the non-ideal motion of a joint. A method is proposed which uses a telescoping magnetic ball-bar to identify these errors on a five-axis machine tool. The motion error sources are individually modelled as polynomial functions of each machine tool joint position. This modelling method easily incorporates the link errors. Once the polynomial coefficients are identified, it is then possible to predict the tool versus workpiece position and orientation errors resulting from these geometric error sources.

Keywords: Five-axis machine tool, geometric errors, calibration, telescoping magnetic ball bar, motion error, link errors, polynomials.

4.3 Introduction

Many parameters influence the quality of machined parts. Amongst them are two groups of geometric error parameters causing tool positioning errors. The first group includes the position independent geometric error parameters (PIGEPs), also called link errors, which describe the relative location between the machine's successive rotary and prismatic joints. Examples of these are squareness errors, parallelism errors, joint offsets, and rotary axes separation errors. The second group includes the position dependent geometric error parameters (PDGEPs), also called motion errors, describing the non-ideal motion of a joint or axis. Examples of these are positioning errors, straightness errors and angular errors such as yaw, pitch, and roll for prismatic axes, and, the angular, axial, radial and tilt errors for rotary axes.

Much research activity has been conducted in the last decade to define, describe and identify the geometric inaccuracies of a machine tool and enhance its performance through compensation in order to produce accurate parts [1, 2, 3, 4]. Laser

interferometers, autocollimators, reference artefacts and dial indicators have been widely used for this purpose [5]. These methods are quite demanding in terms of cost, time and skill in order to realise the measurements. In recent years, the ball-bar method has been used to measure inaccuracies of machine tools by analysing the tool-tip position relative to the part table for specific paths. Originally, Bryan developed [6, 7] and applied the ball-bar as a replacement for the circular comparison standards of circular tests for machine tool. Circular tests were also used by Knapp[8, 9] for checking kinematic errors of machine tools and CMMs. Kakino et al [10], Burdekin and Park [11] worked on the relationship between three-axis machine tool errors and measurement results acquired by ball-bar on a circular path for fix error estimation. Kunzman and Waldele [12] used fixed ball-bar test to estimate the linear displacement errors and squareness error of CMM. In these approaches, several things are common. They use circular paths of one of the balls relative to the other accomplished on either the xy, yz and xz planes of the machine tool. Secondly, the models were developed for lathe or three-axis prismatic milling machine. In 1994, Hai et al [13] applied telescoping ball-bar to measure three-axis machine tool motion errors using polynomials. This model had to define all coefficients by repeating the ball-bar test for several level of each plan which is very time-consuming procedure. In 1997, Pahk [14] used a telescoping ball-bar and developed a polynomial concept to identify three-axis machine tool errors. Although Pahk used polynomials to represent the geometric errors, its work concentrated on three-axis machine tools and he represented the error parameters as dependent polynomial function, which is not representative generally. For example, Pahk represented the positioning error as polynomials without the zero terms, and angular errors as derivatives of straightness.

An extension of the use of the ball bar for the calibration of the misalignment, axis separation and joint offsets of rotary axes was demonstrated by Driels [14]. He used a fix-length ball-bar to calibrate the position independent geometric error parameters of a robot made of six rotary axes modeled using a modified D-H formulation. Although it is

widely accepted in the modelling of industrial robots. D-H modelling is rarely used in the field of machine tools.

In this paper we present a new approach to identify a five axis machine tool geometric errors using independent polynomial functions and ball-bar readings not contained to circular path. The geometric error sources include both the position independent parameters (squareness, etc.) and the position dependent ones (straightness, yaw, etc.). These error sources are individually modelled as polynomial functions of the individual machine tool joint coordinate. These errors have a cumulative effect on the actual relative location between the tool and the workpiece and so directly influence the readings from a telescoping magnetic ball-bar connected between the tool attachment and the table normally supporting the workpiece. An sensitivity Jacobian matrix represents the sensitivity of the ball bar readings to the machine geometric error sources. It is developed using the Newton-Euler equation for a specific machine tool topology, geometry and joint coordinates. This sensitivity Jacobian matrix and the data acquired during the ball bar procedure are used to iteratively estimate the coefficients of each polynomial by solving a linear system of equations. The identified polynomials can then be used to predict the tool tip versus part feature location errors using a forward kinematic model based on homogenous transformation matrices and incorporating the effect of geometric errors. They can also guide maintenance operation for the particular machine.

4.4 Five-axis machine tool forward model

The kinematic model of a machine tool is used to calculate the relative location between a tool frame t rigidly attached to the tool attachment point and a part frame w rigidly attached to the table . From the base or foundation frame F we define a tool branch and a workpiece feature branch using their homogenous transformation matrix (HTM) ${}^{F}\boldsymbol{T}_{t}$ and ${}^{F}\boldsymbol{T}_{w}$ respectively. ${}^{I}\boldsymbol{T}_{t}$ denotes the 4-by-4 HTM representing the pose (position and

orientation) of frame i with respect to frame j. Thus, the pose of t relative to w is given as

$$ {}^{w}\boldsymbol{T}_{t} = [{}^{F}\boldsymbol{T}_{w}]^{-1} \cdot {}^{F}\boldsymbol{T}_{t} \qquad (45) $$

As an example, the joint coordinates of a Matsuura milling machine, available at our facilities (Figure 4.7a), are defined as $\boldsymbol{\theta} = [z\ y\ x\ a\ c]^{T}$. At $\boldsymbol{\theta} = [0\ 0\ 0\ 0\ 0]^{T}$ the reference frames of all joints coincide (see Fig. 4.1). It can also be noted that the x axis of the X joint frame (unit vector $\hat{\mathbf{i}}_X$) is nominally aligned with the x axis of the A joint frame (unit vector $\hat{\mathbf{i}}_A$) and, the z axis of the Z joint frame (unit vector $\hat{\mathbf{k}}_Z$) is nominally aligned with the spindle for all values of $\boldsymbol{\theta}$.

Each nominal link and non-ideal joint combination $\boldsymbol{D}_S$ can be modelled by the product of 3 HTMs (see Fig. 4.2).

$$ \boldsymbol{D}_S = \boldsymbol{D}_{1S}\,\boldsymbol{D}_{2S}\,\boldsymbol{D}_{3S} \qquad (46) $$

$\boldsymbol{D}_{1S}$ is the nominal link HTM defined as:

$$ \boldsymbol{D}_{1S} = \textit{trans}(\hat{\mathbf{i}}, a_x(s))\ \textit{trans}(\hat{\mathbf{j}}, a_y(s))\ \textit{trans}(\hat{\mathbf{k}}, a_z(s))\ \textit{rot}(\hat{\mathbf{k}}, a_z(s))\ \textit{rot}(\hat{\mathbf{j}}, a_y(s))\ \textit{rot}(\hat{\mathbf{i}}, a_x(s)) \qquad (47) $$

where for example $\textit{trans}(\hat{\mathbf{i}}, a_x(s))$ is a HTM for a linear transformation by a nominal value $a_x(s)$ along the $\hat{\mathbf{i}}$ direction; $\textit{rot}(\hat{\mathbf{i}}, \alpha_x(s))$ is a HTM for a rotation of nominal value $\alpha_x(s)$ around $\hat{\mathbf{i}}$. For the target Matsuura machine tool S represents either of Z, Y, X, A, or C and all nominal values are null. The joint HTM $\boldsymbol{D}_{2S}$ describes the nominal motion of the joint frame,

$$ \boldsymbol{D}_{2S} = \textit{trans}(\mathbf{dir}, s) \text{ for prismatic joint; } \boldsymbol{D}_{2S} = \textit{rot}(\mathbf{dir}, s) \text{ for a rotary joint} \qquad (48) $$

where for prismatic joints **dir** is either of $\hat{\mathbf{i}}$, $\hat{\mathbf{j}}$ or $\hat{\mathbf{k}}$ and s (the joint coordinate) is x, y or z, for X, Y, Z respectively. Whereas for rotary joints **dir** is $\hat{\mathbf{i}}$ for A, and $\hat{\mathbf{k}}$ for C, and s is a or c, the displacement angle.

$\boldsymbol{D}_{3S}$describes the joint motion errors (PDGEPs) (see Fig. 4.3).

$$\boldsymbol{D}_{i} = \textit{trans}(\mathbf{i}, e_x(s))\,\textit{trans}(\mathbf{j}, e_y(s))\,\textit{trans}(\mathbf{k}, e_z(s))\,\textit{rot}(\mathbf{k}, \gamma_z(s))\,\textit{rot}(\mathbf{j}, \gamma_y(s))\,\textit{rot}(\mathbf{i}, \gamma_x(s)) \quad (49)$$

where $e_x(s)$, $e_y(s)$, and $e_z(s)$ are the linear errors as functions of the joint coordinate s along joint S, and similarly, $\gamma_x(s)$, $\gamma_y(s)$, and $\gamma_z(s)$ are the angular errors (roll, pitch and yaw) (see Fig. 4.2 and Fig. 4.3). All error terms are functions of the joint coordinate.

Because of the various machine errors just described, the actual tool tip and the workpiece feature do not coincide as nominally planned. However the $\boldsymbol{D}_i$ matrices for a particular machine may be used to calculate the resultant positioning errors for any multi-axis machine with an arbitrary serial combination of rotary and prismatic joints. The difference between the tool tip frame and the workpiece feature frame, ${}^{w}\boldsymbol{E}_t$ (see Fig. 4.1) may be represented as an HTM and calculated as follows:

the tool branch is given by

$${}^{b}\boldsymbol{T}_t = \boldsymbol{D}_z\,\boldsymbol{T}_t \quad (50)$$

and the workpiece feature branch is

$${}^{b}\boldsymbol{T}_w = \boldsymbol{D}_y\,\boldsymbol{D}_x\,\boldsymbol{D}_a\,\boldsymbol{D}_c\,\boldsymbol{T}_w. \quad (51)$$

The complete kinematic chain can be obtained as:

$${}^{b}\boldsymbol{T}_t = {}^{b}\boldsymbol{T}_w\ {}^{w}\boldsymbol{E}_t \quad (52)$$

and finally:

$${}^{w}\boldsymbol{E}_t = [{}^{b}\boldsymbol{T}_w]^{-1}\,{}^{b}\boldsymbol{T}_t. \quad (53)$$

The HTMs of the machine kinematics model will be used to: a) simulate an imperfect machine and generate virtual measurement data for validation purposes, b) generate the sensitivity Jacobian matrix, which expresses the sensitivity of the ball-bar readings to the error parameters and c) predict the location errors of the tool-tip versus the part feature for a given set of joint coordinates and tool and workpiece geometry.

4.5 Representing error parameters as polynomials functions

Considering the three prismatic joints of a five-axis machine tool there are 18 (3×6) such motion errors and 3 constant errors i.e. one squareness error between the Y and X axes, and two squareness errors for the Z axis. Furthermore the geometric errors of the two rotary axis of the five axis machine tool will be modelled using 12 motion errors and 5 constant errors. For a ZFYXAC machine topology, these include two alignment errors between the A and the X axes, one angular offset for the A axis, one squareness error between the C and A axes and one axis to axis distance between axes A and C. In this work we represent all 38 geometric error parameters of the machine tool using 30 polynomial functions of joint coordinates (see Fig. 4.4).

To represent such motion error parameters (PDGEPs), the Chebyshev polynomial [16] is chosen. This polynomial has orthogonal characteristics and can generate a better condition number for the sensitivity Jacobian matrix. The general form of Chebyshev polynomials is:

$$T_n(s_N) = \cos n\theta \tag{54}$$

where n is a nonnegative integer, θ=arcos(s_N) and $0 \le \theta \le \pi$. $T_n(s_N)$ is defined by equ. (54) on the interval $-1 \le s_N \le 1$. The Chebyshev polynomial of degree 3 is used in this work, without lost of generality, and is defined as:

$$p(s_N) = c_0 T_0(s_N) + c_1 T_1(s_N) + c_2 T_2(s_N) + c_3 T_3(s_N) \tag{55}$$

where

$$\begin{aligned} T_0(s_N) &= 1 \\ T_1(s_N) &= s_N \\ T_2(s_N) &= 2s_N^2 - 1 \\ T_3(s_N) &= 4s_N^3 - 3s_N \end{aligned} \tag{56}$$

and c_0, c_1, c_2, c_3 are the coefficients. The general form of a Chebyshev term of degree n is expressed as:

$$T_n(s_N) = 2s_N T_{n-1}(s_N) - T_{n-2}(s_N) \qquad \text{with} \qquad n \geq 2 . \tag{57}$$

Where s_N is the normalised S joint coordinate value over its range:

$$s_N = \frac{d_s - d_{s(\text{median})}}{\text{range} \div 2}$$

$$\text{range} = d_{s(\max)} - d_{s(\min)} \tag{58}$$

$$d_{s(\text{median})} = \frac{d_{s(\min)} + d_{s(\max)}}{2}$$

In general for each error, e, on the machine tool, the polynomial is presented as:

$$p_e(s_N) = c_0^e T_0(s_N) + c_1^e T_1(s_N) + c_2^e T_2(s_N) + c_3^e T_3(s_N) \tag{59}$$

where s_N represents the normalised joint coordinate (y, x, a, c, z) and e represents one of the six motion errors of particular each particular axis (such as $e_x(s)$, $e_y(s)$, $e_z(s)$, $\gamma_x(s)$, $\gamma_y(s)$ and $\gamma_z(s)$). For example, the polynomial representing the horizontal straightness error on the Y axis, $e_x(y)$ can be expressed as:

$$p_{e_x}(y) = c_0^{e_x} T_0(y) + c_1^{e_x} T_1(y) + c_2^{e_x} T_2(y) + c_3^{e_x} T_3(y) \tag{60}$$

4.6 Sensitivity Jacobian matrix generation

From the nominal links and joint coordinate at each pose, the sensitivity Jacobian matrix, $\boldsymbol{J}$, is obtained using Newton-Euler's equation. This matrix determines the changes in the tool versus workpiece feature location $\boldsymbol{\delta\tau}$ resulting from changes in the machine error parameters $\boldsymbol{\delta p}$.

$$\delta\tau = J.\ \delta p \tag{61}$$

The sensitivity Jacobian matrix is built using transport matrices. A transport matrix is generated using a HTM and propagates the effect of an error twist $[e_x\ e_y\ e_z\ \gamma_x\ \gamma_y\ \gamma_z]^T$ occurring in one reference frame onto another frame rigidly connected to the former

$$^{\{B\}}dt_B = {}^B_A C\, {}^{\{A\}}dt_A \tag{62}$$

where $^{\{B\}}dt_B$ is the propagated twist (small displacement) at B, expressed in frame B, $^{\{A\}}dt_A$ is the causal twist in A, expressed in frame A, and ${}^B_A C$ is a 6-by-6 transport matrix [17, 18, 19]. The transport matrix can be formed using sub-matrices of an HTM as follows :

$$\text{if } {}^A_B T = \begin{bmatrix} {}^A_B R & {}^{\{A\}}P_B \\ 000 & 1 \end{bmatrix} \quad \Rightarrow \quad {}^B_A C = \begin{bmatrix} {}^A_B R^T & {}^A_B R^T \left[{}^{\{A\}}P_B \times \right]^T \\ 0\ 0\ 0 & \\ 0\ 0\ 0 & {}^A_B R^T \\ 0\ 0\ 0 & \end{bmatrix} \tag{63}$$

Since the tool path information (cutter location file) is presented in the tool frame, the error should be transformed to the tool-frame. For the machine considered, this can be accomplished by forming a sensitivity Jacobian matrix as follow:

$$^{\{t\},f}dt_t = J \cdot dP \tag{64}$$

where $^{\{t\},f}dt_t$ is a twist with size $6m$-by-1 representing the errors in t to f and express them in t. J is the sensitivity Jacobian matrix with size $(6m)$-by-n, and dP is the error parameter column matrix with n elements. The number of poses and error parameters are m and n respectively.

For example for a ZFYXAC machine (see Fig. 4.1), the sensitivity Jacobian matrix is

$$^{t,f}_t J = \left[-{}^t_F C \cdot {}^f_F C^{-1} \cdot {}^{\{f\},F}_f J \quad {}^{\{t\},F}_t J \right] \tag{65}$$

where

$$ {}^{\{t\},F}_{f}\boldsymbol{J} = \left| {}^{f}_{t}\boldsymbol{C} \quad {}^{f}_{\chi}\boldsymbol{C} \quad {}^{f}_{\zeta}\boldsymbol{C} \quad {}^{f}_{\zeta}\boldsymbol{C} \quad {}^{f}_{\zeta}\boldsymbol{C} \quad {}^{f}_{w}\boldsymbol{C} \quad {}^{f}_{t}\boldsymbol{C} \right|_{6\times(7+6t)} \tag{66} $$

$$ {}^{\{t\},F}_{t}\boldsymbol{J} = \left| {}^{t}_{F}\boldsymbol{C} \quad {}^{t}_{Z}\boldsymbol{C} \quad {}^{t}_{S}\boldsymbol{C} \quad {}^{t}_{t}\boldsymbol{C} \right|_{6\times(4+6t)} \tag{67} $$

and

$$ {}^{f}_{F}\boldsymbol{C}^{-1} = {}^{F}_{f}\boldsymbol{C} \tag{68} $$

In equation (66), ${}^{\{t\},F}_{f}\boldsymbol{J}$ expresses the sensitivity of the feature frame location f observed from the foundation frame F and expressed in the feature frame f to causal error parameters within the feature branch. Note that the two $\boldsymbol{C}$ matrices in equation (65) are used to combine the two branches into one continuous chain from the tool to the feature. ${}^{f}_{t}\boldsymbol{C}$ is $I_{6\times6}$, and other elements of this equation are calculated as:

$$ \begin{aligned} {}^{f}_{\chi}\boldsymbol{C} &= {}^{f}_{t}\boldsymbol{C} \cdot {}^{t}_{w}\boldsymbol{C} \\ {}^{f}_{\zeta}\boldsymbol{C} &= {}^{f}_{w}\boldsymbol{C} \cdot {}^{w}_{\zeta}\boldsymbol{C} \\ {}^{f}_{\zeta}\boldsymbol{C} &= {}^{f}_{\zeta}\boldsymbol{C} \cdot {}^{\zeta}_{\zeta}\boldsymbol{C} \\ {}^{f}_{\zeta}\boldsymbol{C} &= {}^{f}_{\zeta}\boldsymbol{C} \cdot {}^{\zeta}_{\zeta}\boldsymbol{C} \\ {}^{f}_{\zeta}\boldsymbol{C} &= {}^{f}_{\zeta}\boldsymbol{C} \cdot {}^{\zeta}_{\zeta}\boldsymbol{C} \\ {}^{f}_{F}\boldsymbol{C} &= {}^{f}_{\zeta}\boldsymbol{C} \cdot {}^{\zeta}_{F}\boldsymbol{C} \end{aligned} \tag{69} $$

In equation (67), ${}^{\{t\},F}_{t}\boldsymbol{J}$ expresses the sensitivity of the tool frame location t observed from the foundation frame F and expressed in the tool frame t to causal error parameters within the tool branch. ${}^{t}_{t}\boldsymbol{C}$ is $I_{6\times6}$, and other elements of this equation are calculated as:

$$ \begin{aligned} {}^{t}_{S}\boldsymbol{C} &= {}^{t}_{t}\boldsymbol{C} \cdot {}^{t}_{S}\boldsymbol{C} \\ {}^{t}_{Z}\boldsymbol{C} &= {}^{t}_{S}\boldsymbol{C} \cdot {}^{S}_{Z}\boldsymbol{C} \\ {}^{t}_{F}\boldsymbol{C} &= {}^{t}_{Z}\boldsymbol{C} \cdot {}^{Z}_{F}\boldsymbol{C} \end{aligned} \tag{70} $$

Fig. 4.5 shows the action of transport matrices for each axis and for both branches. For the C arrows, the origin of the arrow indicates the frame where the causal error parameters occur. The arrow tip indicates the frame where the resulting effect is propagated and calculated.

4.6.1 Generation of the extended sensitivity Jacobian Matrix for Coefficients

From equation (64), the sensitivity Jacobian matrix has dimensions of 6m-by-66,where m is the number of poses. Each column of this matrix represents the sensitivity of all tool versus feature pose errors to a specific error parameter . However, some of these columns do not correspond to errors on the machine tool. These columns are present because they facilitate the software implementation. They are associated with twist occurring at the foundation, at the tool tip and at the feature. Therefore, the corresponding columns are useless and are removed from the calculated sensitivity Jacobian matrix. In our system there exists 30 machine tool error parameters carried by ${}^{1}_{1}\boldsymbol{C}$, ${}^{1}_{2}\boldsymbol{C}$, ${}^{1}_{3}\boldsymbol{C}$, ${}^{1}_{4}\boldsymbol{C}$ and ${}^{1}_{5}\boldsymbol{C}$ plus 12 location errors for the part and tool fixations (6 for each) carried by ${}^{1}_{4}\boldsymbol{C}$ and ${}^{1}_{3}\boldsymbol{C}$. Therefore, the sensitivity Jacobian matrix has 42 columns. Since each machine tool error parameter is modelled as a polynomial function of degree 3, each requires 4 coefficients and the corresponding column of these errors will be extended to the number of coefficients (i.e. 4). As a result, the extended sensitivity Jacobian matrix, $\boldsymbol{J}_e$ then represents the sensitivity of the tool versus feature pose error to changes in the Chebyshev coefficients and it now has 30*4+12=132 columns.

From equation (59) and (61) the first partial derivatives of a particular tool versus pose error twist with respect to the Chebyshev coefficients are:

$$\begin{aligned}
\frac{\partial \tau}{\partial c_0^e} &= \frac{\partial \tau}{\partial p_e(s)} \cdot \frac{\partial p_e(s)}{\partial c_0^e} = \frac{\partial \tau}{\partial p_e(s)} \cdot T_0(s) \\
\frac{\partial \tau}{\partial c_1^e} &= \frac{\partial \tau}{\partial p_e(s)} \cdot \frac{\partial p_e(s)}{\partial c_1^e} = \frac{\partial \tau}{\partial p_e(s)} \cdot T_1(s) \\
\frac{\partial \tau}{\partial c_2^e} &= \frac{\partial \tau}{\partial p_e(s)} \cdot \frac{\partial p_e(s)}{\partial c_2^e} = \frac{\partial \tau}{\partial p_e(s)} \cdot T_2(s) \\
\frac{\partial \tau}{\partial c_3^e} &= \frac{\partial \tau}{\partial p_e(s)} \cdot \frac{\partial p_e(s)}{\partial c_3^e} = \frac{\partial \tau}{\partial p_e(s)} \cdot T_3(s)
\end{aligned} \tag{71}$$

so each term in the sensitivity Jacobian matrix is replaced as follows to express the sensitivity of the tool versus feature pose to changes in the Chebyshev coefficients.

$$\frac{\partial \tau}{\partial p_e(s)} \Rightarrow \frac{\partial \tau}{\partial p_e(s)} \cdot \begin{bmatrix} T_0(s) & T_1(s) & T_2(s) & T_3(s) \end{bmatrix} \tag{72}$$

The extended sensitivity Jacobian matrix has the form of the *Vendermond* matrix.

4.7 Minimal and Complete set of PDGEPs

The extended sensitivity Jacobian matrix, J_e has 132 columns and accounts for the effect of 132 variables : the tool location error parameters, the workpiece location error parameters and all potential machine error coefficients (for cubic polynomials). This initial model is referred to as the maximal-complete model because it can fully represent the geometric errors sources and may have an excessive number of variables to do so. In table 4.1, column **a** shows these error variables. There are 30x4 coefficients representing the machine tool error parameters and 12 location errors of the part on the table and the tool on the spindle (6 for each). The J_e matrix including these unknown objects is an ill-conditioned matrix. Hereafter, we explain the variable reduction of this model towards a minimal-complete model, which has the minimum number of parameters and coefficients required to completely explain the geometric error characteristics of the real machine tool.

The ill-conditioning of J_e indicates that some columns are linear combinations of others. The variables corresponding to those columns form a confounded variable group and

removing at least one variable of such a group is necessary. The objective is to determine a minimum set of variables, which can completely explain the tool versus part feature pose errors.

4.7.1 Mathematical analysis of the extended sensitivity Jacobian matrix

The identification of all potential set-up parameters and coefficients of the machine model (132 variables in total) is not possible because the system is ill-conditioned. Through a mathematical analysis of the extended sensitivity Jacobian matrix associated with this model, the number of parameters and coefficients that can be selected can be defined.

Initially the J_e matrix is singular due to the presence of redundant variables. A number of matrix properties are now proposed to reduce the number of variables.

The column rank of a matrix is the maximum number of independent columns. It is also equal to the number of non-zero singular values (defined below). An m-by-n matrix with $m \geq n$ is said to be of full rank if its rank = n or rank deficient if its rank < n.

The condition number of matrix J_e is :

$$\mathbf{Cond}(J_e) = \frac{s_{max}}{s_{min}} \tag{73}$$

where σ_{max} and σ_{min} are the largest and smallest singular values of J_e respectively. If J_e is rank deficient, then $\sigma_{min} = 0$ and $Cond(J_e)$ is infinite. The smaller the $Cond(J_e)$, the more independent its columns are.

The singular value are calculated using the singular value decomposition (SVD). In linear algebra, a set of vectors is defined to be independent if none of them can be expressed as a linear combination of the others. By analysing the SVD of the J_e matrix

the dependent columns (redundant variables) can be found. A singular value decomposition of the m-by-n real matrix J_e is any factorisation of the form

$$J_e = U\Sigma V^T \tag{74}$$

where U is an m-by-m orthogonal matrix, V is an n-by-n orthogonal matrix, and Σ is an m-by-n diagonal matrix $\sigma_{ij} = 0$ if i ? j and $\sigma_{ij} \geq 0$ if i = j. The quantities σ_i are the singular values of J_e, and the columns of U and V are called the left and right singular vectors. Here m is the total number of poses and n is the total number of variables (parameters and coefficients) which is also the number of singular values. Note that the singular values are in decreasing order along the diagonal.

Using the notions of *rank*, *cond* and *size* of a matrix, and the SVD, we can analyse whether or not a matrix is singular, how many independent columns exist, what columns are dependent on each other, and to what degree of dependence. The matrix is singular if its number of columns (hereafter called its size) exceeds its rank. The difference between the rank and size indicates the number of redundant parameters. This is confirmed by a very large condition number. An analysis of the column of V corresponding to a zero or near zero singular value reveals confounded variables. Note that the V column of interest will be the last one given that the singular values are in decreasing order. The dominant variables (coefficients or parameters of the model) are those with relatively large elements in the V column. If in the column of V, the values of two elements are ±0.707, it means that they are completely confounded and their effects on the solution are identical except maybe for the sign. This is confirmed by the presence of two columns of the J_e matrix being identical except maybe for their sign. In this case one of two variables must be removed. In a more complex case of variable coupling, i.e. more than two variables involved, the group of confounded parameters will be formed from those parameters which have relatively large elements in the last column of V. In this case one parameter of the group must be removed. Removing one coefficient means removing its corresponding column in the extended sensitivity Jacobian matrix. Once a column is removed, an updated extended sensitivity Jacobian

matrix is generated. Then the analysis related to the updated matrix continues to find new confounded parameter groups. It is important to ensure that the removal of a variable does not reduce the rank of the matrix since this means that the tool versus feature pose error can no longer be completely predicted.

To select the parameter or coefficients to be removed from a confounded group, several strategies are used.

I Part and tool related parameters

The error parameters pertaining to the tool and part locations are often determined during a set-up procedure and thus are independent from the machine tool error sources. Therefore in a confounded group of variables we keep those tool and part parameters.

II PIGEP parameters

Within a group of confounded variables, those coefficients corresponding to PIGEPs are systematically kept during the model reduction because they correspond to machine error parameters well recognised in the field of machine tool. An important task is to establish the correspondence between these constant parameters and the coefficients of the polynomial functions. These PIGEPs are a squareness error between the X and Y axes ($\gamma_{Z,X}$), parallelism errors between the A and the X ($\gamma_{Z,A}$, $\gamma_{Y,A}$), squareness errors for the Z axis ($\gamma_{X,Z}$, $\gamma_{Y,Z}$), joint offset for the A axis ($\gamma_{X,A}$), and axis separation and squareness errors for the C axis ($e_{Y,C}$, $\gamma_{X,C}$) [20]. Table 4.2 lists the correspondence between the PIGEPs and the polynomial coefficients. For example the chosen coefficient corresponding to the squareness error $\gamma_{Z,X}$ is the zero order coefficient of the Y axis, $\gamma_Z(y)_0$, see Fig. 4.6. An alternative choice could have been $e_Y(x)_1$. A similar correspondence can be seen between $\gamma_{Z,A}$, $\gamma_{Y,A}$ and $\gamma_{Y,C}$ and, $\gamma_Z(x)_0$, $\gamma_Y(x)_0$ and $\gamma_Y(a)_0$ respectively. The joint angular offset $\gamma_{X,A}$ corresponds to $\gamma_X(x)_0$. The axis separation $e_{Y,C}$ corresponds to $e_Y(a)_0$. The squareness $\gamma_{Y,Z}$ can be associated either to $\gamma_Y(y)_0$ or $e_Y(z)_1$, and arbitrarily we chose $e_Y(z)_1$. Finally, the squareness $\gamma_{X,Z}$ corresponds only to $e_X(z)_1$. Table

4.2 lists these parameters and their corresponding coefficients. See also table 4.1 column d.

III Considering the condition number of the extended sensitivity Jacobian matrix

If the selection of a coefficient for removal cannot be made on the basis of strategies I or II then we remove the coefficient leading to the smallest conditioning number once removed. It results in a reduction of the numerical propagation of measurement noise in the calibration data onto the identified machine error variables.

4.7.2 Selection procedure

A matlab simulation was used to generate a series of 600 machine configurations as well as the associated extended sensitivity Jacobian matrix which had the following characteristics : Dimensions=(600×6)-by-132; Rank=104; Conditioning number = 8 .

A rank of 104 for a matrix with a column size of 132 indicates that 28 variables should be removed. To remove these variables, we begin by determining groups of confounded variables by analysing the columns of V obtained from equation (73). In the last column of matrix V, the variables, which are confounded together, can be recognised. For keeping or removing a variable we follow the strategies numbered I to III. If strategy number I is not valid we use strategy number II and so on. Once a variable is removed, the extended sensitivity Jacobian matrix is updated and then a new SVD analysis started. This procedure is continued until the size of the last updated extended sensitivity Jacobian matrix becomes equal to its rank. The resulting matrix is a reduced sensitivity Jacobian J_r matrix. Table 4.3 shows the group of confounded variables, those to be removed, the strategy used to select the removed variables, and the changes in the mathematical characteristics of the J_r.

In table 4.1, column **a** shows all error parameters and coefficients, column **b** shows those removed, column **c** shows all parameters and coefficients to be identified, column **d**

shows the coefficients of column **c** representing PIGEPs, and column **e** shows the coefficients of column **c** representing PDGEPs. There are 104 parameters and coefficients to be identified (including 92 coefficients plus 2×6 errors for feature and tool fixing points).

The numerical simulation show that the minimal-complete model consists in 104 variables (parameters and coefficients) . These variables are sufficient to completely predict the tool versus feature pose errors of a machine afflicted by geometric errors both on position independent and position dependent parameters when a cubic polynomial representation is used.

4.7.3 Remarks on the number of coefficients and parameters

To calibrate a multi-axis machine tool modelled as polynomial functions for its geometric errors parameters, the minimal number of parameters and coefficients $N_{p\&c}$ to be identified can be calculated from the following equations:

$$N_{p\&c} = N_p + N_c \tag{75}$$

The number of position independent geometric error parameter N_p was established by Everett [21]:

$$N_p = 4R+2P+6 \tag{76}$$

Where R and P are the number of rotary and prismatic joints respectively. In our study the value of N_p for a machine of ZFYXAC topology is 20 [20] since R=2 and P=3 as is the case with most five-axis machine tool. The number of coefficients N_c necessary to model the motion errors with polynomial functions of degree 3 can then be established at 104-20=84. This value for N_c can be explained as follows. Initially all motion error parameter polynomials have n+1 coefficients. Where n represents the degree of polynomials. However all zero order terms are position independent, thus are not motion errors, and as such are accounted for in N_p. Also in principle for prismatic joints, the linear terms of the straightness errors (2 per joint) are not motion errors and so the first-

order terms are not required for motion error modelling. With regards to rotary joints, all above zero-order terms are required. Therefore, the number of coefficients can be calculated as:

$$N_c = P(6(n+1-1)-2) + R(6(n+1-1)). \quad (77)$$

By substitution of N_p and N_c in equation (75) we have:

$$N_{p\&c} = 4R + 6n(R+P) + 6 \quad (78)$$

For example, the ZFYXAC machine having 2 rotary joints and 3 prismatic joints, and using Chebyshev polynomials of degree 3, $N_{p\&c} = 104$.

4.8 Using a ball-bar to identify the parameters and coefficients

In practice, it is difficult to measure the complete pose (position and orientation) errors of the tool relatively to the workpiece. The telescoping magnetic ball-bar is a convenient instrument but only detects the orientation of the pose error along its measurement axis (Fig. 4.7). However, it is possible to transform the reduced sensitivity Jacobian matrix in order to model the functionality of the TMBB.

First the tool position error must be orientated along the ball bar axis. From Fig. 4.8, the orientation matrix $\boldsymbol{R}$ is calculated as:

$$\boldsymbol{R} = \boldsymbol{R}_1 * \boldsymbol{R}_2$$

$$\boldsymbol{R}_1 = \boldsymbol{rot}(\hat{\mathbf{k}}, \beta - 90) \quad \text{where}$$

$$\beta = \text{atan2}(d_y, d_x) \text{ and} \quad (79)$$

$$\boldsymbol{R}_2 = \boldsymbol{rot}(\hat{\mathbf{i}}_1, -\gamma) \quad \text{where}$$

$$\gamma = \text{atan2}(d_{xy}, d_z).$$

Where d (in figure 4.8) is the distance between frames w and t, d_x, d_y, d_z are the Cartesian co-ordinates of frame t in frame w and d_{xy} is the orientation of d on the xy

plan. $\boldsymbol{R}$ is used at the end of each branch to orient the feature and tool frame along the ball-bar axis.

This effectively aligns one of the axes of the reference frame of expression of the translation components of the error twist with the ball bar axis. As a result, the new component corresponding to the aligned axis directly provides the virtual distance measurement of the TMBB. This mathematical technique maintains the availability of a linear system of equations. It allows the generation of an identification Jacobian matrix where each line represents the effect of a machine parameter coefficient onto the ball to ball distance thus maintaining the availability of a linear system of equations. Having instead calculated the distance from the initial unaligned components (with the squares and square root operations thus required) would have not permitted the development of a linear system. As will be shown later, the availability of a linear system greatly simplifies solving for the unknowns parameters.

In order to propagate the effects of the coefficients and parameters onto the ball bar readings, a matrix called the identification Jacobian matrix $\boldsymbol{J}_{\mathrm{I}}$ is derived from the reduced sensitivity Jacobian matrix $\boldsymbol{J}_{\mathrm{r}}$. This matrix has m lines instead of the $6m$ lines of the reduced sensitivity Jacobian matrix. However $\boldsymbol{J}_{\mathrm{I}}$ is less rich, thus the need to measure more poses for the machine calibration.

In order to generate the ball bar measurement at each configuration, the position of the tool branch ball relative to the workpiece branch ball is calculated for two cases: 1) with the machine tool parameters at their estimated values from which ${}^{\mathrm{w}}\boldsymbol{T}_{\mathrm{t}}^{\mathrm{predicted}}$ is calculated, and 2) for a true machine tool from which ${}^{\mathrm{w}}\boldsymbol{T}_{\mathrm{t}}^{\mathrm{true}}$ is calculated. The difference between the ball to ball distances obtained from ${}^{\mathrm{w}}\boldsymbol{T}_{\mathrm{t}}^{\mathrm{true}}$ and ${}^{\mathrm{w}}\boldsymbol{T}_{\mathrm{t}}^{\mathrm{predicted}}$ respectively, represents the virtual measurement value for one configuration. These differences for all test configurations are concatenated vertically to form the measured data column matrix $\Delta\boldsymbol{b}$. The ball to ball distance is calculated directly from the norm of the translation vector contained within the HTMs ${}^{\mathrm{w}}\boldsymbol{T}_{\mathrm{t}}^{\mathrm{true}}$ and ${}^{\mathrm{w}}\boldsymbol{T}_{\mathrm{t}}^{\mathrm{predicted}}$.

Each ball of the ball-bar only requires a position error and no orientation error. Considering this, the number of unknowns of the minimum-complete set to be identified will decrease to 98 parameters and coefficients (104-3-3=98).

A single socket strategy (a single ancrage at the tool and at the workpiece table) cannot provide an identification Jacobian matrix of rank 98. The measurements from the ball bar are not constraining the solution sufficiently. For example, the mathematical results for an identification Jacobian matrix using one-socket and having 140 poses give a rank of 66. The simulations have been repeated for different situations with different configurations and with large numbers of poses, but the rank did not increase above 78. Thus it appears that the maximum number of parameters and coefficients, which can be identified with a single ball bar set-up strategy, can not be more than 78.

However, the measurement data set can be enriched using the additional TMBB set-ups through the use of different ball positions at the tool attachment point (the spindle) and at the workpiece table.

4.8.1 Three-set-up method to acquire data

A two set-up strategy was also tried, but the number of identifiable parameters and coefficients remained less than the number of parameters and coefficients, which must be identified for a complete model. Finally a three ball-bar -set-up strategy was found successful. As seen in Fig. 4.9 a three set-up strategy adds 6 position error parameters per set-up (3 for the spindle ball and three for the workpiece table ball. The orientation parameters are not required. Therefore, for a three set-up strategy, the number of parameters and coefficients to be identified will be those of the minimal-complete system (92 coefficients) plus 3x6 positioning errors for ball position errors which gives a total of 110 unknowns to be identified. Table 4.4 column **a** show these parameters and coefficients.

It is important to point out here that such a procedure relies on the hypothesis that the machine errors are primarily of a systematic nature i.e. that the machine repeatability is relatively good.

4.9 Procedure to identify the parameters and coefficients of the minimal-complete model

To identify the parameters and coefficients, equation (80) must be solved iteratively. In this equation, $?\boldsymbol{b}$ are the ball-bar readings as a column matrix, and $\boldsymbol{J}_1$ is a matrix of rectangular type. A pseudo-inverse matrix [22] has been applied to solve for the unknowns :

$$\Delta \boldsymbol{b} = \boldsymbol{J}_1 \cdot \boldsymbol{dP} \tag{80}$$

where $\boldsymbol{J}_1^+$ is called pseudo-inverse of *Moore-Penrose* of $\boldsymbol{J}_1$ which can be calculated from its SVD:

$$\boldsymbol{J}_1^+ = \boldsymbol{V}\boldsymbol{S}^+\boldsymbol{U}^T. \tag{81}$$

The Newton method [23] is used to find the best solution for $\boldsymbol{\delta P}$ through an iteration procedure. The details procedures, to identify the parameters and coefficients is shown in Fig. 4.10 and proceeds as follows:

1. Initially set the variables to be identified to their nominal (null) values and potential error parameters to the non-null true values.
2. Calculate the difference between the true and predicted ball bar lengths, $\Delta \boldsymbol{b}$, for all ball bar locations using the true tool pose ${}^{w}\boldsymbol{E}_t^{true}$ (calculated using the true variable values) and the predicted one ${}^{w}\boldsymbol{E}_t^{pred.}$ (calculated using the last identified values and the forward kinematic model).
3. Generate the identification Jacobian matrix for the last identified variable values and at the machine configurations being used for the ball bar test.

4. Solve equation (80) and update the identified values.
5. Repeat steps 2, 3 and 4 until the change in the identified variables is smaller than some convergence criteria compatible with the application context (e.g. simulation with or without noise on the data, virtual or real machine and data etc.).

4.9.1 Verification of the identified parameters and coefficients

The identified solution is judged using the following criteria :

1. If we impose non-zero values to the complete and minimal parameter set, are the identified parameters identical to the real parameters ?
2. If we impose non-zero values on all potential error parameters then is the calculated twist, representing the position and orientation of the tool relative to the workpiece identical for the true and identified parameters for configurations other than those used for the calibration procedure?

4.10 Simulation procedure and results

Two calibration simulations were conducted using specially written Matlab code. Simulation A involves imposing non-null values for all 138 potential parameters and coefficients of the maximal-complete model and then attempting to assign values (identify through calibration) to the 110 parameters and coefficients of the minimal-complete model in order to obtain a model that perfectly mimics the true machine erroneous behaviour. Simulation B involves imposing non-null values only to the 110 parameters and coefficients of the minimal-complete model and then performing the calibration. In this second simulation, we would anticipate the identified model not only to mimic the true machine behaviour but also to have exactly the same parameter and coefficient values as the true machine.

For simulation A 180 poses have been used to identify the 110 parameters and coefficients (see table 4.4 column **c**) of the three set-up strategy. Table 4.4 shows the

results of simulation A. Column **a** names all parameters and coefficients, column **c** shows the parameters and coefficients to be identified, column **b** shows the true values of each parameter of column **a**, and finally column **d** shows the corresponding identified values of parameters and coefficients of column **c**. At the 14^{th} iteration the variable change is smaller than 10^{-14}.The difference between the pose errors calculated for the calibration configurations, using the true variable values and the identified ones was smaller than 10^{-14}. Similar results are obtained when using configurations other than those used for calibration.

Table 4.5 shows the results of simulation B. Column **e** shows the parameters and coefficients to be identified and column **f** shows the corresponding true values. Column **g** shows the calculated values for these parameters and coefficients. Column **h** shows the difference between column **f** and **g**. The unknowns parameters and coefficients are all identified to better than 10^{-13}.

In all the tests, the identification Jacobian matrix has a condition number below 3500 and a rank of 110.

4.11 Conclusion

A model has been developed to calibrate a five-axis machine tool for position dependent and position independent geometric errors using the type of data acquired from a telescoping magnetic ball-bar. The mathematical solution uses the sensitivity Jacobian matrix which expresses the sensitivity of the tool-tip versus workpiece feature position to the machine geometric error sources. These error sources were modelled by Chebyshev polynomials and integrated in an sensitivity Jacobian matrix. The Chebyshev polynomials are used because of their better numerical conditioning due to their orthogonal properties .

Because there are initially more polynomial coefficients than is strictly necessary to model the error sources, a strategy is proposed to reduce the number of coefficients to a

minimal-complete model set. A formula for the required number of parameters is also proposed.

Then, a three-socket ball-bar strategy was used to identify these parameters and simulations are conducted using specially written Matlab programs and functions. The unknown coefficients and ball position parameters were calculated through a system of linear equation made of the identification Jacobian matrix and the ball-bar readings. Then, the identified polynomials are used to predict the tool-tip error for a number of machine configurations. The results confirm that the machine error polynomials can be successfully calibrated.

The selected parameters were then identified using the ball-bar measurements procedure.

Acknowledgements

This work was made possible through the financial support of Rene Mayer's NSERC Grant N° 155677-98 and Clément Fortin's NSERC Grant 36396-98.

Reference

[1] Shin, V. C., Chin, H. and Brink M. J., 1991, Characterization of CNC machining centers. Journal of Manufacturing System, v. 10, No. 5.

[2] Donmez, M. A., Blomquist, D. S., Hocken, R. J., Liu, C. R., and Barash, M. M., 1986, *A general methodology for Machine Tools Accuracy Enhancement by Error Compensation*, Precision Engineering, Vol. 8, No. 4, pp. 187-196.

[3] Donmez, M. A., Liu, C. R., and Barash, M. M., 1987, *A generalized Mathematical Model for Machine Tool Errors*, Modeling, Sensing, and Controling of Manufacturing Process, ASME Wwinter Annual Conference, PED-Vol. 23/DSC-Vol.4, pp. 231-243.

[4] Duffie, N. A., and Malmberg, S. J., 1987, *Error Diagnosis and Compensation Using Kinematic Model and Position Error data*, Annals of CIRP, Vol. 36, No. 1, pp. 355-358.

[5] ASME B5.54-1992, Methods for performance evaluation of computer numerically controlled machining centers, An American National Standard.

[6] Bryan J. B., 1982, *A simple method for testing easuring machine and machine tools Part 1: Principles and applications*, Precision Engineering, 4(2).

[7] Bryan J. B., 1982, *A simple method for testing measuring machine and machine tools Part 2: Construction details*, Precision Engineering, 4(2).

[8] Knapp, W., 1983, "Circular test for Three-Coordinate Measuring Machines and Machine Tools," Precision Enginerring, V17, pp.115-124.

[9] Knapp, W., 1983, "Test of the Three-Dimensional Uncertainty of Machine Tools and Measuring Machines and Its Relation to the Machine Errors," Annals of CIRP, V32(1), pp.459-464..

[10] Kunmann, H., and Waldele, F., 1983, On Testing Corrdinate Measuring Machines (CMM) with Kinematic Referenece Standards (KRS), Annals of CIRP, V32(1).

[11] Hai, N., Yuan, J., and Ni, J., 1994, "Revese Kinematic Analysis of Machine Tool Error Using Telescoping Ball Bar", PED-Vol.68-1, Manufacturing Science and Engineering, Volume 1, ASME.

[12] Pahk H. J., Kim Y. S. and Moon J. H., 1997, *A New Technique for Volumetric Error Assessment of CNC Machine Tools Incorporating Ball Bar Measurement and 3D Volumetric Error Model*, Int. J. Mach. Tools Manufac., **37**(11), pp. 1583-1596.

[13] Kakino Y., Ihara Y. and Shinohara A., 1993, *Accuracy Inspection of NC Machine Tools by Double Ball Bar Method*, Hanser Publishers.

[14] Burdekin, M. and Park, I., A computer Aided System for Assessing the Contouring Accuracy of NC Machine Tools, Proc. 28th MATADOR Conf., Manchester, 1988.

[15] Driels M. R., 1993, "Using Passive End-Point Motion Constraints to Calibrate Robot Manipulators, Trans. Of the ASME, Vol. 115.

[16] Rivlin, J. J., 1974, "The Chebyshev Polynomials", John Willy & Sons, New York.

[17] Craig, J. J., 1989, "Introduction to Robotics, Mechanics and Controls", Second Edition, Addison-Wesley Publishing Company.

[18] Cloutier, G., Mayer, J. R. R., 1999, "Modelisation de Machine en Fabrication Mecanique", Course material offered in the Mechanical Engineering Department, Ecole Polytechnique de Montreal.

[19] Hayati, S., Tso K. and Roston G., 1988, "Robot Geometry Calibration", IEEE international Conference on Robotics and Automation, Vol. 2, April 24-29 1988, Philadelphia, Pennsylvania.

[20] Mayer, J.R.R., Mir, Y.A., Fortin, C., 2000, "Calibration of a Five-Axis Machine Tool for Position Independent Geometric Error Parameters Using a Telescoping Magnetic Ball-Bar", MATADOR International Conference, 2000, UK.

[21] Everett L. J. and Suryohadiprojo A. H., 1988, *A study of kinematic models for forward calibration of manipulators*, IEEE Int. Conf. on Robotics and Automation, pp. 798-800.

[22] Golub, G.H., and Loan, V., 1989, "Matrix Computations", The Johns Hopkins University Press.

[23] Ciarlet, P.G., 1998, "Introduction à l'analyse numérique matricielle et à l'optimisation", Masson, ISBN 2100041673.

Table 4.1 Summary of the variables in relation to the maximal-complete and minimal-complete models.

Axis	All axis and set-up error terms for a 5-axes machine tool	a Maximals-complete model variables	b The coefficients removed	c Minimals-complete model variables	d Coefficient corresponding to PIGEPs	e Coefficient corresponding to PDGEPs
Y						
X						
A						
C						
W						
Z						
t						

Table 4.2 The PIGEPs and their corresponding polynomial coefficients in the PDGEP model.

PIGEPs for target machine (ZFYXAC)	Corresponding coefficients in the polynomials based PDGEP model
$\gamma_{Z,X}$	$\gamma_Z(y)_0$
$\gamma_{X,A}$	$\gamma_X(x)_0$
$\gamma_{Y,A}$	$\gamma_Y(x)_0$
$\gamma_{Z,A}$	$\gamma_Z(x)_0$
$e_{Y,A}$	$e_Y(a)_0$
$\gamma_{X,C}$	$\gamma_X(a)_0$
$\gamma_{X,Z}$	$e_X(z)_1$
$\gamma_{X,Z}$	$e_X(z)_1$

Table 4.3 Group of confounded variables and the removed coefficients.

Group of coupled variables	The coefficients to be removed	Strategies used	Variation of mathematical menes of the observation matrix		
			size	rank	cond
$\chi_4(1)$ & $\chi_4(2)_b$	$\chi_4(2)_b$	I	800X132	104	-
$\chi_4(1)$ & $\chi_4(2)_b$	$\chi_4(2)_b$	I	800X131	104	-
$c_4(1)$ & $c_4(2)_b$	$c_4(2)_b$	I	800X130	104	-
$c_4(1)$ & $c_4(2)_b$	$c_4(2)_b$	I	800X129	104	-
$c_4(1)$ & $c_4(2)_b$	$c_4(2)_b$	I	800X128	104	-
$c_4(c)_b$ & $c_4(W)$	$c_4(c)_b$	I	800X127	104	-
$c_4(c)_b$ & $c_4(W)$	$c_4(c)_b$	I	800X126	104	-
$c_4(c)_b$ & $c_4(W)$	$c_4(c)_b$	I	800X125	104	4.7E32
$\chi_4(d)_b$ & $\chi_4(c)_b$	$\chi_4(c)_b$	III	800X124	104	7.0E32
$c_4(d)_b$ & $c_4(W)$	$c_4(d)_b$	I	800X123	104	9.4E32
$\chi_4(c)_b$ & $c_4(W)$ & $c_4(W)$ & $\chi_4(W)$	$\chi_4(c)_b$	I	800X122	104	7.7E32
$\chi_4(c)_b$ & $c_4(W)$ & $c_4(W)$ & $c_4(W)$ & $\chi_4(W)$	$\chi_4(c)_b$	I	800X121	104	6.2E32
$c_4(d)_b$ & $\chi_4(d)_b$ & $c_4(W)$ & $c_4(W)$ & $\chi_4(W)$ & $c_4(1)$	$c_4(d)_b$	I, II, III	800X120	104	4.9E32
$\chi_4(1)_b$ & $c_4(W)$ & $c_4(W)$ & $\chi_4(W)$ & $\chi_4(d)_b$	$\chi_4(d)_b$	I, II, III	800X119	104	3.9E32
$c_4(1)_b$ & $c_4(1)$	$c_4(1)_b$	I	800X118	104	2.9E32
$\chi_4(d)_b$ & $c_4(W)$ & $c_4(W)$ & $\chi_4(W)$	$\chi_4(d)_b$	I	800X117	104	9.2E28
$c_4(1)_b$ & $c_4(1)$	$c_4(1)_b$	I	800X116	104	7.7E28
$c_4(1)_b$ & $\chi_4(1)_b$ & $c_4(2)_b$	$c_4(1)_b$	II	800X114	104	6.3E17
$c_4(1)_b$ & $c_4(1)$	$c_4(1)_b$	I	800X113	104	7.9E17
$c_4(1)_b$ & $c_4(1)$	$c_4(1)_b$	I	800X112	104	6.5E17
$c_4(1)_b$ & $\chi_4(1)_b$ & $\chi_4(1)_b$	$c_4(1)_b$	II, III	800X111	104	5.3E17
$c_4(1)_b$ & $c_4(1)$	$c_4(1)_b$	I	800X110	104	9.4E16
$c_4(1)_b$ & $c_4(1)$	$c_4(1)_b$	I	800X109	104	7.2E16
$\chi_4(1)_b$ & $\chi_4(d)_b$	$\chi_4(1)_b$	III	800X108	104	4.9E17
$c_4(1)_b$ & $\chi_4(1)_b$ & $\chi_4(2)_b$	$c_4(1)_b$ & $\chi_4(2)_b$	II, III	800X107	104	4.8E16
$c_4(1)_b$ & $\chi_4(d)_b$ & $c_4(2)_b$ & $\chi_4(2)_b$	$c_4(1)_b$	II, III	800X106	104	2.6E16
$\chi_4(1)_b$ & $c_4(2)_b$ & $\chi_4(2)_b$	$\chi_4(1)_b$	II, III	800X105	104	2.3E16
			800X104	104	1.6E3

Table 4.4 Results of simulation A : Non-null values are applied to all maximal-complete model variables.

Axis	All axis and set-up error terms for a 5-axes machine tool	a Maximum-complete model variables	b* True values for the variables of column a (10E-3)	c Minimum-complete model variables	d* Identified values for the variables of column c respectively (10E-3)
Y	$e_{x,Y}$	$e_x(y)_0\ e_x(y)_1\ e_x(y)_2\ e_x(y)_3$	6.3, 0.8, -0.4, 0.1	$e_x(y)_2\ e_x(y)_3$	-0.3819, 0.0996
	$e_{y,Y}$	$e_y(y)_0\ e_y(y)_1\ e_y(y)_2\ e_y(y)_3$	9.9, -1.1, 0.0, -0.1	$e_y(y)_1\ e_y(y)_2\ e_y(y)_3$	-1.1043, 0.0356, -0.0582
	$e_{z,Y}$	$e_z(y)_0\ e_z(y)_1\ e_z(y)_2\ e_z(y)_3$	36.5, 0.2, 0.0, 0.0	$e_z(y)_2\ e_z(y)_3$	0.0091, -0.0027
	$\chi_{x,Y}$	$\chi_x(y)_0\ \chi_x(y)_1\ \chi_x(y)_2\ \chi_x(y)_3$	9.8, 0.0, 0.0, 0.0	$\chi_x(y)_1\ \chi_x(y)_2\ \chi_x(y)_3$	0.0165, 0.0110, 0.0058
	$\chi_{y,Y}$	$\chi_y(y)_0\ \chi_y(y)_1\ \chi_y(y)_2\ \chi_y(y)_3$	7.2, 0.1, 0.0, 0.0	$\chi_y(y)_1\ \chi_y(y)_2\ \chi_y(y)_3$	0.1063, -0.0143, 0.0147
	$\chi_{z,Y}$	$\chi_z(y)_0\ \chi_z(y)_1\ \chi_z(y)_2\ \chi_z(y)_3$	2.1, 0.1, 0.0, 0.0	$\chi_z(y)_0\ \chi_z(y)_1\ \chi_z(y)_2\ \chi_z(y)_3$	2.1422, 0.05629, -0.0088, 0.0087
X	$e_{x,X}$	$e_x(x)_0\ e_x(x)_1\ e_x(x)_2\ e_x(x)_3$	75.3, 0.3, -1.1, 0.4	$e_x(x)_1\ e_x(x)_2\ e_x(x)_3$	0.2808, -1.1149, 0.3701
	$e_{y,X}$	$e_y(x)_0\ e_y(x)_1\ e_y(x)_2\ e_y(x)_3$	6.5, 0.1, -0.5, 0.0	$e_y(x)_2\ e_y(x)_3$	-0.5071, -0.0102
	$e_{z,X}$	$e_z(x)_0\ e_z(x)_1\ e_z(x)_2\ e_z(x)_3$	6.3, 0.9, 0.6, 0.3	$e_z(x)_2\ e_z(x)_3$	0.5920, 0.3390
	$\chi_{x,X}$	$\chi_x(x)_0\ \chi_x(x)_1\ \chi_x(x)_2\ \chi_x(x)_3$	11.2, 0.0, 0.0, 0.0	$\chi_x(x)_0\ \chi_x(x)_1\ \chi_x(x)_2\ \chi_x(x)_3$	11.2094, 0.0473, -0.0398, 0.0183
	$\chi_{y,X}$	$\chi_y(x)_0\ \chi_y(x)_1\ \chi_y(x)_2\ \chi_y(x)_3$	-2.0, 0.0, -0.1, 0.0	$\chi_y(x)_0\ \chi_y(x)_1\ \chi_y(x)_2\ \chi_y(x)_3$	-2.0425, -0.0218, -0.0971, 0.0186
	$\chi_{z,X}$	$\chi_z(x)_0\ \chi_z(x)_1\ \chi_z(x)_2\ \chi_z(x)_3$	-6.0, 0.0, 0.0, 0.0	$\chi_z(x)_0\ \chi_z(x)_1\ \chi_z(x)_2\ \chi_z(x)_3$	-6.0418, -0.0399, -0.0181, 0.0151
A	$e_{x,A}$	$e_x(a)_0\ e_x(a)_1\ e_x(a)_2\ e_x(a)_3$	2.7, 1.3, 0.8, -0.8	$e_x(a)_1\ e_x(a)_2\ e_x(a)_3$	1.3152, 0.8060, -0.8387
	$e_{y,A}$	$e_y(a)_0\ e_y(a)_1\ e_y(y)_2\ e_y(a)_3$	22.1, -28.1, 11.7, -2.1	$e_y(a)_0\ e_y(a)_1\ e_y(a)_2\ e_y(a)_3$	22.1330, -28.1317, 11.7257, -2.1005
	$e_{z,A}$	$e_z(a)_0\ e_z(a)_1\ e_z(a)_2\ e_z(a)_3$	4.4, 40.6, -19.2, 4.2	$e_z(a)_1\ e_z(a)_2\ e_z(a)_3$	40.6451, -19.1666, 4.2065
	$\chi_{x,A}$	$\chi_x(a)_0\ \chi_x(a)_1\ \chi_x(a)_2\ \chi_x(a)_3$	76.6, -5.9, 2.8, -0.6	$\chi_x(a)_1\ \chi_x(a)_2\ \chi_x(a)_3$	-5.9454, 2.8220, -0.6383
	$\chi_{y,A}$	$\chi_y(a)_0\ \chi_y(a)_1\ \chi_y(a)_2\ \chi_y(a)_3$	12.7, -10.7, 5.0, -1.1	$\chi_y(a)_0\ \chi_y(a)_1\ \chi_y(a)_2\ \chi_y(a)_3$	12.7338, -10.6801, 4.9712, -1.1090
	$\chi_{z,A}$	$\chi_z(a)_0\ \chi_z(a)_1\ \chi_z(a)_2\ \chi_z(a)_3$	4.8, -5.4, 2.4, -0.5	$\chi_z(a)_1\ \chi_z(a)_2\ \chi_z(a)_3$	-5.4069, 2.3983, -0.4954
C	$e_{x,C}$	$e_x(c)_0\ e_x(c)_1\ e_x(c)_2\ e_x(c)_3$	2.4, 0.8, 0.1, 0.0	$e_x(c)_1\ e_x(c)_2\ e_x(c)_3$	0.8420, 0.1308, 0.0031
	$e_{y,C}$	$e_y(c)_0\ e_y(c)_1\ e_y(c)_2\ e_y(c)_3$	27.5, -0.2, 0.3, -0.2	$e_y(c)_1\ e_y(c)_2\ e_y(c)_3$	-0.1519, 0.3092, -0.2415
	$e_{z,C}$	$e_z(c)_0\ e_z(c)_1\ e_z(c)_2\ e_z(c)_3$	3.6, -0.3, -0.1, 0.0	$e_z(c)_1\ e_z(c)_2\ e_z(c)_3$	-0.2611, -0.0715, -0.0138

	χ_C	$\chi(c)_0$ $\chi(c)_1$ $\chi(c)_2$ $\chi(c)_3$	16.7, 0.1, 0.0, 0.0	$\chi(c)_1$ $\chi(c)_2$ $\chi(c)_3$	0.0570, -0.0397, 0.0170
	χ_C	$\chi(c)_0$ $\chi(c)_1$ $\chi(c)_2$ $\chi(c)_3$	48.6, 0.1, 0.0, 0.0	$\chi(c)_1$ $\chi(c)_2$ $\chi(c)_3$	0.0590, -0.0122, 0.0083
	χ_C	$\chi(c)_0$ $\chi(c)_1$ $\chi(c)_2$ $\chi(c)_3$	9.0, -0.1, 0.0, 0.0	$\chi(c)_1$ $\chi(c)_2$ $\chi(c)_3$	-0.0612, 0.0324, -0.0158
w_1		$E_x(w)_1$, $e_x(w)_1$, $e_z(w)_1$	4.6, 2.9, -5.3	$e_x(w)_1$, $e_x(w)_1$, $e_z(w)_1$	7.0176, 2.9165, -1.6960
w_2		$E_x(w)_2$, $e_x(w)_2$, $e_z(w)_2$	4.6, 2.9, -5.3	$e_x(w)_2$, $e_x(w)_2$, $e_z(w)_2$	4.6397, -47.9830, 119.2135
w_3		$E_x(w)_3$, $e_x(w)_3$, $e_z(w)_3$	4.6, 2.9, -5.3	$e_x(w)_3$, $e_x(w)_3$, $e_z(w)_3$	38.3278, 53.3549, -124.4962
Z	$e_x z$	$e_x(z)_0$ $e_x(z)_1$ $e_x(z)_2$ $e_x(z)_3$	90.9, -41.5, -0.3, -1	$e_x(z)_1$ $e_x(z)_2$ $e_x(z)_3$	-41.5118, -0.3018, -0.0796
	$e_x z$	$e_x(z)_0$ $e_x(z)_1$ $e_x(z)_2$ $e_x(z)_3$	6.1, 0.4, 0.0, 0.0	$e_x(z)_1$ $e_x(z)_2$ $e_x(z)_3$	0.3942, -0.0137, -0.0104
	$e_z z$	$e_z(z)_0$ $e_z(z)_1$ $e_z(z)_2$ $e_z(z)_3$	9.0, -0.9, 0.1, 0.1	$e_z(z)_1$ $e_z(z)_2$ $e_z(z)_3$	-0.9339, 0.14529, 0.0979
	χ_z	$\chi(z)_0$ $\chi(z)_1$ $\chi(z)_2$ $\chi(z)_3$	50.4, -0.1, 0.0, 0.0	$\chi(z)_1$ $\chi(z)_2$ $\chi(z)_3$	-0.0618, -0.0345, -0.0191
	χ_z	$\chi(z)_0$ $\chi(z)_1$ $\chi(z)_2$ $\chi(z)_3$	51.6, -0.1, 0.0, 0.0	$\chi(z)_1$ $\chi(z)_2$ $\chi(z)_3$	-0.0579, 0.0411, 0.0024
	χ_z	$\chi(z)_0$ $\chi(z)_1$ $\chi(z)_2$ $\chi(z)_3$	3.2, 0.0, 0.0, 0.0	$\chi(z)_1$ $\chi(z)_2$ $\chi(z)_3$	0.0125, 0.0375, 0.0041
t_1		$e_x(t)_1$, $e_x(t)_1$, $e_z(t)_1$	-11.9, 8.0, 14.6	$e_x(t)_1$, $e_x(t)_1$, $e_z(t)_1$	-18.3010, 22.3442, 14.5626
t_2		$e_x(t)_2$, $e_x(t)_2$, $e_z(t)_2$	-11.9, 8.0, 14.6	$e_x(t)_2$, $e_x(t)_2$, $e_z(t)_2$	-11.8725, 8.0374, 14.5626
t_3		$e_x(t)_3$, $e_x(t)_3$, $e_z(t)_3$	-11.9, 8.0, 14.6	$e_x(t)_3$, $e_x(t)_3$, $e_z(t)_3$	-5.3688, -3.1101, -18.8496

Values are rounded off for presentation propose

Table 4.5 Results of simulation B : Non-null values are applied only to the minimal-complete model variables.

Axis	e Minimal-complete model variables	f corresponding true values for the variables of column e respectively	g corresponding identified values for the variables of column e respectively	h Difference between columns f and g (10^{-13})
Y	$e_x(y)_2$	-0.00038190000000	-0.00038190000001	0.0059
	$e_x(y)_1$	0.00009960000974	0.00009960000964	0.0993
	$e_x(y)_1$	-0.00110430000000	-0.00110430000000	-0.0019
	$e_x(y)_2$	0.00003560000000	0.00003560000000	0.0046
	$e_x(y)_1$	-0.00005820001272	-0.00005820001271	-0.0117
	$e_z(y)_2$	0.00000919998510	0.00000919998519	-0.0885
	$e_z(y)_1$	-0.00000270000377	-0.00000270000381	0.0378
	$\chi_x(y)_1$	0.00001659999313	0.0001659999314	-0.0115
	$\chi_x(y)_2$	0.00001109999853	0.00001109999853	-0.0042
	$\chi_x(y)_1$	0.00000589999890	0.00000589999890	-0.0016
	$\chi_z(y)_1$	0.00010639999941	0 00010639999941	0.0187
	$\chi_z(y)_2$	-0.00001430000085	-0.00001430000084	-0.0045
	$\chi_z(y)_1$	0.00001470000036	0.00001470000036	0 0027
	$\chi_z(y)_0$	0.00214220000191	0.00214220000189	0.0106
	$\chi_z(y)_1$	0.00005629999925	0.00005629999926	-0.0123
	$\chi_z(y)_2$	-0.00000880000123	-0.00000880000121	-0.0171
	$\chi_z(y)_1$	0.00000870000114	0.00000870000114	0.0013
X	$e_x(x)_1$	0.00028080000000	0.00028080000000	0.0071
	$e_x(x)_2$	-0.00111490000611	-0.00111490000610	-0.0052
	$e_x(x)_1$	0.00037019999562	0.00037019999568	-0.0579
	$e_x(x)_2$	-0.00050710000000	-0.00050710000000	-0.0008
	$e_x(x)_1$	-0.00001020000287	-0.00001020000287	-0.0006
	$e_z(x)_2$	0.00059200002779	0.00059200002785	-0.0565
	$e_z(x)_1$	0.00033909999353	0.00033909999355	-0.0231
	$\chi_x(x)_0$	0.01120949975437	0.01120949975436	0.0119
	$\chi_x(x)_1$	0.00004730000010	0.00004730000010	-0.0062
	$\chi_x(x)_2$	-0.00003989999732	-0.00003989999732	-0.0007
	$\chi_x(x)_1$	0.00001839999796	0.00001839999796	0.0020
	$\chi_z(x)_0$	-0.00204250000158	-0.00204250000158	0.0004
	$\chi_z(x)_1$	-0.00002180000195	-0.00002180000194	-0.0045
	$\chi_z(x)_2$	-0.00009719999613	-0.00009719999614	0.0062
	$\chi_z(x)_1$	0.00001860000025	0.00001860000025	0.0028
	$\gamma_x(x)_0$	-0.00604180000049	-0.00604180000049	0.0076
	$\gamma_x(x)_1$	-0.00003999999844	-0.00003999999845	0.0093
	$\gamma_z(x)_1$	-0.00001810000165	-0.00001810000164	-0.0014
	$\gamma_z(x)_2$	0.00001510000144	0.00001510000143	0.0048
	$\gamma_z(x)_1$			
A	$e_x(a)_1$	0.00131519999997	0.00131520000023	-0.2668
	$e_x(a)_2$	0.00080610000001	0.00080609999993	0.0812
	$e_x(a)_1$	-0.00083870000596	-0.00083870000595	-0.0058
	$e_x(a)_0$	0.02213309887471	0.02213309887466	0.0504
	$e_x(a)_1$	-0.02813170000000	-0.02813170000001	0.0071

	$e_3(a)_2$	0.01172570003272	0.01172570003267	0.0544
	$e_3(a)_3$	-0.00210050002152	-0.00210050002146	-0.0651
	$e_2(a)_1$	0.04064520000001	0.04064519999999	0 0180
	$e_2(a)_2$	-0.01916669998215	-0.01916669998218	0.0288
	$e_2(a)_3$	0.00420650000015	0.00420650000014	0.0100
	$\chi_1(a)_1$	-0.00594540000000	-0.00594540000000	-0.0004
	$\chi_1(a)_2$	0.00282200000333	0.00282200000338	-0.0431
	$\chi_1(a)_3$	-0.00063830000185	-0.00063830000188	0.0286
	$\chi_1(a)_0$	0.01273380073317	0.01273380073317	0.0006
	$\chi_2(a)_1$	-0.01068010000000	-0.01068010000000	-0.0013
	$\chi_2(a)_2$	0.00497129999868	0.00497129999869	-0.0088
	$\chi_2(a)_3$	-0.00110909999840	-0.00110909999841	0.0092
	$\chi_3(a)_1$	-0.00540690000000	-0.00540690000000	-0.0029
	$\chi_3(a)_2$	0.00239830000218	0.00239830000221	-0.0315
	$\chi_3(a)_3$	-0.00049549999944	-0.00049549999946	0.0213
C	$e_1(c)_1$	0.00084200000000	0.00084200000000	0.0015
	$e_1(c)_2$	0.00013086730899	0.00013086730902	-0.0257
	$e_1(c)_3$	0.00000310236679	0.00000310236679	0.0028
	$e_2(c)_1$	-0.00015190000000	-0.00015190000000	-0.0023
	$e_2(c)_2$	0.00030920000000	0.00030920000000	-0.0042
	$e_2(c)_3$	-0.00024150000000	-0.00024150000000	0.0036
	$e_3(c)_1$	-0.00026110000000	-0.00026110000000	0.0005
	$e_3(c)_2$	-0.00007150000000	-0.00007150000000	-0.0038
	$e_3(c)_3$	-0.00001380000000	-0.00001380000000	0.0004
	$\chi_1(c)_1$	0.00005705438836	0.00005705438835	0.0042
	$\chi_1(c)_2$	-0.00003976820712	-0.00003976820713	0.0046
	$\chi_1(c)_3$	0.00001700000000	0.00001700000000	0.0005
	$\chi_2(c)_1$	0.00005905279408	0.00005905279407	0.0071
	$\chi_2(c)_2$	-0.00001228290869	-0.00001228290869	0.0001
	$\chi_2(c)_3$	0.00000839556672	0.00000839556672	-0.0003
	$\chi_3(c)_1$	-0.00006120000000	-0.00006120000000	0.0005
	$\chi_3(c)_2$	0.00003240000000	0.00003240000000	0.0002
	$\chi_3(c)_3$	-0.00001589160945	-0.00001589160945	0.0030
w_1	$e_1(w)_1$	0.00701769999826	0.00701769999829	-0.2520
	$e_2(w)_1$	0.00291650000663	0.00291650000659	0.4065
	$e_3(w)_1$	-0.00169609994919	-0.00169609994927	0.8341
w_2	$e_1(w)_2$	0.00463969999999	0.00463970000001	-0.2247
	$e_2(w)_2$	-0.04798309731772	-0.04798309731774	0.1454
	$e_3(w)_2$	0.11921359683634	0.11921359683636	-0.1899
w_3	$e_1(w)_3$	0.03832784179696	0.03832784179697	-0.0881
	$e_2(w)_3$	0.05335497714163	0.05335497714163	0.0617
	$e_3(w)_3$	-0.12449626942914	-0.12449626942914	0.2151
Z	$e_1(z)_1$	-0.04151190000000	-0.04151189999999	-0.0972
	$e_1(z)_2$	-0.00030189998495	-0.00030189998498	0.2971
	$e_1(z)_3$	-0.00007969999374	-0.00007969999374	0.0055
	$e_2(z)_1$	0.00039430000000	0.00039429999999	0.0950
	$e_2(z)_2$	-0.00001370000000	-0.00001370000000	-0.0186
	$e_2(z)_3$	-0.00001040000000	-0.00001040000000	0.0241
	$e_3(z)_1$	-0.00093390000000	-0.00093390000000	0.0103

	$e_2(2)_2$	0.00014530000000	0.00014529999999	0.0923
	$e_2(2)_3$	0.00009790000000	0.00009790000000	-0.0227
	$\chi_1(2)_1$	-0.00006185927788	-0.00006185927785	-0.3505
	$\chi_1(2)_2$	-0.00003455381887	-0.00003455381888	0.1506
	$\chi_1(2)_3$	-0.00001916346670	-0.00001916346671	0.0868
	$\chi_2(2)_1$	-0.00005790000000	-0.00005790000000	-0.0069
	$\chi_2(2)_2$	0.00004110000000	0.00004110000000	0.0261
	$\chi_2(2)_3$	0.00000240000000	0.00000240000000	0.0068
	$\gamma_2(2)_1$	0.00001250143051	0.00001250143050	0.1370
	$\gamma_2(2)_2$	0.00003750080420	0.00003750080420	0.0362
	$\gamma_2(2)_3$	0.00000410044589	0.00000410044589	-0.0038
t_1	$e_1(t)_1$	-0.01830106094477	-0.01830106094474	-0.0272
	$e_1(t)_2$	0.02234428513662	0.02234428513652	0.1036
	$e_1(t)_3$	0.01456260001271	0.01456260001257	0.1434
t_2	$e_1(t)_1$	-0.01187260000003	-0.01187259999984	-0.1885
	$e_1(t)_2$	0.00803740000000	0.00803740000000	0.0064
	$e_1(t)_3$	0.01456259999999	0.01456260000000	-0.0105
t_3	$e_1(t)_1$	-0.00536880359126	-0.00536880359126	0.1013
	$e_1(t)_2$	-0.00311010842865	-0.00311010842865	-0.0745
	$e_1(t)_3$	-0.01884961360836	-0.01884961360836	0.3847

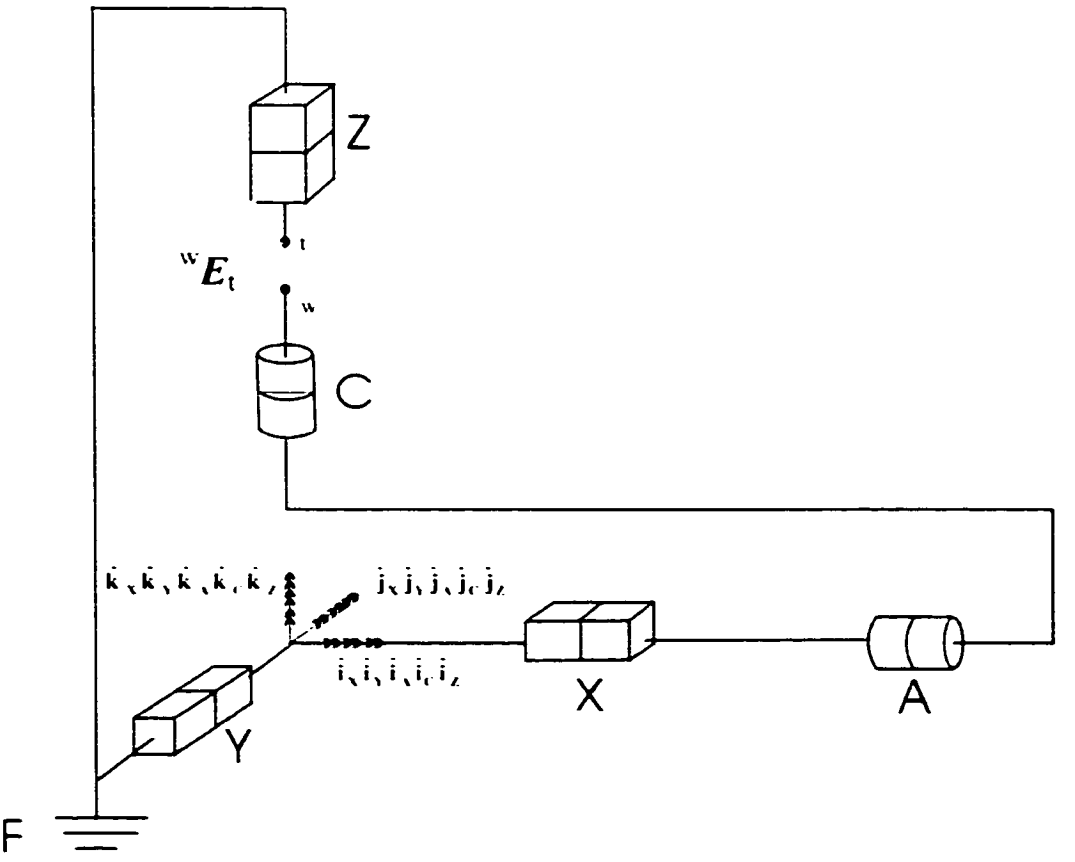

Figure 4.1 Joint frames at zero coordinate $\theta=[0\ 0\ 0\ 0\ 0]^T$.

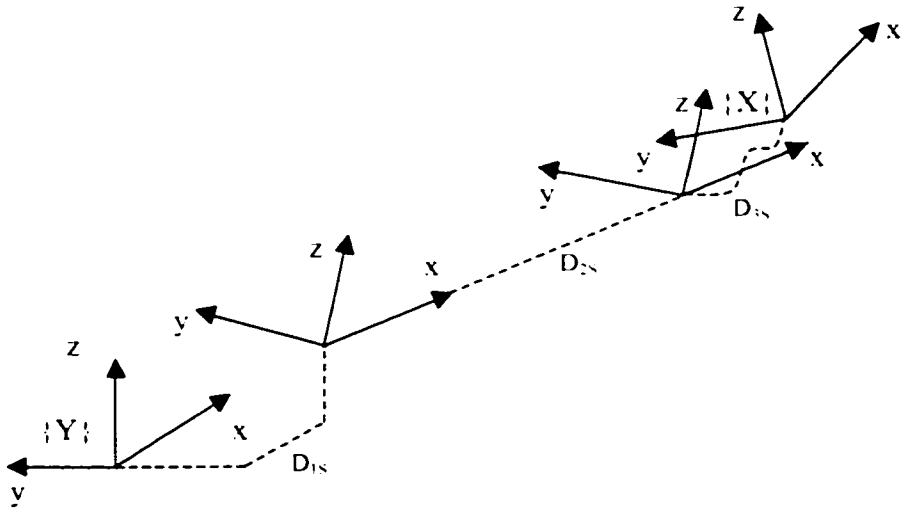

Figure 4.2 Sub-HTM of each joint-link transformation from referenec {Y} to reference {X}.

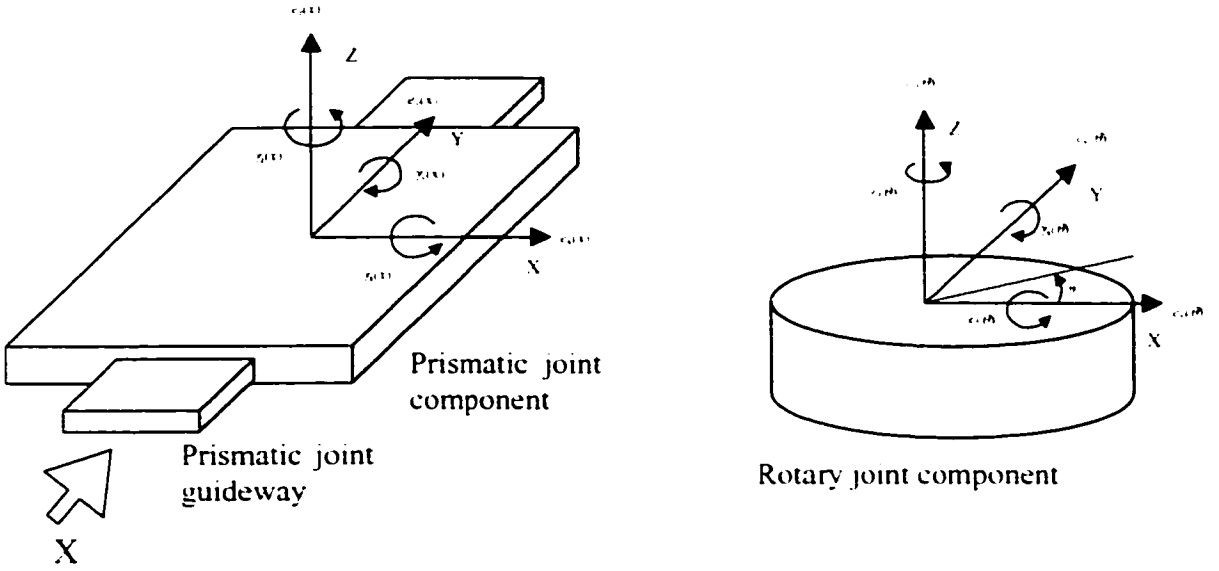

Figure 4.3 Linear and angular errors for prismatic and rotary joints.

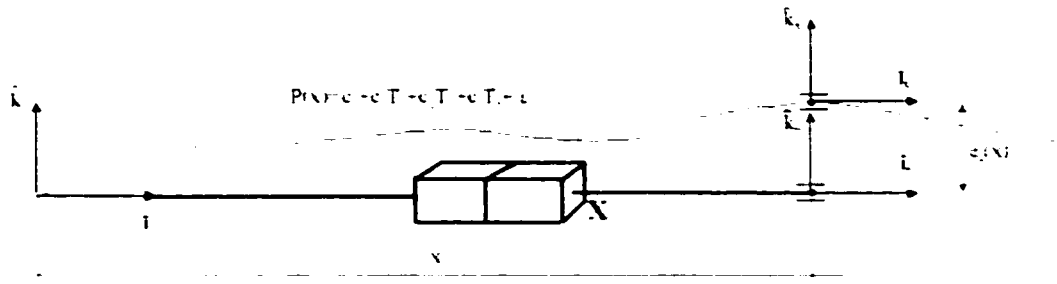

Figure 4.4 Polynomial representation of a PDGEP parameters.

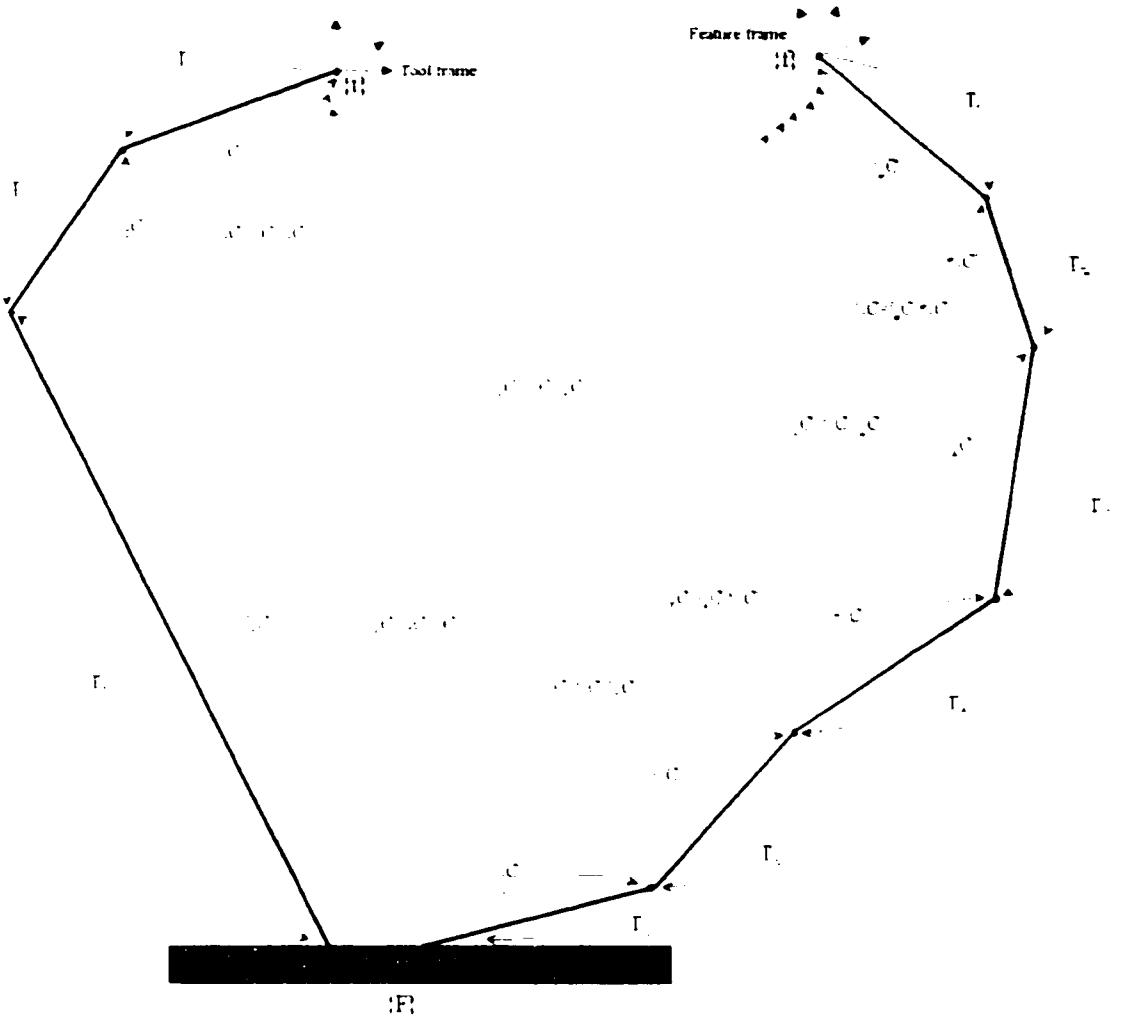

Figure 4.5 The construction and propagation routes of the transport matrices in relation to the machine topology and the individual joint HTMs.

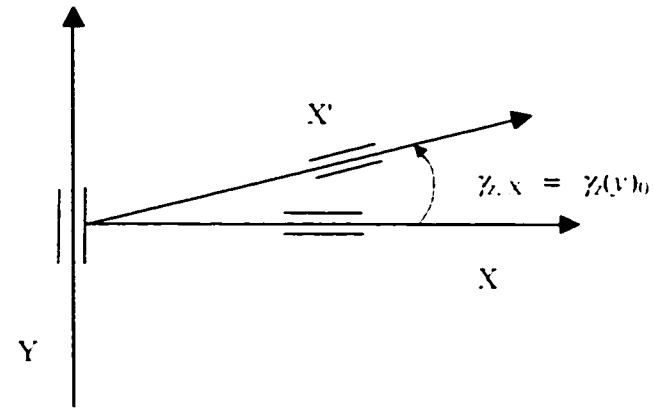

Figure 4.6 Correspondence between $\gamma_{z,x}$ and $\gamma_z(y)_0$

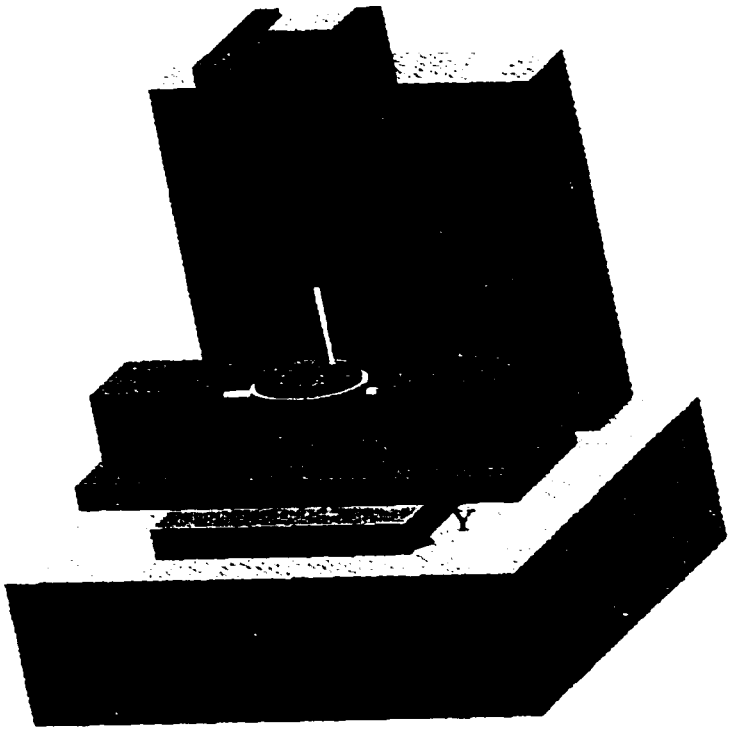

Fig. 4.7a Matsuura

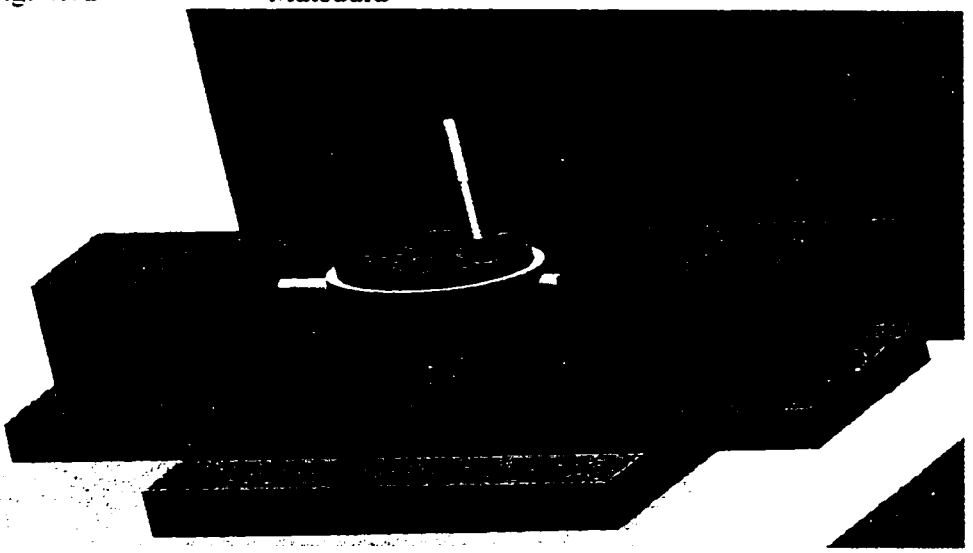

Fig. 4.7b Ball-bar set-up

Figure 4.7 Matsuura machine tool with a ball-bar set-up.

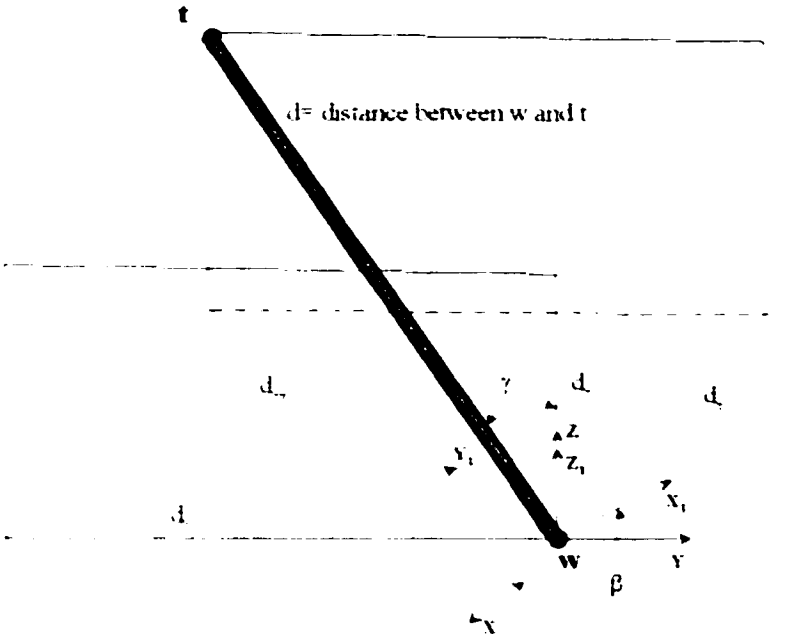

Figure 4.8 Orientation of the machine positioning error twist in the direction of the ball-bar.

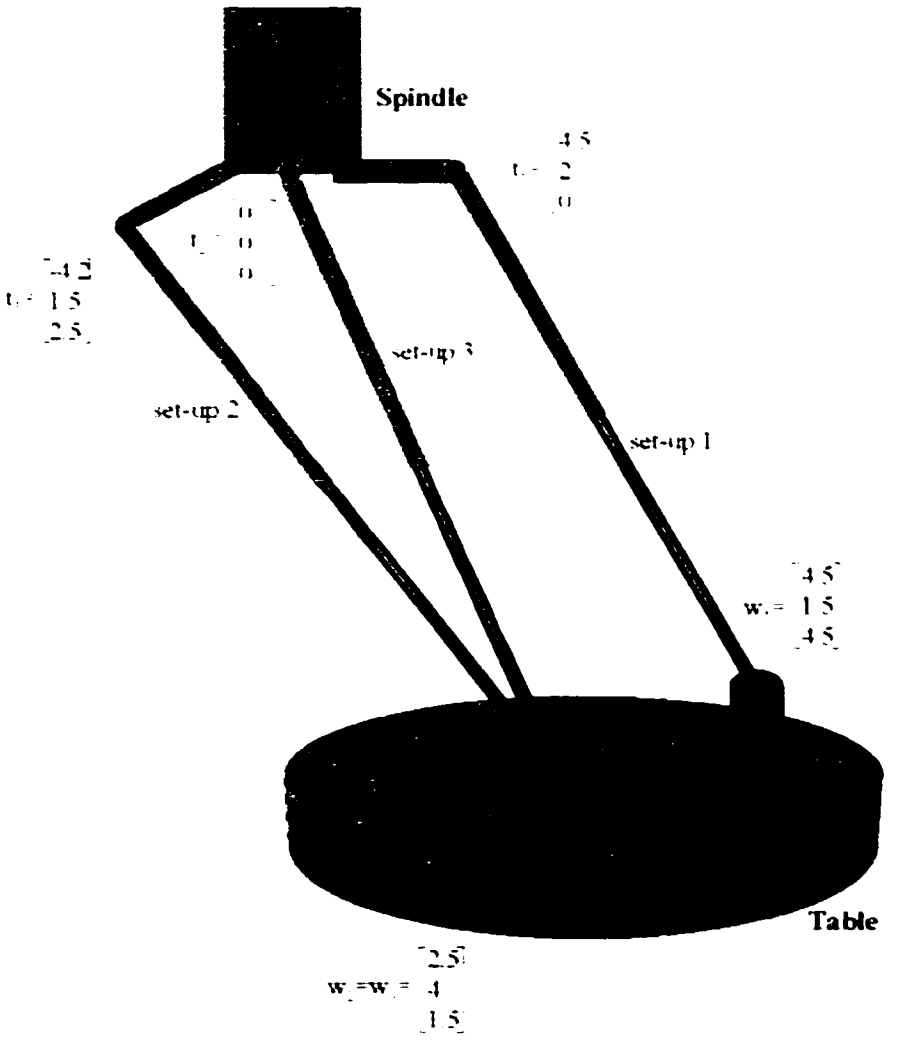

Figure 4.9 Three set-up strategy. Each set-up is performed separately.

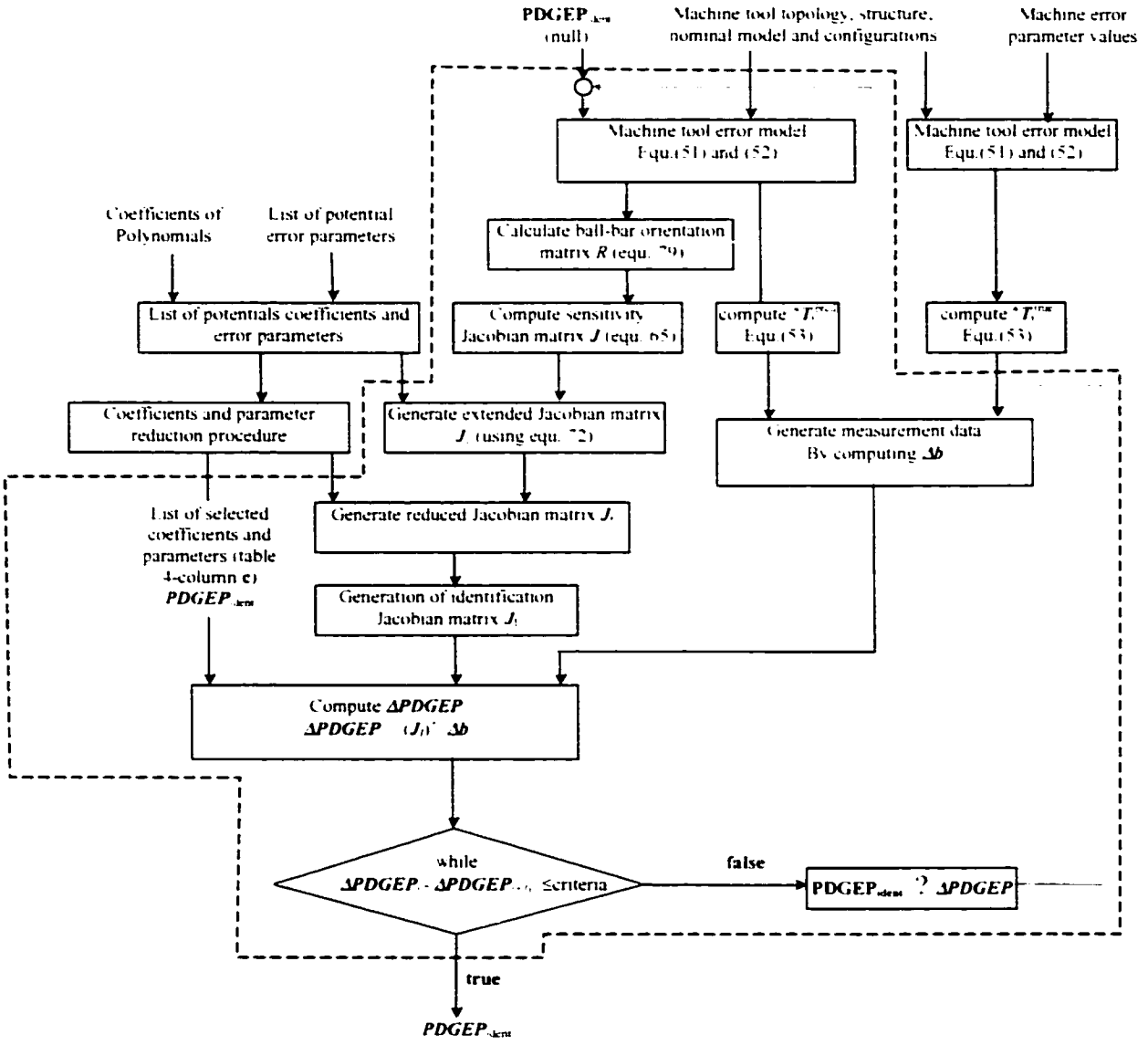

Figure 4.10 Graph presenting the simulation algorithm for PDGEPs.

CHAPTER 5: TOOL PATH ERROR PREDICTION OF A FIVE-AXIS MACHINE TOOL WITH GEOMETRIC ERRORS

Y. A. Mir, J.R.R. Mayer*, and C. Fortin

*‡Mechanical Engineering Department
École Polytechnique de Montréal
P. O. Box 6079, Station «Downtown»
Montréal, Québec, Canada

Submitted in June 2001 to the Journal of Engineering Manufacture
*To whom correspondence should be addressed:rene.mayer@meca.polymtl.ca

5.1 Présentation du chapitre et liens utiles

Dans ce chapitre une méthode est présentée pour prévoir l'effet des erreurs géométriques des machines-outils sur la position de bout d'outil. On considère les deux catégories d'erreurs, les liaisons (les paramètres d'erreurs géométriques indépendants de la position) et les erreurs de mouvement (les paramètres d'erreurs géométriques dépendants de la position). Dans les chapitres précédents, les paramètres d'erreurs ont été identifiés. Ces derniers sont utilisés dans une procédure de prédiction d'erreurs pour calculer les erreurs associées au bout d'outil pour des emplacements de commande donnés sur une surface. La surface prévue est comparée avec la surface nominale de la pièce et ensuite la différence est comparée avec la zone de tolérance. Le résultat donne l'information utile au gammiste pour décider si vraiment la machine-outil choisie est capable d'exécuter l'opération dans la tolérance désirable. Une réponse négative à cette question mène à un

changement de la machine-outil, du processus ou simplement à une compensation de l'erreur de la machine outil. Une méthodologie est aussi suggérée pour intégrer cette méthode dans un environnement CAO/FAO.

5.2 Abstract

Predicting the actual tool path of a machine tool prior to machining a part provides useful data in order to ensure or improve the dimensional accuracy of the part. The actual tool path can be estimated by accounting for the effect of the machine tool geometric error parameters on the tool path. In CAD/CAM systems, the nominal tool path (or CL data) is directly generated from the curves and surfaces to be machined and the errors of the machine tool are not considered. In order to take these errors in consideration, they must first be identified and then used in the machine tool forward kinematic model. In this paper a method is presented to identify the geometric errors of machine tools and predict their effect on the tool-tip position. Both the link errors (position independent geometric error parameters) and the motion errors (position independent geometric error parameters) are considered. The nominal and predicted tool paths are compared and an assessment is made of the resulting surfaces with respect to the desired part profile tolerance. A methodology is also suggested to integrate this tool within a CAD/CAPP/CAM environment.

Keywords: Five-axis machine tool calibration, cutter location file, tool path error prediction.

5.3 Introduction

The ability to simulate the machining operation and predict the accuracy of the result during the early stages of process plan development is an important research issue in CAD/CAM, computer-aided process planning (CAPP), and also for the virtual machining concept **[1, 2, 3, 4, 5]**. It allows manufacturing engineers to predict the resulting shape of a part before its actual production in order to verify machining and

other operation parameters before a first part is made thus reducing the cost of trial and error. It can also reduce cost and increase the quality of parts through early corrective actions.

Producing an accurate part depends to a great extent on the realisation of an accurate tool path. The machine tool errors, which exist during machining, have to be identified and their influence on the machining of a surface predicted. Errors due to kinematic inaccuracies of the machine tool components strongly influence the quality of parts. Many research activities have been conducted in the last two decades to identify the geometric inaccuracies of the machine tool and to enhance its performance in order to produce more accurate parts **[6, 7, 8, 9]**. In recent years, the ball-bar has found widespread acceptance alongside laser interferometers to measure inaccuracies of machine tools by inspecting the tool attachment point motion inaccuracies**[10, 11, 12, 13]**.

Accurately positioning the tool-tip to a desired point is key to producing a precise part. There are several error sources, which prevent positioning the tool to the desired location a to machine a specific geometric feature on a part. Amongst them are geometric errors of machine tools, temperature variation of machine tool, tool deflection, tool wear, and interpolation and control algorithms. Much work has been done on the tool path generation, through analysing other factors such as tool collision, tool deflection, exact interpolation etc. Morishing et al. **[14]** applied a 3D configuration space to avoid tool collision when generating tool path for complex geometry by generating a modified version of CL data. Leu et al. developed a methodology to verify the NC machining tool path due to tool deflection **[15, 16, 17]**. Korean **[18]** worked on the development of interpolator in order to overcome the difficulty of generating tool trajectories that follow exactly the curvature of the geometric elements designed in CAD model. Ge **[19]** developed an approach in which sculptured surface are represented directly in terms of Bezier and B-spline motions of the cutting tool. By this approach Ge tried to bring the tool movement close to the design curve in a reverse manner.

Frey developed a concept to generate cutting tool trajectory using swept envelope **[20]**. In this approach the tool is represented as a solid which can move following a curve defined into another solid. In this work the effects of the errors of the machine tool on the movement of the tool have been considered for a grinding machine. The method is limited to tool shapes that have a revolution symmetry. The interpolation algorithms of the machine controller and its impact on the tool trajectories and thus on the machined part is not addressed.

The machining of a part takes place by positioning the tool-tip at locations defined in the CL data file. In order to achieve these tool-tip positions and orientations we calculate the corresponding joint coordinate values of the machine tool axes. These values are calculated through an inverse kinematic model. When each axis moves for positioning the tool-tip, the errors associated with that axis and its actual position intervene.

In this study we consider the effect of the geometric errors of a five axis machine tool on the accuracy of a machined part and we propose a complete calibration procedure for both the position independent geometric error parameters (PIGEPs) and the position dependent geometric error parameters (PDGEPs) using a telescoping magnetic ball-bar and an identification procedure. It requires the development of a geometric model of the machine, polynomial functions to represent the position dependent parametric errors, and an identification sensitivity Jacobian matrix to quantify the sensitivities of the ball bar measurements to machine tool errors. An assessment of the conformity of parts to be produced can be done by analysing the predicted tool path and resulting surface. To do so a nominal CL data file is generated on the basis of the machining process plan. Then the corresponding trajectory of the tool can be generated directly from a CAD/CAM system. The predicted (imperfect) trajectory can be calculated by considering the identified errors of the machine tool for the planned trajectory. The nominal and predicted surfaces so generated following each of this trajectory leads to two different surfaces here named the nominal and predicted surfaces. The nominal and predicted surfaces are compared and the departure is evaluated against the desired profile tolerance

on the part drawing. This analysis helps the process planner select an appropriate machine tool and process. If required, a compensation procedure can then be suggested to correct the actual tool trajectory.

An illustrative example is presented for a milling process on a machine tool with a ZFYXAC topology. First a nominal CL data is generated directly from CAD/CAM . Then a predicted CL-data is generated . The surfaces related to these two CL data are compared and analysed in order to verify whether the real model is within tolerance or not.

5.4 Error modelling and identification

In this section a procedure is presented to identify the geometric errors of a five-axis machine tool. These error are individually modelled as polynomial functions of the individual machine tool joint position. It is then possible to predict the tool-tip position and orientation errors for a given machining task.

5.4.1 Direct kinematic model of a five-axis serial machine tool

The kinematic model describes the relative location between a workpiece feature frame w rigidly attached to the table and a tool frame t rigidly attached to the tool attachment point (see Figure 5.1a). From the base or foundation frame F we define a tool branch and a workpiece feature branch using their homogenous transformation matrix (HTMs) ${}^{F}\mathbf{T}_{t}$ and ${}^{F}\mathbf{T}_{w}$ respectively. ${}^{j}\mathbf{T}_{i}$ denotes the 4x4 HTM representing the pose (position and orientation) of frame i with respect to frame j. Thus, the pose of t relative to w is given as

$$ {}^{w}\mathbf{T}_{t} = [{}^{F}\mathbf{T}_{w}]\text{-}1 \; {}^{F}\mathbf{T}_{t} \qquad (82) $$

The HTM for a non-ideal link and joint combination including the nominal description and the imperfections in the link and joint can be modelled using 3 HTMs (see Figure 5.1b).

$$\mathbf{D}_S = \mathbf{D}_{1S}\,\mathbf{D}_{2S}\,\mathbf{D}_{3S} \tag{83}$$

$\mathbf{D}_{1S}$ is the nominal link HTM, $\mathbf{D}_{2S}$ describe the nominal motion of the joint frame and $\mathbf{D}_{3S}$ describe the form errors of joint motion. For a machine tool with ZFYXAC topology S can be either of Z, Y, X, A, or C and all nominal parameters are null. $\mathbf{D}_S$ is used to calculate the resultant positioning errors for any multi-axis machine with an arbitrary serial combination of rotary and prismatic joint **[21, 22]**.

For joint X for example:

$$\mathbf{D}_X = \mathbf{D}_{1X}\,\mathbf{D}_{2X}\,\mathbf{D}_{3X} \tag{84}$$

where, $\mathbf{D}_{1X}$ is the nominal link HTM defined as:

$$\mathbf{D}_{1X} = \mathbf{trans}(\hat{\mathbf{i}}, a_x(x))\,\mathbf{trans}(\hat{\mathbf{j}}, a_y(x))\,\mathbf{trans}(\hat{\mathbf{k}}, a_z(x))\,\mathbf{rot}(\hat{\mathbf{k}}, \alpha_z(x))\,\mathbf{rot}(\hat{\mathbf{j}}, \alpha_y(x))\,\mathbf{rot}(\hat{\mathbf{i}}, \alpha_x(x)) \tag{85}$$

where for example $\mathbf{trans}(\hat{\mathbf{i}}, a_x(x))$ is the HTM for a linear displacement by a value $a_x(x)$ along the $\hat{\mathbf{i}}$ direction; $\mathbf{rot}(\hat{\mathbf{i}}, \alpha_x(x))$ is the HTM for a rotation of $\alpha_x(x)$ around $\hat{\mathbf{i}}$. The joint HTMs $\mathbf{D}_{2X}$ describes the nominal motion of the joint.

$$\mathbf{D}_{2X} = \mathbf{trans}(\hat{\mathbf{i}}, x) \text{ for a prismatic joint} \tag{86}$$

$\mathbf{D}_{3X}$ describes the form errors (and link errors) of the joint motion (PDGEPs).

$$\mathbf{D}_{3X} = \mathbf{trans}(\hat{\mathbf{i}}, e_x(x))\,\mathbf{trans}(\hat{\mathbf{j}}, e_y(x))\,\mathbf{trans}(\hat{\mathbf{k}}, e_z(x))\,\mathbf{rot}(\hat{\mathbf{k}}, \gamma_z(x))\,\mathbf{rot}(\hat{\mathbf{j}}, \gamma_y(x))\,\mathbf{rot}(\hat{\mathbf{i}}, \gamma_x(x)) \tag{87}$$

where $e_x(x)$, $e_y(x)$ and $e_z(x)$ are the linear errors along joint X and $\gamma_x(x)$, $\gamma_y(x)$ and $\gamma_z(x)$ are the angular errors (roll, pitch and yaw) along the joint. Similar operations are required for the Y, A, C and Z axes.

Because of the various machine errors, the actual tool tip frame and the workpiece feature frame do not coincide by an error ${}^{w}\mathbf{E}_t$ (see Fig. 5.1a) calculated as follows for the ZFYXAC topology machine tool :

$$
\begin{aligned}
{}^{F}\mathbf{T}_{t} &= \mathbf{D}_{z}\mathbf{T}_{t} \\
{}^{F}\mathbf{T}_{w} &= \mathbf{D}_{y}\,\mathbf{D}_{x}\,\mathbf{D}_{a}\,\mathbf{D}_{c}\,\mathbf{T}_{w}. \\
{}^{F}\mathbf{T}_{t} &= {}^{F}\mathbf{T}_{w}\ {}^{w}\mathbf{E}_{t}
\end{aligned}
\qquad (88)
$$

and finally:

$$
{}^{w}\mathbf{E}_{t} = [{}^{F}\mathbf{T}_{w}]^{-1}\ {}^{F}\mathbf{T}_{t} \qquad (89)
$$

5.4.2 Polynomials representation

The Chebyshev polynomials **[23]** are chosen to model the link and motion error parameters (PIGEPs and PDGEPs). These polynomial have orthogonal characteristics and can generate a better numerical conditioning of the associated sensitivity Jacobian matrix. The general form of Chebyshev polynomials is:

$$
T_{n}(s_{N}) = \cos n\theta \qquad (90)
$$

where n is a nonnegative integer, s_N is the normalized joint coordinate, $\theta=\arccos(s_N)$ and $0 \le \theta \le \pi$. $T_n(s_N)$ is defined by equation (90) on the interval $-1 \le s_N \le 1$. Chebyshev polynomials of degree 3 are used in this work, without lost of generality, and are defined as:

$$
p(s_{N}) = c_{0}T_{0}(s_{N}) + c_{1}T_{1}(s_{N}) + c_{2}T_{2}(s_{N}) + c_{3}T_{3}(s_{N}) \qquad (91)
$$

where

$$
\begin{aligned}
T_{0}(s_{N}) &= 1 \\
T_{1}(s_{N}) &= s_{N} \\
T_{2}(s_{N}) &= 2s_{N}^{2} - 1 \\
T_{3}(s_{N}) &= 4s_{N}^{3} - 3s_{N}
\end{aligned}
\qquad (92)
$$

and c_0, c_1, c_2, c_3 are the coefficients.

In general for each error type e on the machine tool, the polynomial is presented as:

$$p_e(s_N) = c_0^e T_0(s_N) + c_1^e T_1(s_N) + c_2^e T_2(s_N) + c_3^e T_3(s_N) \quad (93)$$

where s is one of x, y, z, a, b or c and e represents one of the six geometric errors of a particular axis (e.g. $e_x(s)$, $e_y(s)$, $e_z(s)$, $\gamma_x(s)$, $\gamma_y(s)$ and $\gamma_z(s)$).

For example the value of $e_y(x)$, the y-direction straightness error of the X axis at its commanded coordinate x_N, is calculated using equation (93) as follows :

$$e_y(x) = c_0^{e_y} T_0(x_N) + c_1^{e_y} T_1(x_N) + c_2^{e_y} T_2(x_N) + c_3^{e_y} T_3(x_N) \quad (94)$$

where $c_0^{e_y}$, $c_1^{e_y}$, $c_2^{e_y}$ *and* $c_3^{e_y}$ are the polynomial coefficients for $e_y(x_N)$ and x_N is a normalised joint coordinate value for the X axis. Therefore, for a given position on the machine tool, thirty polynomials are evaluated, which represent 30-errors (positions and angular) of a five axis machine tool (six error for each axis). In addition to these errors, there exist also errors for fixing the part and tool on the table and spindle respectively, which must also be considered. Once these errors are calculated, they are introduced in the forward kinematic error model (equation (83)) to calculate the tool-tip error relative to the part.

5.4.3 Error identification

With a perfect machine tool structure ${}^{w}\mathbf{E}_t$ is null. However in reality imperfections exist and therefore, the errors should be identified. The machine error parameters can be identified using data collected with a ball bar instrument contained in vertical matrix $\boldsymbol{\delta\tau}$. This requires the modelling of the motion errors with polynomial functions in order to obtain a reasonable number of unknown variables contained in vertical matrix $\boldsymbol{\delta p}$ for the identification algorithm. Furthermore, in order to facilitate the calculation of these unknowns, a linear model relating the effect of the unknown variables on the ball bar measurement is generated using Newton-Euler equations.

5.4.3.1 Generation of the sensitivity Jacobian matrix

From the nominal links and joint coordinate at each pose, the sensitivity Jacobian matrix, **J**, is obtained using Newton-Euler's equation for a specific machine tool topology, geometry and joint position. This matrix determines the changes in the tool versus workpiece feature location $\boldsymbol{\delta\tau}$ resulting from small changes in the machine error parameters $\boldsymbol{\delta p}$.

$$\boldsymbol{\delta\tau} = \boldsymbol{J}\,\boldsymbol{\delta p} \tag{95}$$

$\boldsymbol{\delta p}$ is a vertical concatenation of one or more 6-by-1 twists. An error twist is made of the vertical concatenation of the three small positional errors and of the three small angular errors associated the moving element of a link-joint combination. $\boldsymbol{\delta\tau}$ is vertical concatenation of the resulting 6-by-1 error twist of the tool frame location relative to the workpiece feature location. The sensitivity Jacobian matrix **J** is built using transport matrices. A transport matrix is generated using a HTM and propagates the effect of an error twist $[e_x\ e_y\ e_z\ \gamma_x\ \gamma_y\ \gamma_z]^T$ occurring in one reference frame onto another frame rigidly connected to the former

$$^{\{B\}}\mathbf{dt}_B = {}^B_A\mathbf{C}\,{}^{\{A\}}\mathbf{dt}_A \tag{96}$$

where $^{\{B\}}\mathbf{dt}_B$ is the propagated twist (small displacement) at B, expressed in frame B, $^{\{A\}}\mathbf{dt}_A$ is the causal twist in A, expressed in frame A, and ${}^B_A\mathbf{C}$ is a 6-by-6 transport matrix **[24, 25, 26]**. The transport matrix can be formed using sub-matrices of an HTM as follows :

$$\text{if } {}^{A}_{B}\mathbf{T} = \begin{bmatrix} {}^{A}_{B}\mathbf{R} & {}^{A}\mathbf{P}_{B} \\ 000 & 1 \end{bmatrix} \quad \Rightarrow \quad {}^{B}_{A}\mathbf{C} = \begin{bmatrix} {}^{A}_{B}\mathbf{R}^{T} & {}^{A}_{B}\mathbf{R}^{T}\left[{}^{A}\mathbf{P}_{B}\times\right]^{T} \\ 0\ 0\ 0 & \\ 0\ 0\ 0 & {}^{A}_{B}\mathbf{R}^{T} \\ 0\ 0\ 0 & \end{bmatrix}. \tag{97}$$

Since the tool path information (cutter location file) is presented in the tool frame, the error should be transformed into the tool-frame. For the machine considered, this can be accomplished by forming a sensitivity Jacobian matrix as follow:

$${}^{\{t\}}\mathbf{dt}_{t} = \mathbf{J}\,\mathbf{dp} \tag{98}$$

where ${}^{\{t\}}\mathbf{dt}_{t}$ is a twist with size $6m$-by-1. $\mathbf{J}$ is the sensitivity Jacobian matrix with size $(6m)$-by-n, and $\mathbf{dp}$ is the error parameter column matrix with n elements. The number of poses and error parameters are m and n respectively.

For example for a ZFYXAC machine, the sensitivity Jacobian matrix is

$${}^{t}_{t}\mathbf{J} = \left[-{}^{t}_{F}\mathbf{C}\cdot{}^{t}_{F}\mathbf{C}^{-1}\cdot{}^{\{t\}F}_{t}\mathbf{J} \quad {}^{\{t\}F}_{t}\mathbf{J}\right] \tag{99}$$

where

$${}^{\{t\}F}_{t}\mathbf{J} = \left[{}^{t}_{t}\mathbf{C} \quad {}^{t}_{1}\mathbf{C} \quad {}^{t}_{1}\mathbf{C} \quad {}^{t}_{1}\mathbf{C} \quad {}^{t}_{1}\mathbf{C} \quad {}^{t}_{1}\mathbf{C} \quad {}^{t}_{t}\mathbf{C}\right|_{6\times(7-6)} \tag{100}$$

$${}^{\{t\}F}_{t}\mathbf{J} = \left[{}^{t}_{F}\mathbf{C} \quad {}^{t}_{2}\mathbf{C} \quad {}^{t}_{3}\mathbf{C} \quad {}^{t}_{t}\mathbf{C}\right|_{6\times(4-6)} \tag{101}$$

and

$${}^{t}_{F}\mathbf{C}^{-1} = {}^{F}_{t}\mathbf{C} \tag{102}$$

In equation (100), ${}^{\{t\}F}_{t}\mathbf{J}$ expresses the sensitivity of the feature frame location f observed from the foundation frame F and expressed in the feature frame f to causal error parameters within the feature branch. Whereas in equation (101), ${}^{\{t\}F}_{t}\mathbf{J}$ expresses the sensitivity of the tool frame location t observed from the foundation frame F and expressed in the tool frame t to causal error parameters within the tool branch.

5.4.3.2 Procedure to identify the coefficients

Equation (103) is a linear system which calculate the relative location errors of the tool-tip to a feature on the workpiece expressed in the tool frame:

$$\left[{}^{(t)_i}\mathbf{t}_i\right] = \left[{}^{(t)_i}_{i}\mathbf{J}\right] \cdot [\mathbf{dp}] \qquad (103)$$

where ${}^{(t)_i}\mathbf{t}_i$ is a twist with (m.6)-by-1, ${}^{(t)_i}_{i}\mathbf{J}$ is the sensitivity Jacobian matrix with (m.6)-by-n, and **dp** is the error parameter matrix with n-by-1, m and n are the number of poses and error parameters respectively.

Each column of the sensitivity Jacobian matrix represents an error term in the system. For a five-axis machine there exist 30 machine tool error parameters represented as polynomials and 12 positioning and orienting errors for part and tool location (6 for each). Therefore, the identification sensitivity Jacobian matrix has a 30+12 columns.

However, since each error parameter of a machine tool is presented as a polynomial function of degree 3, each of these errors will be represented by 4 coefficients. Accomplishing this results in a new Jacobian matrix called the extended sensitivity Jacobian matrix with 30x4+12=132 columns. The extension is performed using a process similar to that used to produce a Vandermonde matrix. In Table 5.1, column **a** shows these error terms. Because of redundancies amongst coefficients of different joints it is necessary to remove some of them to form a minimal-complete model which nevertheless fully represents the erroneous geometric behaviour of the imperfect machine just as the maximal-complete model does. The minimal-complete number of parameters and coefficients can be selected using geometric insight of the physical behaviour of the machine tool and mathematical analysis of the extended sensitivity Jacobian Matrix [22]. The resulting matrix is a reduced sensitivity Jacobian matrix $\mathbf{J}_r$ and can be used to identify the parameters and coefficients. Column **c** in Table 5.1, shows these parameters, column **a** shows all 132 error parameters including redundant one and column **b** shows those parameters that have been removed.

In order to propagate the effects of the coefficients and parameters onto the ball bar readings, a matrix called the identification Jacobian matrix $\mathbf{J}_I$ is derived from the reduced sensitivity Jacobian matrix. This matrix has m lines instead of the 6m lines of the reduced sensitivity Jacobian matrix because the ball bar only detects the orientation of the positional changes along its axis which passes through the two balls.

An analysis of the identification Jacobian for a single ball bar setup shows that there can never be enough measurement configuration used to successfully identify the retained parameters and coefficients. It is necessary to add two more measurement set-ups for a total of three to fully calibrate the five-axis machine tool. Figure 5.2 shows three set-ups used in turns and the position of each socket on the table and spindle. Figure 5.3 illustrates the identification procedure to calculate the coefficients of the polynomials and the sockets position error parameters. Column **d** of Table 5.2 shows the identified values of the coefficients and sockets' position errors. Although the identified values differ sometimes significantly from the true ones, it was verified that the identified machine behaves geometrically like the true one. The differences are due to redundancies in the definition of the true machine. Further tests this time only applying non null true values to the minimal-complete set of variables results in identified values that are identical to the true ones.

5.5 Verification of tool path

During process plan development, a CAD model of a part is selected, then a feature is chosen to be machined and the machining resources defined, finally a process is selected for operating on the feature. It is then highly desirable to assess the compatibility of the machining resource and associated machining sequence with the drawing tolerance. The machining accuracy of a part depends partly on the positioning accuracy of the tool-tip for the specified tool trajectories required to produce the workpiece.

5.5.1 Procedure to predict the tool versus workpiece position error

Usually the tool trajectories are represented by a series of positions and orientations contained in the CL data file for a specific geometric element and are generated directly from the CAD/CAM system once the preliminary steps of tool definition are completed on a CAM system. The joint coordinate values for each machine tool joint, are then calculated using the machine tool inverse kinematics model. Next, each joint coordinate value (axis command position) is introduced in the polynomial functions to calculate the geometric errors associated with that axis. Once these errors are calculated, they are introduced in the forward kinematics error model (equation (83)). Figure 5.4 shows the steps to predict the tool-tip versus workpiece error.

5.5.2 Generation of tool trajectory

In a modern CAD/CAM system, the tool trajectory is generated following several steps of process planning. The general procedure is presented in Figure 5.5.

Figure 5.6 shows the part to be analysed in the following illustrative example. A curve named $curve_{nominal}$ on the surface of the part is selected, then the corresponding tool path is generated from a CAM system. The tool path information including the machine tool topology, tool radius and type, tool tip position and orientation are presented in the CL data file. The CL data representing the tool tip position and tool orientation are expressed by $(x_c, y_c, z_c, i_c, j_c, k_c)$, where (x_c, y_c, z_c) stands for the cutter tip position and (i_c, j_c, k_c) stands for the cutter orientation. In CATIA [CATIA 2000] for example the CL data can be generated using the NC-SET functions.

5.5.3 Generation of the $CL_{predicted}$ and $curve_{predicted}$

The $CL_{predicted}$ is the position and orientation of the tool relative to the part when the geometric errors of the machine tool are considered. To calculate its values, first the joint coordinate values for $CL_{nominal}$ are calculated through an inverse kinematics procedure. Then these values and the geometric error values are considered within the

forward kinematics error model of equation (83) and finally from the equation (89) the new tool position and orientation $CL_{predicted}$ are calculated (see Figure 5.4).

From the $CL_{predicted}$, a new curve named $curve_{predicted}$ is generated in a CAD modeller (CATIA) as shown in Figure 5.6.

5.5.4 Comparison of two curves

The difference between the predicted and nominal curves is compared to a line profile tolerance associated to the part drawing.

To compare $curve_{predicted}$ with $curve_{nominal}$ we first select a series of equally spaced points on $curve_{nominal}$ (see Figure 5.7), secondly we generate the normal vectors at these points and thirdly we create a line segment, named L_d, starting from the points located on $curve_{nominal}$ to the $curve_{predicted}$ in the direction of the normal vectors. The comparison with the tolerance zone is made between the value of L_d at a given point and the value of the bi-lateral tolerance $\pm T/2$. In the 3D CAD package CATIA **[27]**, these two curves can be compared using the ANALYSE+RELATIVE functions. Figure 5.7 shows $curve_{nominal}$, the profile tolerance zone and the out-of-tolerance zone. The presence of an out-of-tolerance zone indicates that the selected machine tool cannot perform the operation satisfactorily.

5.5.5 Comparison of two surfaces

The capability of the machine tool (based on its geometric errors) to accurately machine a specific surface is assessed as follows. A surface is selected ($surface_{nominal}$) from which the $CL_{nominal}$ data file is generated directly from the CAD/CAM. The next operation involves calculating the joint coordinate values for each position in the $CL_{nominal}$ file. Then the corresponding machine tool errors for these configurations are calculated using the polynomial functions. Next from the forward kinematics error model new positions are predicted and used to generate the new surface using the same process used for $surface_{nominal}$. The surface is generated from the curves, themselves

generated from the $CL_{predicted}$ points. The new surface, named $surface_{predicted}$, is compared to the $surface_{nominal}$ and the difference analysed with respect to the specified tolerance.

The surface profile tolerance zone is a volume generated by offsetting (on both sides) the nominal surface in a direction normal to the nominal surface at each point of the surface. The offsets in each direction may, or may not, be disposed equally [28] . Figure 5.8a shows the $surface_{nominal}$ and its profile tolerance zone. The comparison between $surface_{nominal}$ and $surface_{predicted}$ proceeds as follows. For the points on the nominal surface P_n, the line between P_n and the point at the intersection of the normal vector with $surface_{predicted}$ (P_r) named $L_{predicted}$ is compared to the profile tolerance $L_{profile}$. If $L_{predicted} < L_{profile}$, then $surface_{predicted}$ is conformed. If not, $surface_{predicted}$ exceeds the tolerance zone. In CATIA, $surface_{predicted}$ can be extracted from the envelope created by the profile tolerance volume. Alternatively they can be compared using an envelope created between $surface_{nominal}$ and $surface_{predicted}$ and another created by the profile surface volume. Figure 5.8b shows the $surface_{nominal}$ and $surface_{predicted}$.

5.5.6 Illustrative example

An example is given in this section to illustrate the error prediction and tool path verification. This example involves the milling of a part having a sculptured surface. This nominal part modelled on CATIA is shown in Figure 5.9a. Figure 5.9b shows the blank before machining. Since the sculptured surface is relatively complex and also because of the relatively tight tolerance imposed, the part needs to be machined by a five-axis machine tool. From the error identification procedure, the error coefficients are identified as described in section 2. Table 5.2 shows these parameters and coefficients and their identified values for the target CFYXAC machine tool. The CL data is generated using NC-SET of CATIA and is used by the error prediction procedure as explained in 3.1 in order to calculate the tool path errors and generate $CL_{predicted}$. A surface named $surface_{predicted}$ is generated from $CL_{predicted}$. Figure 5.9c shows the surfaces resulting from the $CL_{nominal}$ and $CL_{predicted}$ data. The two parts resulting from $surface_{nominal}$ and $surface_{predicted}$ are superposed in Figure 5.9d. These two surfaces are then compared

to see if the volume between the two surfaces is within the surface profile tolerance zone. Figure 5.9e shows the volume between the two top surfaces and Figure 5.9f shows the volume and the tolerance zone. Figure 5.9g shows the portions of the volume that are out-of-tolerance indicating a need to change machine tool or to take corrective measures such as to compensate the errors for producing an acceptable part.

5.5.7 Integration within a computer aided process planning and CAD/CAM system

Having information about the inaccuracy of the surface or volume to be machined, before committing actual resources, is highly desirable in process plan development and in the product development phase. As explained earlier, a software is developed that uses the information of machine tool actual data stored in machine tool database and identifies its geometric errors and then verifies if the current machining operation can satisfy the requirements on the quality of the part. It becomes more useful when we can generate the part's actual shape generated under the current status of machine tool and compared with its nominal shape within a CAD/CAM system. A general overview of the integration of this tool in a process planning system and CAD/CAM system is shown in Figure 5.10. First a machine tool is selected. Then a nominal tool path is generated with the CAD/CAM modeller using the machining parameters selected by the process planner. This nominal tool path is compared with the predicted tool path for the selected machine tool. This information is analysed by the process planner for corrective actions if necessary.

5.6 Conclusion

This study proposes an approach to predict the influence of the geometric errors of a five-axis machine tool on a machined surface and to assess this surface against the desired surface profile tolerance. An error identification procedure has been presented to identify the parametric errors of the five-axis machine tool. A forward kinematic error model of the machine tool was presented and a sensitivity Jacobian matrix was formed

to show the sensibility of the ball-bar measurements to the geometric error parameters. The identified error parameters were then used in an error prediction procedure to calculate the errors associated with the tool-tip for a given command location. For surface machining, the tool-tip positions and orientations stored in a CL data file are then used in the error prediction module to calculate the corresponding predicted positions and orientation using the geometric errors considered. The predicted surface is compared with the part nominal surface and then difference is compared to the tolerance zone. The result provides useful information to the process planner in deciding whether or not the selected machine tool is capable of performing the operation within the desired tolerance. A negative answer to this question leads to either a change of machine tool, process, or simply to a compensation of the machine error via the post processor.

Acknowledgements

This work was performed with the support of Rene Mayer's NSERC Grant N° 155677-98 and Clément Fortin's NSERC Grant 36396-98.

References

1 **Elmaraghy H. A.** Evolution and future perspectives of CAPP. *Annals CIRP*, 42(2), pp. 739-751, 1993.

2 **Huang Y., Oliver J. H.** Integrated Simulation, Error Assessment, and Tool Path Correction for Five-Axis Milling. *Journal of Manufacturing Systems*, V. 14, No. 5, 1995.

3 **Bzymek Z. M.** Design and Utilization of Virtual Machines and Processes. MH-Vol. 5/MED-Vol.9, *Industrial Virtual Reality: Manufacturing and Design Tool for the Next Millennium ASME*, 1999.

4 **Ebrahimi M., Whalley R.** Machine Tool Syntheses in Virtual Machining. *Int. J. of Materials and Product Technology*, Vol. 13, Nos 3-6, 1998.

5 **ElMounayri H., Spence A. D., Elbestawi M. A.** Milling Process Simulation-A Generic Solid Modeller Based Paradigm. *Journal of Manufacturing Science and Engineering, Transaction of ASME*, Vol. 120, 1998.

6 **Shin, V. C., Chin, H. and Brink M. J.** Characterization of CNC machining centers. *Journal of Manufacturing Systems*, v. 10, No. 5, 1991.

7 **Donmez, M. A., Blomquist, D. S., Hocken, R. J., Liu, C. R., and Barash, M. M.** A General Methodology for Machine Tools Accuracy Enhancement by Error Compensation. *Precision Engineering*, Vol. 8, No. 4, pp. 187-196, 1986.

8 **Donmez, M. A., Liu, C. R., and Barash, M. M.** A generalized Mathematical Model for Machine Tool Errors, Modeling, Sensing, and Controling of Manufacturing Process, *ASME Winter Annual Conference*, PED-Vol. 23/DSC-Vol.4, pp. 231-243, 1987.

9 **Duffie, N. A., and Malmberg, S. J.** Error Diagnosis and Compensation Using Kinematic Model and Position Error Data. *Annals of CIRP*, Vol. 36, No. 1, pp. 355-358, 1987.

10 **Bryan J. B.** A simple method for testing measuring machine and machine tools Part 1: Principles and applications. *Precision Engineering*, 4(2), 1982.

11 **Bryan J. B.** A simple method for testing measuring machine and machine tools Part 2: Construction details. *Precision Engineering*, 4(2), 1982.

12 **Hai, N., Yuan, J., and Ni, J.** Reverse Kinematic Analysis of Machine Tool Error Using Telescoping Ball Bar. *PED-Vol.68-1, Manufacturing Science and Engineering*, Volume 1, ASME, 1994.

13 **Kakino Y., Ihara Y. and Shinohara A.** Accuracy Inspection of NC Machine Tools by Double Ball Bar Method. Hanser Publishers, 1993.

14 **Morishing K., Takeuchi Y., Kase K.** Tool Path Generation Using C-Space for 5-Axis Control Machining. *Journal of Manufacturing Science and Engineering*, Transaction of ASME, Vol. 121, 1999.

15 **Leu M. C., Wang L., Blackmore D.** A verification programme for 5-axis NC machining with General APT Tools. *Annals of CIRP*, Vol. 46/1, 1997.

16 **Leu M. C., Lu F., Blackmore D.** Simulation of NC Machining with Cutter Deflection by Modelling Deformed Swept Volumes. *Annals of CIRP*, Vol. 47/1, 1998.

17 **Lim E. M., Menq C.-H., Yen D. W.** Integrated planning for precision machining of complex surfaces-III: Compensation of dimensional errors. *International Journal of Machine Tools and Manufacture*, Vol. 37, No. 9, 1997.

18 **Korean Y.** Five-Axis Surface Interpolators. *Annals of CIRP*, Vol. 44/1, 1995.

19 **Ge Q. J.** Kinematics-Driven Geometric Modeling: A Framework for simultaneous NC Tool-Path Generation and Sculptured Surface Design. Proceedings of the 1996 IEEE, *International Conference on Robotics and Automation*, 1996.

20 **Frey D. D., Otto K. N., Pflager W.** Swept Envelopes of Cutting Tools in Integrated Machine and Workpiece Error Budgeting. *ASEM Journal of Mechanical Design*, 1998.

21 **Mayer J.R.R., Mir, Y.A., Fortin, C.** Calibration of a Five-Axis Machine Tool for Position Independent Geometric Error Parameters Using a Telescoping Magnetic Ball-Bar. *MATADOR International Conference*, UK, 2000.

22 **Mir Y. A., Mayer J.R.R, Fortin C.** Calibration of a Five-Axis Machine Tool Link and motion errors Using Telescoping Magnetic Ball-Bar. Submitted to the *Journal of Machine Tool and Manufacture*, 2001

23 **Rivlin, J. J.** The Chebyshev Polynomials. John Willy & Sons, New York, 1974.

24 **Craig, J. J.** Introduction to Robotics, Mechanics and Controls. Second Edition, Addison-Wesley Publishing Company, 1974.

25 **Cloutier, G., Mayer, J. R. R.** Modélisation de Machine en Fabrication Mécanique. Course material offered in the Mechanical Engineering Department, Ecole Polytechnique de Montreal, 1999.

26 **Hayati, S., Tso K. and Roston G.** Robot Geometry Calibration. IEEE international *Conference on Robotics and Automation*, Vol. 2, Philadelphia, Pennsylvania, April 24-29 1988.

27 **CATIA SOLUTIONS** A CAD/CAM package developed by Dassault systems, http://www.catia.com.

28 **ASME Y14.5, 1994.**

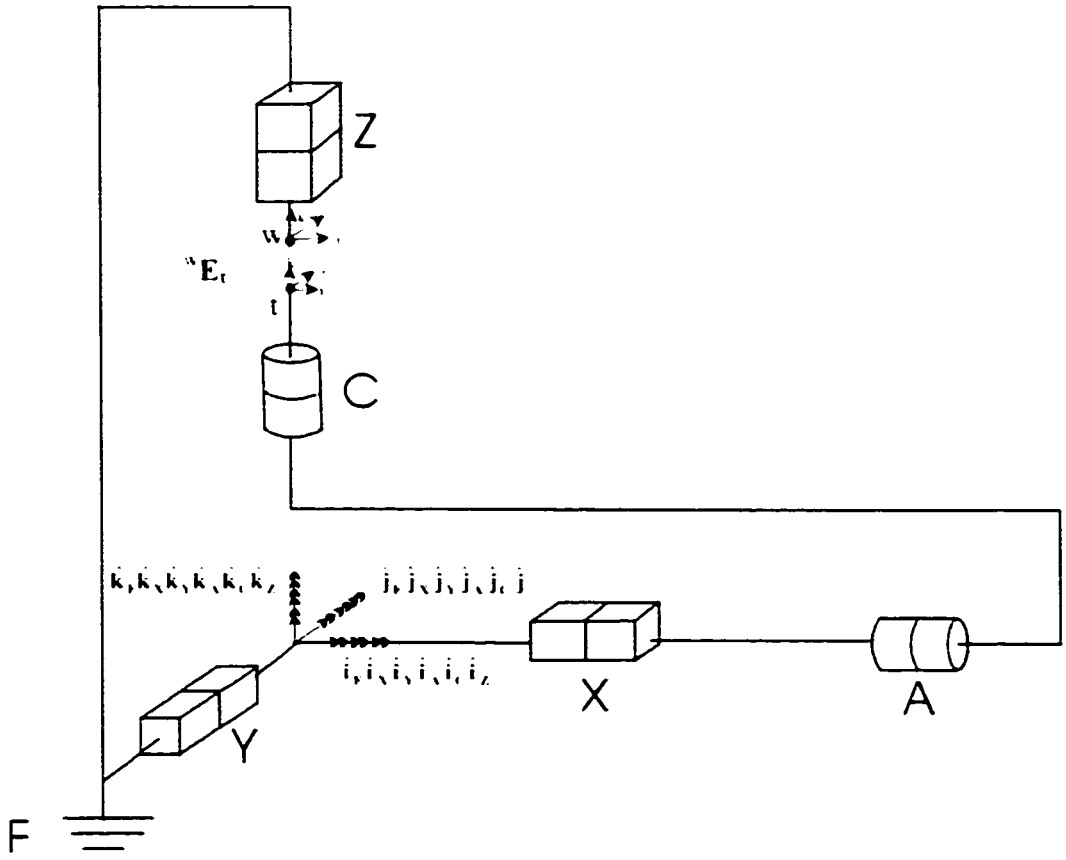

Figure 5.1a Joint frames at joint coordinate $\theta = [0\ 0\ 0\ 0\ 0]^T$.

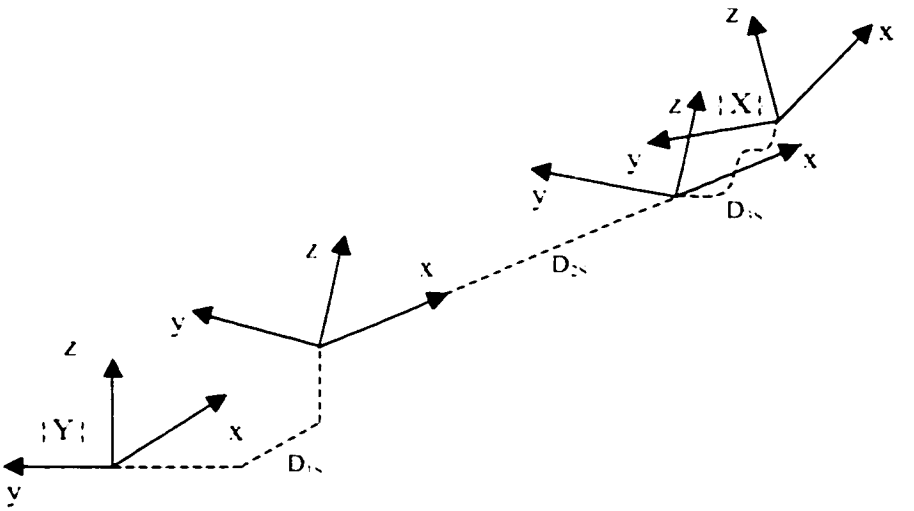

Figure 5.1b Sub-HTMs of each joint-link transformation.

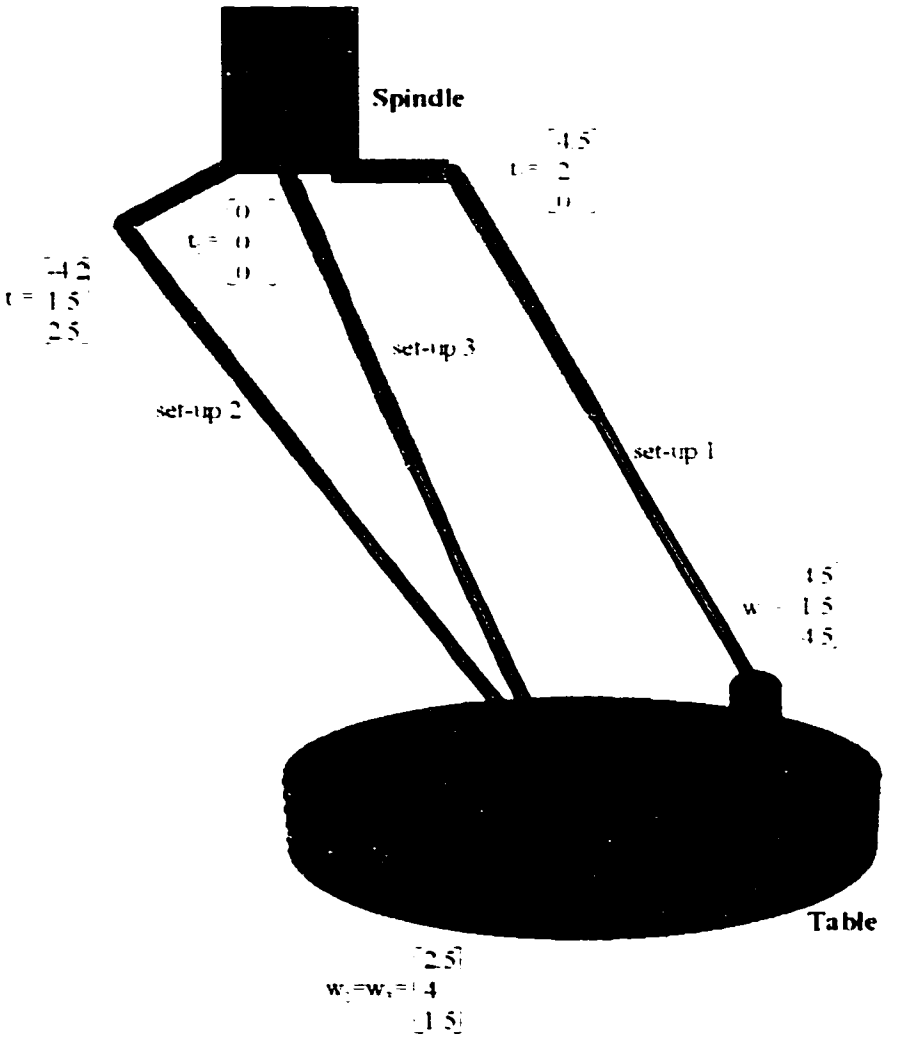

Figure 5.2 The three set-ups and the position of each socket.

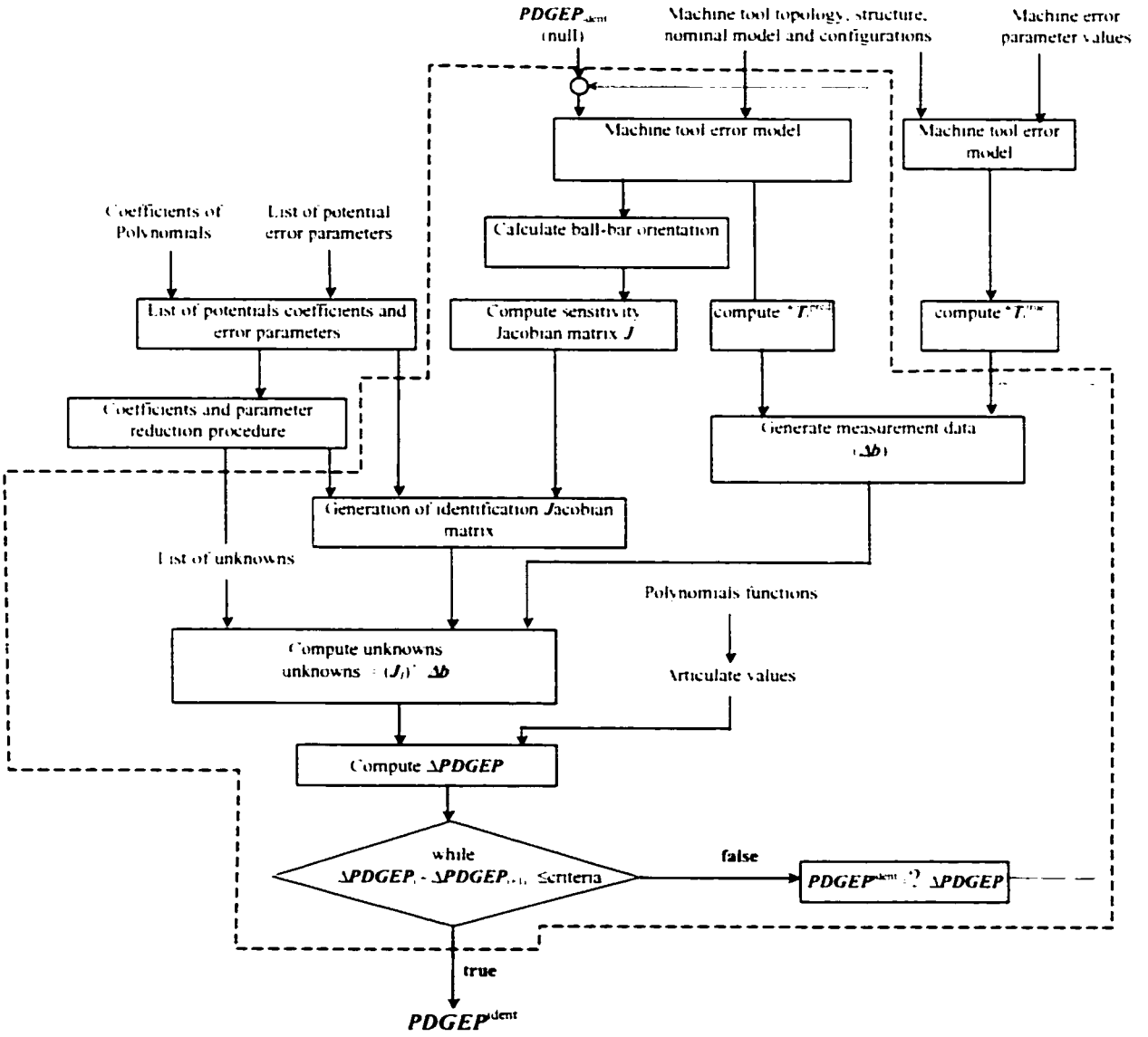

Figure 5.3 A general overview of the identification procedures.

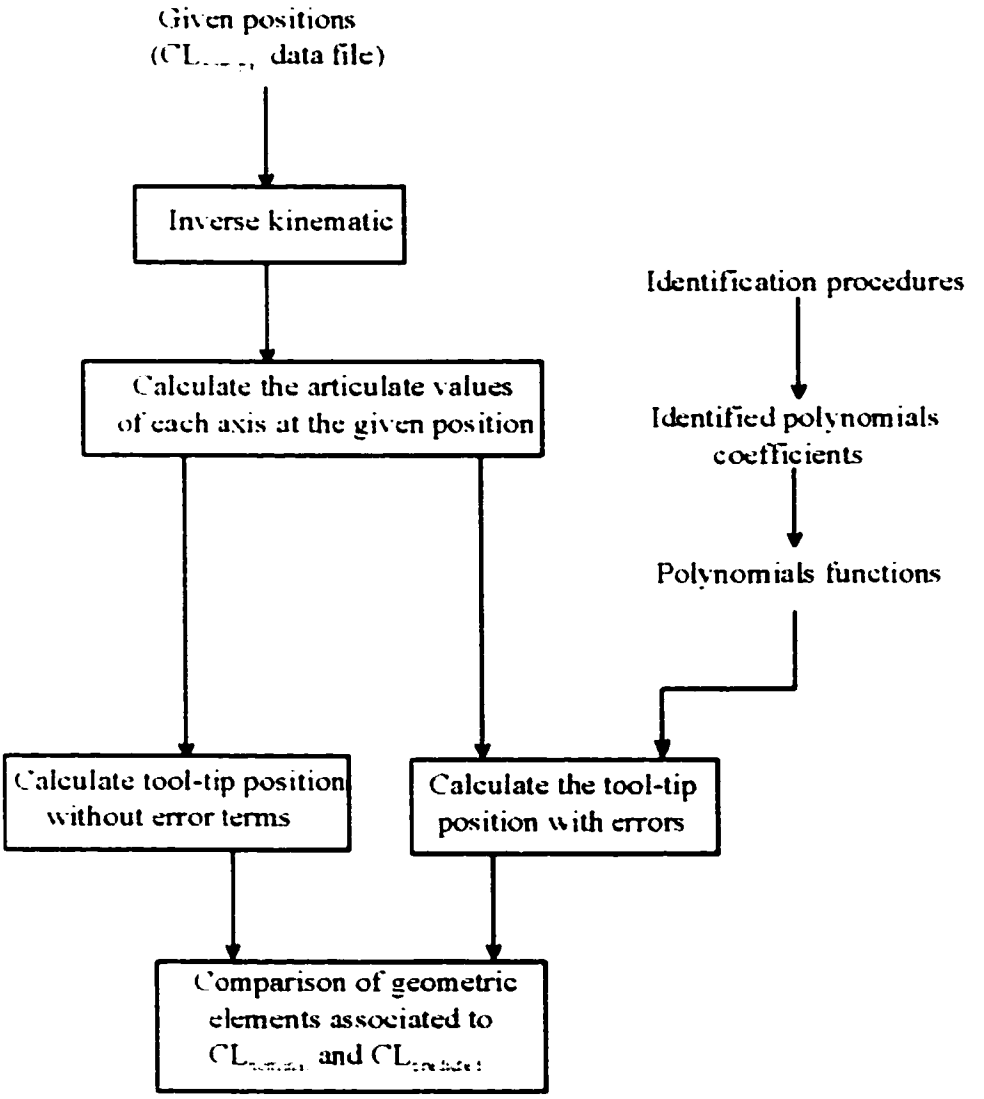

Figure 5.4 Steps to predict the errors of a machine tool for a given position.

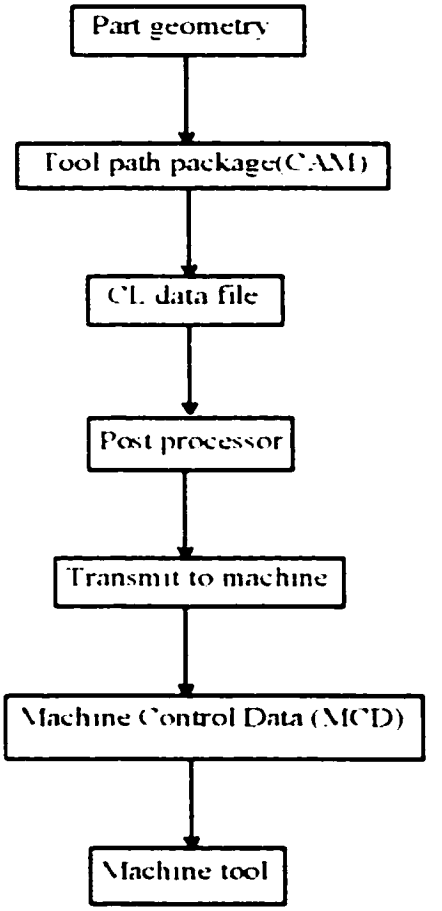

Figure 5.5 A general overview of generating tool path on machine tool.

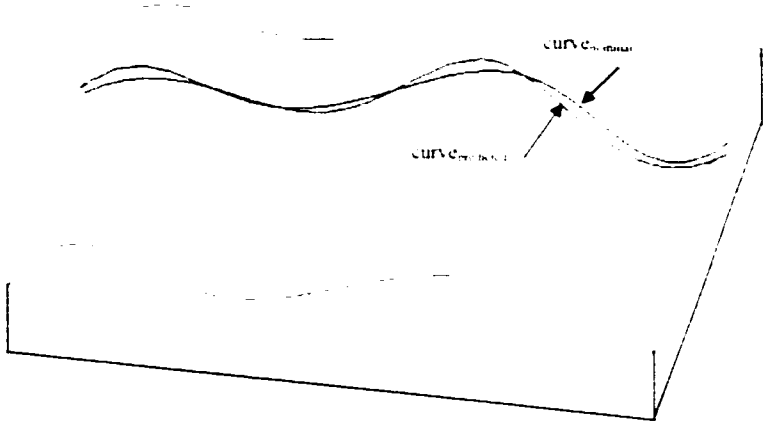

Figure 5.6 Nominal and predicted curves on the surface to be machined

4.7a

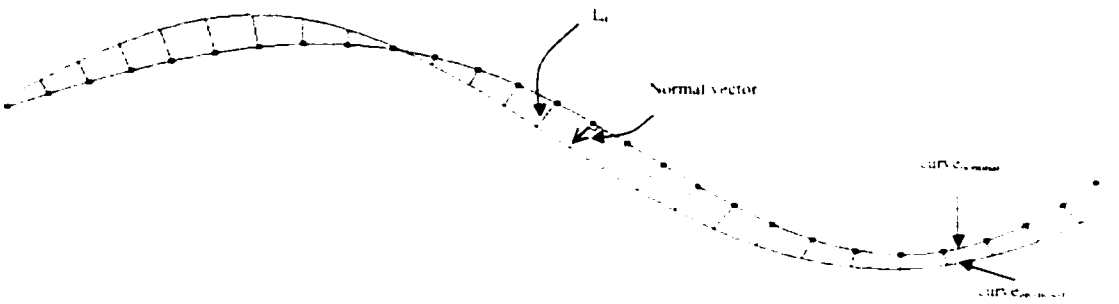

4.7b

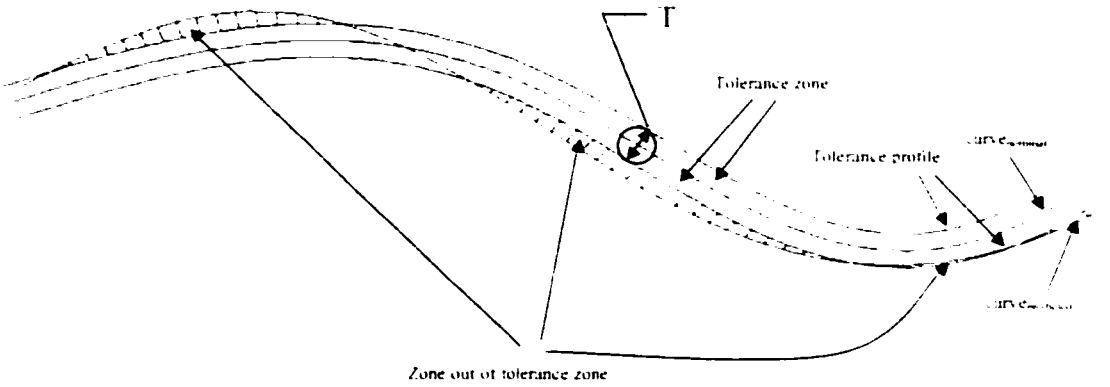

Figure 5.7 Comparison of two curves, profile tolerance and zone out of tolerance zone.

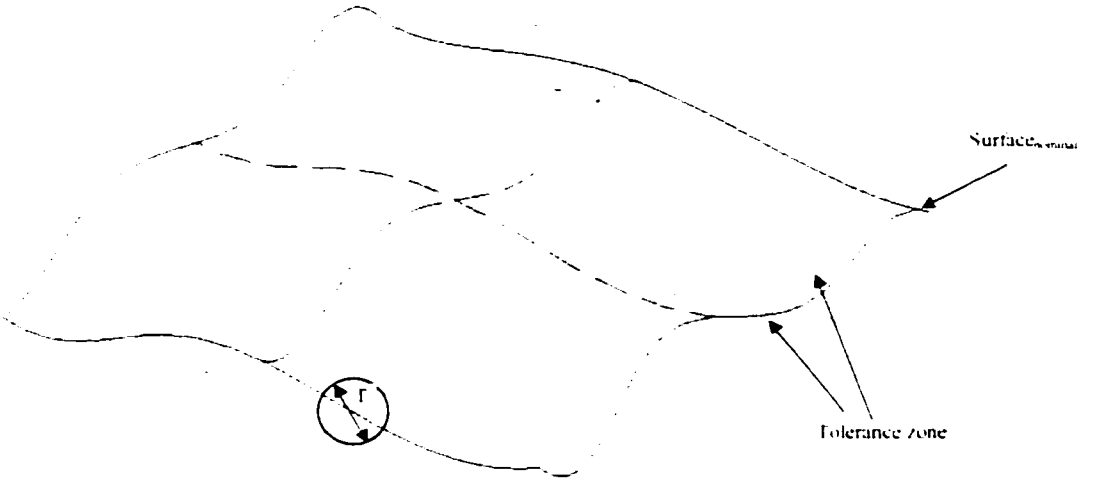

Figure 5.8a Surface$_{nominal}$ and profile tolerance zone.

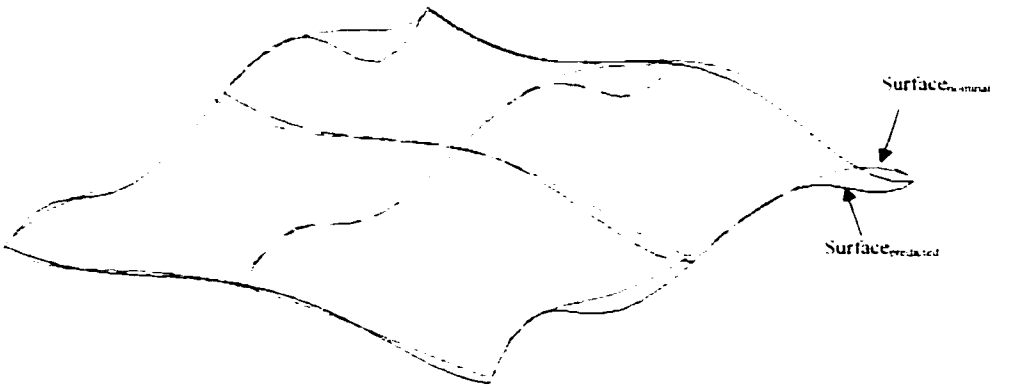

Figure 5.8b Surface$_{nominal}$ and surface$_{predicted}$.

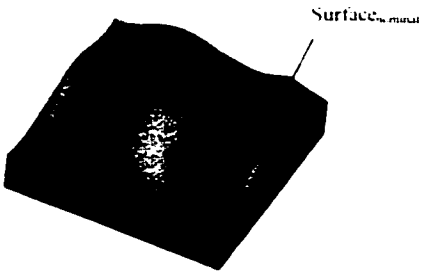

Fig. 5.9a Surface of the part to be machined.

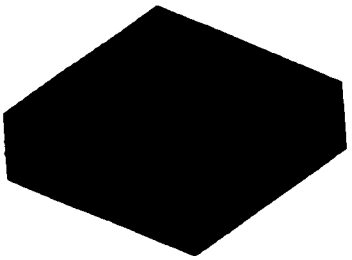

Fig. 5.9b Raw material.

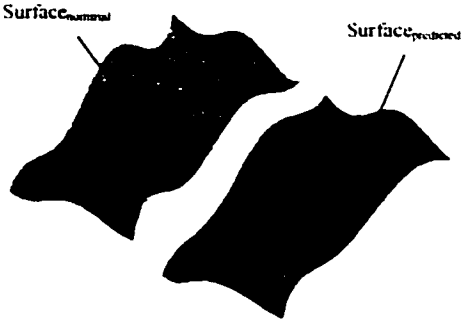

Fig. 5.9c The surface$_{nominal}$ and surface$_{predicted}$.

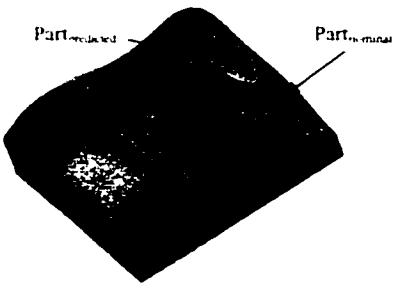

Fig. 5.9d Superposed nominal and predicted parts.

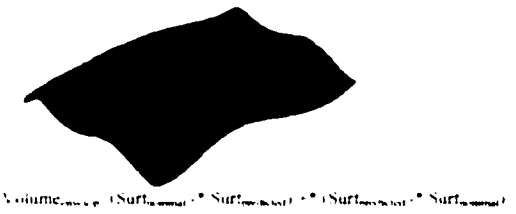

Fig.5.9e Volume between two top surfaces.

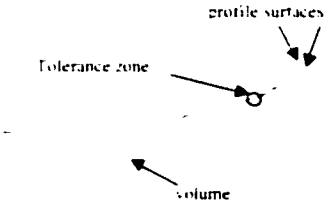

Fig. 5.9f Volume and tolerance zone.

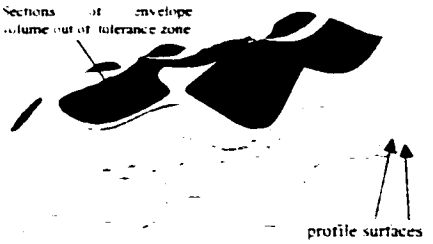

Fig. 5.9g A section of volume that is located out of tolerance zone.

Figure 5.9 Illustrative example of tool path verification.

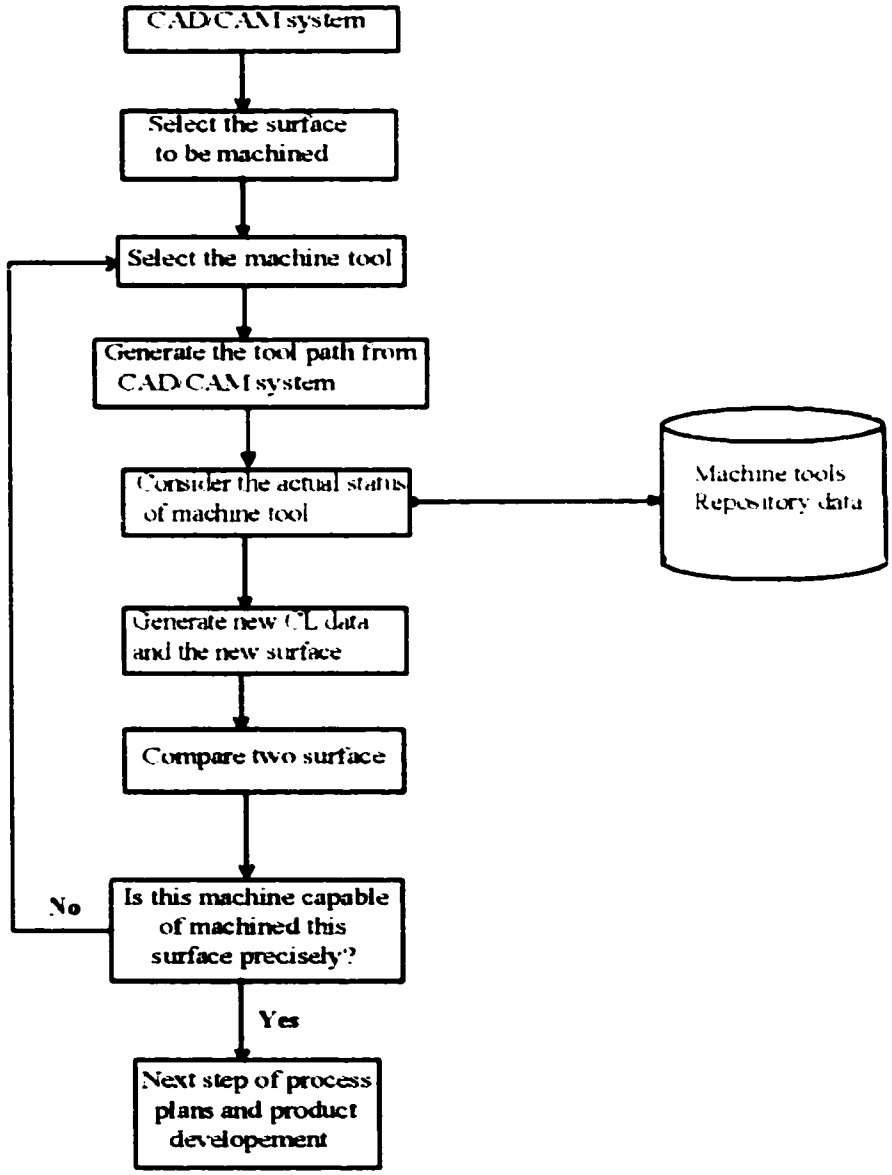

Figure 5.10 Integration of tool path error prediction in product and process plans development cycle.

Table 5.1: Summary of the variables in relation to the maximal-complete and minimal-complete models.

Axis	All axis and set-up error terms for a 5-axes machine tool	a Maximal-complete model variables	b The coefficients removed	c Minimal-complete model variables
Y	$e_{x,Y}$	$e_x(Y)_0\ e_x(Y)_1\ e_x(Y)_2\ e_x(Y)_3$	$e_x(Y)_0\ e_x(Y)_1$	$e_x(Y)_2\ e_x(Y)_3$
	$e_{y,Y}$	$e_y(Y)_0\ e_y(Y)_1\ e_y(Y)_2\ e_y(Y)_3$	$e_y(Y)_0$	$e_y(Y)_1\ e_y(Y)_2\ e_y(Y)_3$
	$e_{z,Y}$	$e_z(Y)_0\ e_z(Y)_1\ e_z(Y)_2\ e_z(Y)_3$	$e_z(Y)_0\ e_z(Y)_1$	$e_z(Y)_2\ e_z(Y)_3$
	$\chi_{x,Y}$	$\chi_x(Y)_0\ \chi_x(Y)_1\ \chi_x(Y)_2\ \chi_x(Y)_3$	$\chi_x(Y)_0$	$\chi_x(Y)_1\ \chi_x(Y)_2\ \chi_x(Y)_3$
	$\chi_{y,Y}$	$\chi_y(Y)_0\ \chi_y(Y)_1\ \chi_y(Y)_2\ \chi_y(Y)_3$	$\chi_y(Y)_0$	$\chi_y(Y)_1\ \chi_y(Y)_2\ \chi_y(Y)_3$
	$\chi_{z,Y}$	$\chi_z(Y)_0\ \chi_z(Y)_1\ \chi_z(Y)_2\ \chi_z(Y)_3$		$\chi_z(Y)_0\ \chi_z(Y)_1\ \chi_z(Y)_2\ \chi_z(Y)_3$
X	$e_{x,X}$	$e_x(X)_0\ e_x(X)_1\ e_x(X)_2\ e_x(X)_3$	$e_x(X)_0$	$e_x(X)_1\ e_x(X)_2\ e_x(X)_3$
	$e_{y,X}$	$e_y(X)_0\ e_y(X)_1\ e_y(X)_2\ e_y(X)_3$	$e_y(X)_0\ e_y(X)_1$	$e_y(X)_2\ e_y(X)_3$
	$e_{z,X}$	$e_z(X)_0\ e_z(X)_1\ e_z(X)_2\ e_z(X)_3$	$e_z(X)_0\ e_z(X)_1$	$e_z(X)_2\ e_z(X)_3$
	$\chi_{x,X}$	$\chi_x(X)_0\ \chi_x(X)_1\ \chi_x(X)_2\ \chi_x(X)_3$		$\chi_x(X)_0\ \chi_x(X)_1\ \chi_x(X)_2\ \chi_x(X)_3$
	$\chi_{y,X}$	$\chi_y(X)_0\ \chi_y(X)_1\ \chi_y(X)_2\ \chi_y(X)_3$		$\chi_y(X)_0\ \chi_y(X)_1\ \chi_y(X)_2\ \chi_y(X)_3$
	$\chi_{z,X}$	$\chi_z(X)_0\ \chi_z(X)_1\ \chi_z(X)_2\ \chi_z(X)_3$		$\chi_z(X)_0\ \chi_z(X)_1\ \chi_z(X)_2\ \chi_z(X)_3$
A	$e_{x,A}$	$e_x(a)_0\ e_x(a)_1\ e_x(a)_2\ e_x(a)_3$	$e_x(a)_0$	$e_x(a)_1\ e_x(a)_2\ e_x(a)_3$
	$e_{y,A}$	$e_y(a)_0\ e_y(a)_1\ e_y(Y)_2\ e_y(a)_3$		$e_y(a)_0\ e_y(a)_1\ e_y(a)_2\ e_y(a)_3$
	$e_{z,A}$	$e_z(a)_0\ e_z(a)_1\ e_z(a)_2\ e_z(a)_3$	$e_z(a)_0$	$e_z(a)_1\ e_z(a)_2\ e_z(a)_3$
	$\chi_{x,A}$	$\chi_x(a)_0\ \chi_x(a)_1\ \chi_x(a)_2\ \chi_x(a)_3$	$\chi_x(a)_0$	$\chi_x(a)_1\ \chi_x(a)_2\ \chi_x(a)_3$
	$\chi_{y,A}$	$\chi_y(a)_0\ \chi_y(a)_1\ \chi_y(a)_2\ \chi_y(a)_3$		$\chi_y(a)_0\ \chi_y(a)_1\ \chi_y(a)_2\ \chi_y(a)_3$
	$\chi_{z,A}$	$\chi_z(a)_0\ \chi_z(a)_1\ \chi_z(a)_2\ \chi_z(a)_3$	$\chi_z(a)_0$	$\chi_z(a)_1\ \chi_z(a)_2\ \chi_z(a)_3$
C	$e_{x,C}$	$e_x(c)_0\ e_x(c)_1\ e_x(c)_2\ e_x(c)_3$	$e_x(c)_0$	$e_x(c)_1\ e_x(c)_2\ e_x(c)_3$
	$e_{y,C}$	$e_y(c)_0\ e_y(c)_1\ e_y(c)_2\ e_y(c)_3$	$e_y(c)_0$	$e_y(c)_1\ e_y(c)_2\ e_y(c)_3$
	$e_{z,C}$	$e_z(c)_0\ e_z(c)_1\ e_z(c)_2\ e_z(c)_3$	$e_z(c)_0$	$e_z(c)_1\ e_z(c)_2\ e_z(c)_3$
	$\chi_{x,C}$	$\chi_x(c)_0\ \chi_x(c)_1\ \chi_x(c)_2\ \chi_x(c)_3$	$\chi_x(c)_0$	$\chi_x(c)_1\ \chi_x(c)_2\ \chi_x(c)_3$
	$\chi_{y,C}$	$\chi_y(c)_0\ \chi_y(c)_1\ \chi_y(c)_2\ \chi_y(c)_3$	$\chi_y(c)_0$	$\chi_y(c)_1\ \chi_y(c)_2\ \chi_y(c)_3$
	$\chi_{z,C}$	$\chi_z(c)_0\ \chi_z(c)_1\ \chi_z(c)_2\ \chi_z(c)_3$	$\chi_z(c)_0$	$\chi_z(c)_1\ \chi_z(c)_2\ \chi_z(c)_3$
w	$e_{x,w}$	$e_x(w)$		$e_x(w)$
	$e_{y,w}$	$e_y(w)$		$e_y(w)$
	$e_{z,w}$	$e_z(w)$		$e_z(w)$
	$\chi_{x,w}$	$\chi_x(w)$		$\chi_x(w)$
	$\chi_{y,w}$	$\chi_y(w)$		$\chi_y(w)$
	$\chi_{z,w}$	$\chi_z(w)$		$\chi_z(w)$
Z	$e_{x,Z}$	$e_x(z)_0\ e_x(z)_1\ e_x(z)_2\ e_x(z)_3$	$e_x(z)_0$	$e_x(z)_1\ e_x(z)_2\ e_x(z)_3$
	$e_{y,Z}$	$e_y(z)_0\ e_y(z)_1\ e_y(z)_2\ e_y(z)_3$	$e_y(z)_0$	$e_y(z)_1\ e_y(z)_2\ e_y(z)_3$
	$e_{z,Z}$	$e_z(z)_0\ e_z(z)_1\ e_z(z)_2\ e_z(z)_3$	$e_z(z)_0$	$e_z(z)_1\ e_z(z)_2\ e_z(z)_3$
	$\chi_{x,Z}$	$\chi_x(z)_0\ \chi_x(z)_1\ \chi_x(z)_2\ \chi_x(z)_3$	$\chi_x(z)_0$	$\chi_x(z)_1\ \chi_x(z)_2\ \chi_x(z)_3$
	$\chi_{y,Z}$	$\chi_y(z)_0\ \chi_y(z)_1\ \chi_y(z)_2\ \chi_y(z)_3$	$\chi_y(z)_0$	$\chi_y(z)_1\ \chi_y(z)_2\ \chi_y(z)_3$
	$\chi_{z,Z}$	$\chi_z(z)_0\ \chi_z(z)_1\ \chi_z(z)_2\ \chi_z(z)_3$	$\chi_z(z)_0$	$\chi_z(z)_1\ \chi_z(z)_2\ \chi_z(z)_3$
t	$e_{x,t}$	$e_x(t)$		$e_x(t)$
	$e_{y,t}$	$e_y(t)$		$e_y(t)$
	$e_{z,t}$	$e_z(t)$		$e_z(t)$
	$\chi_{x,t}$	$\chi_x(t)$		$\chi_x(t)$
	$\chi_{y,t}$	$\chi_y(t)$		$\chi_y(t)$
	$\chi_{z,t}$	$\chi_z(t)$		$\chi_z(t)$

Table 5.2: Results of simulations A: Non-null values are applied to all maximal-complete model variables.

Axis	All axis and set-up error terms for a 5-axes machine tool	a Maximum-complete model variables	b* True values for the variables of column a 10E-3	c Minimum-complete model variables	d* Identified values for the variables of column c respectively 10E-3
Y					
X					
A					
C					
w_1					
w_2					
w_3					
Z					
t_1					
t_2					
t_3					

*values are rounded off for presentation propose

CONCLUSION ET DISCUSSION GÉNERALE

Les systèmes de GAO revêtent une importance grandissante dans les industries de fabrication moderne. La GAO fournit un lien direct entre la conception et la fabrication et réduit le temps nécessaire entre la conception et la fabrication. Le système GAO doit être intégré complètement dans un environnement de CAO/FAO. Le domaine GAO a été graduellement développé ces deux dernières décennies et différentes technologies sont impliquées. Cependant, leur succès dans l'industrie tarde à venir. Les problèmes principaux sont les changements rapides de technologies de fabrication/production, le manque de méthodologies précises, le manque d'intégration avec CAO/FAO, la dépendance sur l'expérience des gammistes etc..

Un concept a été présenté pour prévoir l'erreur paramétrique d'une machine-outil à cinq axes. Différents paramètres peuvent être la cause des erreurs incluant le comportement cinématique de la machine, l'effet thermique, l'effet dynamique, des charges, etc. Ce travail examine les causes géométriques d'erreurs sur les machines-outils.

La présence d'erreurs sur des machines-outils affecte la qualité d'une pièce usinée. Ainsi en identifiant les paramètres d'erreurs de la machine-outil, leur propagation sur la pièce peut être évaluée pour prévoir si cette machine, avec un processus choisi, est capable de produire une pièce de tolérances désirables. Cela peut aider le gammiste à choisir un paramètre approprié pour produire cette pièce.

On a proposé une approche pour l'étalonnage des paramètres d'erreurs géométriques indépendants de la position d'une machine-outil à cinq axes. La matrice de transformation homogène a été utilisée pour la modélisation de la machine-outil, une matrice Jacobienne a été développée sur la base de la transformation nominale de composants de machine-outil et ensuite une série minimale mais complète de paramètres d'erreurs a été définie. Ensuite l'emploi de la BBMT a été simulé pour acquérir des lectures de longueur pour un certain nombre de configurations de machine. Les simulations montrent des résultats excellents.

Une procédure d'étalonnage complète a aussi été développée pour une machine-outil à cinq axes pour les erreurs géométriques dépendant de la position en employant encore une fois la barre à billes télescopique. L'emploi de la barre à billes a été simulé pour l'acquisition des données pour l'étalonnage sans employer de trajectoire circulaire. Le modèle est basé sur la matrice Jacobienne pour exprimer la sensibilité de la position de bout d'outil versus des sources d'erreurs géométriques de la machine. Les sources d'erreurs de machine-outil ont été individuellement modélisées par des polynômes de Chebychev et intégrés dans la matrice d'observation. Le polynôme de Chebychev a été employé à cause de ses avantages sur la procédure de calcul. Les coefficients des polynômes ont été calculés par une équation linéaire de la matrice d'observation et la lecture de barre à billes. Les valeurs de polynômes ont été utilisées pour prévoir l'erreur de bout d'outil pour une valeur articulée donnée. Les paramètres ont été identifiés par une procédure d'identification complète. À cause de la redondance entre des paramètres d'erreurs, une stratégie a été créée pour choisir un paramètre approprié à partir de chaque groupe de paramètres couplés. D'une procédure d'identification complète, un nombre minimal mais complet de coefficients a été identifié. Une stratégie de barre à billes à trois ancrages a été utilisée pour identifier ces paramètres. Finalement, quelques critères ont été employés pour évaluer si les paramètres identifiés sont acceptables. Un logiciel de simulation a été développé en code Matlab^{TM} afin d'accomplir les procédures.

La vérification de la performance de la machine-outil pour exécuter une opération dans une tolérance souhaitable a aussi été examinée. Une fois les erreurs de la machine-outil identifiées, elles sont alors utilisées pour calculer les erreurs associées au bout d'outil pour une position donnée. Pour un usinage de surface, les positions de bout d'outil sont stockées dans un fichier de données CL (CL nominal) produit directement d'un système de CAO/FAO. Ces positions sont transmises au module de prédiction d'erreurs pour calculer les erreurs associées à chacune de ces positions qui formera le CL réel. La nouvelle surface est alors produite en utilisant CL_{reel}, qui est calculé en considérant l'erreur associée à chacune des positions de $CL_{nominal}$. La nouvelle surface est comparée avec la surface de pièce (la surface nominale) et la différence est comparée à la zone de

tolérance. Le résultat donne l'information aux gammistes sur le processus pour décider si vraiment la machine-outil choisie est capable d'exécuter l'opération dans la tolérance désirable. La réponse négative à cette question mène au changement de la machine-outil, du processus ou peut simplement mener à compenser l'erreur de la machine par une correction du post-processeur.

Recommandations pour travaux futurs

La confirmation expérimentale du travail de simulation est nécessaire afin de mettre en application le concept dans l'industrie.

Un des buts d'identification des erreurs de machine-outil est d'empêcher la propagation de ces erreurs sur la surface de pièce, pour cela une procédure de compensation doit être élaborée soit au post-processeur ou au niveau des contrôleurs.

Le développement d'une voie plus simple (par exemple utilisation de la barre à billes) pour identifier les erreurs thermique et dynamique de la machine-outil d'une façon appropriée peut être intégré avec la méthode d'identification des erreurs géométriques.

Plus de recherches sont nécessaires pour choisir le type de polynômes et leur degré pour représenter exactement le comportement d'erreurs du mouvement sur des machines-outils.

L'optimisation de la procédure de simulation ainsi que la recherche du nombre optimal et approprié de configurations pour chaque topologie de machines-outils sont recommandées.

BIBLIOGRAPHIE

Alting L. and Zhang H. C., "Computer aided process planning: the state-of-the-art survey", *International Journal of Production Research*, 27(4), pp. 553-585, 1989.

Bryan J. B., A simple method for testing measuring machine and machine tools Part 1: Principles and applications, Precision Engineering, 4(2), 1982.

Bryan J. B., A simple method for testing measuring machine and machine tools Part 2: Construction details, Precision Engineering, 4(2), 1982.

Chang T.C and Wysk R. A., An Introduction to Automated Process Planning Systems, Prentice-Hall, Englewood Cliffs, New Jersey, 1985.

Ciarlet, P.G., "Introduction à l'analyse numérique matricielle et à l'optimisation", Masson, 1982.

Cloutier, G., Mayer, J. R. R., "Modélisation de Machine en Fabrication Mécanique", Course offered in Mechanical Engineering Department, École Polytechnique de Montréal, 1999.

Craig, J. J., "Introduction to Robotics, Mechanics and Controls", Second Edition, Addison-Wesley Publishing Company, 1989.

Donmez, M. A., Blomquist, D. S., Hocken, R. J., Liu, C. R., and Barash, M. M., "A general methodology for Machine Tools Accuracy Enhancement by Error Compensation," Precision Engineering, Vol. 8, No. 4, pp. 187-196, 1986.

Donmez, M. A., Liu, C. R., and Barash, M. M., "A generalised Mathematical Model for Machine Tool Errors," Modelling, Sensing, and Controlling of Manufacturing Process, ASME Winter Annual Conference, PED-Vol. 23/DSC-Vol.4, pp. 231-243, 1987.

Driels M. R., Using Passive End-Point Motion Constraints to Calibrate Robot Manipulators, Trans. of the ASME, Vol. **115**, 560-566, 1993.

Duffie, N. A., and Malmberg, S. J.,"Error Diagnosis and Compensation Using Kinematic Model and Position Error data, " Annals of CIRP, Vol. 36, No. 1, pp. 355-358, 1987.

Elmaraghy H. A., "Evolution and future perspectives of CAPP", Annals CIRP, 42(2), pp. 739-751, 1993.

Elshennawy A. K. and Ham I., "Performance Improvement in Coordinate Measuring Machines by Error Compensation," Journal of Manufacturing Systems, v9, n2, 1990, pp151-158.

Evershiem, W. and Cobanoglu, M. T., "Integrated process planning and part programming system for machining Forging dies", Proc. of CIRP Int. Workshop on CAPP, Hannover, Sept. 21-22, 1989, pp.37-53.

Eversheim W. and Schulz J. "CIRP technical reports: Survey of computer aided process planning systems". Annals CIRP, 34(2), pp. 607-614, 1985.

Ferreira P. M. and Liu C. R., "A Method for estimating and Compensating Quasi-static Errors of Machine Tools," ASME Transactions Journal of Engineering for Industry v115, 1993, pp149-159.

Fortin C., Mascle C., Mayer J. R. R., Cloutier G. M., Balazinski M., Mir, Y. A., Belanger I., "An Interactive Computer Aided Process Planning System for Manufacturing, Assembly and Inspection", 32nd International MATADOR conference, July 1997.

Frey, D.D., Otto K. N. and Pflager W., "Swept Envelopes of Cutting Tools in Integrated Machine and part Error Budgeting", accepted for publication in Annals of the CIRP, 1997.

Fussell, B. K., Ersoy, C., and Jerad, R. B., "Computer Generated CNC Machining Feed-rates", ASME Japan/USA Symposium on Flexible Automation , Vol. 1, pp. 377-384, 1992.

Fussel, B. K., and Srinivasan, K., "An Investigation of the End Milling Process Under Varying Machining Conditions", ASME Journal of Engineering for Industry, Vol. , 1989.

Ham, I. and Lu, S. C-Y., "New developments of CAPP in USA and Japan", Proc. of CIRP Int. Workshop on CAPP, Hannover, Sept. 21-22, 1989, pp.1-23.

Hayati, S., Tso K. and Roston G., 1988, "Robot Geometry Calibration", IEEE International Conference on Robotics and Automation, Vol. 2, April 24-29 1988, Philadelphia, Pennsylvania.

Hocken, R. J., "Technology of Machine Tools, vol. 5, Machine Tool Accuracy", Machine tool task force, 1980.

Hocken, R. J., Simpson, J. A, Borchardt, B., Lazar, J., Reeve, C., and Stein, P., "Three Dimension Metrology," Annals of CIRP, Vol. 26, No. 1, pp. 403-408, 1977.

Huang Y. and Oliver J. H., "Integrated Simulation, Error Assessment, and Tool Path Correction for Five-Axis NC Milling", Journal of Manufacturing Systems, Vol. 14/No. 5, 1995.

Kakino Y., Ihara Y. and Shinohara A., Accuracy Inspection of NC Machine Tools by Double Ball Bar Method, Hanser Publishers, 1993.

Kim K. I. and Kim K., "Parametric Tool Path Planning Based on New Variable STEP Strategy for Sculptured Surfaces", Transaction of NAMRI/SME, Volume XXI, 1993.

Kiridena S. B. and Ferreira P. M., "Kinematic Modelling of Quasistatic Errors of Three axis Machining Centers," International Journal of Machine Tools & manufacture v34, n1, 1994a, pp85-100.

Kiridena S. B. and Ferreira P. M., "Parameter Estimation and Model Verification of First Order Quasistatics Error Model for Three-Axis Machining Centers," International Journal of Machine Tools & Manufacture v34, n1, 1994b, pp101-125.

Kiridena S. B. and Ferreira P. M., "Computational Approaches to Compensating Quasistatic Errors of Three-Axis Machining Centers," International Journal of Machine Tools & Manufacture V34, 1994c, pp127-145.

Kiridena V. and Ferreira P. M., "Mapping the Effects of Positioning Errors on the Volumetric Accuracy of Five-axis CNC Machine Tools," International Journal of Machine Tools & Manufacture, V33, n3, 1993, pp. 417-437.

Kreng V. B., Liu C. R., and Chu C. N., "A Kinematic Model for Machine Tool Accuracy Characterisation," International Journal of Advanced Manufacturing Technology, n9, 1994, pp79-86.

Kunmann, H., and Waldele, F., On Testing Coordinate Measuring Machines (CMM) with Kinematic Reference Standards (KRS), Annals of CIRP, V32(1), 1983.

Leu M. C., Wang L., Blackmore D., "A verification programme for 5-axis NC machining with General APT Tools", Annals of CIRP, Vol. 46/1, 1997.

Leu M. C., Lu F., Blackmore D., "Simulation of NC Machining with Cutter Deflection by Modelling Deformed Swept Volumes", Annals of CIRP, Vol. 47/1, 1998.

Leung H. C., "Annotated bibliography on Computer Aided Process Planning", Int. J Adv Manuf. Techno., Vol 12, pp. 309-329, 1996.

Mayer, J.R.R., Mir, Y.A., Fortin, C., "Calibration of a Five-Axis Machine Tool for Position Independent Geometric Error Parameters Using a Telescoping Magnetic Ball-Bar", MATADOR International Conference, 2000, UK.

Morishing K., Takeuchi Y., Kase K., "Tool Path Generation Using C-Space for 5-Axis Control Machining", Journal of Manufacturing Science and Engineering, Transaction of ASME, Vol. 121, 1999.

Mou J., Donmez M. A., and Cetinkunt S., "An Adaptive Error Correction Method Using Feature-Based Analysis Techniques for Machine Performance Improvement, Part 1: Theory Derivation," ASME Transactions Journal of Engineering for Industry v117, 1995, pp584-590.

Mou J., Donmez M. A., and Cetinkunt S., "An adaptive Error Correction Method Using Feature-Based Analysis Techniques for Machine Performance Improvement, Part 2: Experimental Verification," ASME Transactions Journal of Engineering for Industry v117, 1995, pp591-600.

Mou J. and Liu C. R.,"An Adaptive Methodology for Machine Tool Error Correction," ASME Transactions Journal of Engineering for Industry v117, 1995, pp389-399.

Mou J. and Liu C. R., "An Error Correction Method for CNC Machine Tools Using Reference Parts," Transaction of the North American Manufacturing Research Institution of SME, v12, 1994, pp275-282.

Mou J. and Liu C. R., "A Method for enhancing the accuracy of CNC Machine Tools for On-Machine Inspection," Journal of Manufacturing Systems v11, n4, 1992, pp229-237.

NIST (National Institute of Science and Technology), http://www.nist.org.

Noble B. and Daniel J. W., "Applied linear algebra", Prentice-hall, second edition, 1977.

Pahk H. J., Kim Y. S. and Moon J. H., A New Technique for Volumetric Error Assessment of CNC Machine Tools Incorporating Ball Bar Measurement and 3D Volumetric Error Model, Int. J. Mach. Tools Manuf., 37(11), pp. 1583-1596, 1997.

Ragunath, V. "Thermal effects on the accuracy of numerically controlled machine-tools". Ph.D. Thesis , Purdue University, West Lafayette, IN, 1985.

Rivlin, J. J., "The Chebyshev Polynomials", John Willy & Sons, New York, 1974.

Schenk, D. E., "Feasibility of automated process planning", PhD thesis, Purdue University, West Lafayette, Indiana, USA, 1966.

Shin, V. C., Chin, H. and Brink M. J., "Characterisation of CNC machining centers. " Journal of Manufacturing System, v. 10, No. 5, 1991.

Tempellof, K. H., "A system of computer sided process planning for machine parts", Advanced Manufacturing Tech., Proc. of 4th Int. IFIP/IFAC Conf., New York 1980.

Trankle H., Effects of position errors in five-axis milling processes, Ph.D. Dissertation, Stuttgart University, Federal Republic of Germany, 1980.

Wang, W. P., "Solid Modelling of Optimising Metal Removal of Three-dimensional NC End Milling", Journal of Manufacturing systems, Vol. 7, No. 1, pp. 57-65, 1988.

Weill R., Spur G. and Eversheim W., "Survey of Computer aided process planning systems", Annals of CIRP, 31(2), pp. 539-552, 1982.

Wysk R. A., Chang T. C. and Ham I., "Automated process planning systems: an overview of ten years of activities", 1st CIRP working seminar, Paris, 22-23 January 1985.

Yazar, Z., Merrick, T., and Altan, T., "Feed Rate Optimisation Based on Cutting Force Calculations in 3-Axis Milling of Sculptured Surfaces", REPORT NO" ERC/NSM-D-92-35, Engineering Research Center, The Ohio State University, Columbus, OH, 1992.

Zhang G., Ouyang R., and Lu B., "A Displacement Method for Machine Geometry Calibration," Annals of CIRP, v37, 1988, pp515-518.

Zhang G., Veale R., Charlton T., Borchardt B., and Hocken R., "Error Compensation of Coordinate Measuring Machines," Annals of CIRP v34, 1985, p445-448.